
Role of immune cells in hereditary myelinopathies

Dissertation zur Erlangung des
naturwissenschaftlichen Doktorgrades
der Bayerischen Julius-Maximilians-Universität Würzburg

vorgelegt von

Dr. med. Antje Kroner-Milsch

aus München

Würzburg 2008

Eingereicht am: 16.07.2008

Mitglieder der Promotionskommission:

Vorsitzender: Prof. M.J. Müller

Gutachter: Prof. R. Martini

Gutachter: Prof. W. Rößler

Tag des Promotionskolloquiums: 24.09.2008

Doktorurkunde ausgehändigt am:



Hiermit erkläre ich, die vorliegende Arbeit selbständig angefertigt und keine anderen als die angegebenen Hilfsmittel verwendet zu haben.

Diese Arbeit hat weder in gleicher noch in ähnlicher Form in einem anderen Prüfungsverfahren vorgelegen.

Ich habe in keinem früheren Verfahren einen akademischen Grad erworben oder zu erwerben versucht, abgesehen vom „Dr. med“.

Würzburg, den

Dr. Antje Kroner-Milsch

Für Erik und meine lieben Eltern

TABLE OF CONTENTS

1. Abstract.....	10
2. Zusammenfassung.....	11
3. Introduction.....	12
3.1 Nerve conduction.....	12
3.2 Nodes of Ranvier.....	12
3.3 Composition of myelin and role of myelin related proteins.....	13
3.4 Human hereditary myelinopathies.....	15
3.5 Animal models for hereditary myelinopathies.....	19
3.6 Role of immune cells in myelin mutants.....	23
3.7 Activation and modulation of the adaptive immune system.....	25
4. Aim of the study.....	27
5. Materials and methods.....	28
5.1 Reagents, chemicals, media, buffers, equipment.....	28
5.2 Methods.....	28
5.2.1 DNA Purification.....	28
5.2.2 PCR (Polymerase chain reaction)	28
5.2.3 Animals and determination of Genotypes.....	28
5.2.3.1 PLP transgenic mice	28
5.2.3.2 P0+/- mice.....	29
5.2.3.3 RAG-1-/- mice.....	29
5.2.3.4 Granzyme B-/- mice.....	29
5.2.3.5 PD-1-/- mice.....	29
5.2.3.6 Double mutants.....	30
5.2.4 Bone marrow chimerization.....	30
5.2.5 Purification of mononuclear cells.....	30
5.2.5.1 Splenocytes.....	30
5.2.5.2 CNS lymphocytes.....	30
5.2.5.3 PNS immune cells.....	31
5.2.6 Flow cytometry.....	31
5.2.7 Tissue preparation and immunohistochemistry.....	31
5.2.8 Assessment of demyelination and axonal damage.....	32
5.2.8.1 Analysis of semithin sections.....	32

5.2.8.2 Electron microscopy.....	32
5.2.8.3 Analysis of myelin status by MBP- immunohistochemistry	33
5.2.9 Quantification of immune cells and apoptotic oligodendrocytes...	33
5.2.10 CDR3 Spectratyping.....	33
5.2.11 Investigation of urine glucose and protein.....	34
5.2.12 Phagocytosis rate of peritoneal macrophages.....	34
5.2.13 Apoptosis in cultured splenocytes.....	34
5.2.14 Detection of cytokines.....	35
5.2.14.1 ELISPOT assays.....	35
5.2.14.2 ELISA.....	35
5.2.15 Electrophysiology.....	35
5.2.16 Behavioral Testing.....	36
5.2.16.1 Rotarod.....	36
5.2.16.2 Sensitivity to mechanical stimuli.....	36
5.2.16.3 Sensitivity to thermal stimuli.....	36
5.2.16.4 Gait studies	37
5.2.17 Statistical analysis.....	37
6. Results.....	38
6.1 Role of immune cells in the CNS.....	38
6.1.1 Granzyme B is involved in the tissue damage of PLPtg mice.....	38
6.1.2 CD8+ T- lymphocytes in the CNS express PD-1.....	41
6.1.3 Numbers of CNS immune cells are significantly elevated in PLPtg/ PD-1-/- double mutants.....	42
6.1.3.1 Elevation of lymphocytes in PLPtg/PD-1-/- mice compared to PLPtg mice.....	43
6.1.3.2 No elevation of macrophages in PLPtg/PD-1-/- mice compared to PLPtg mice.....	43
6.1.4 Numbers of immune cells are significantly elevated in PLPtg PD-1-/- transplanted bone marrow chimeras (BMCs)	45
6.1.5 PD-1 deficiency leads to an increase of granzyme B+ T- lymphocytes and pre-apoptotic profiles in oligodendropathy- induced neuroinflammation.....	47

6.1.6 Pathological features are enhanced in PLPtg/PD-1 ^{-/-} double mutated mice.....	48
6.1.7 T- cell CDR3 spectratyping analysis: robust clonal expansions in the CNS of PD-1 ^{-/-} and PLPtg/PD-1 ^{-/-} mice.....	51
6.1.8 Urinary protein and glucose are not elevated in the absence of PD-1	53
6.1.9 Peripheral immune parameters do not differ between mutant mouse strains.....	53
6.1.9.1 Immune cell subsets.....	54
6.1.9.2 Phagocytic activity of macrophages.....	54
6.1.9.3 Stimulation induced apoptosis.....	55
6.1.9.4 Cytokine levels.....	56
6.1.10 CNS T- cells are prone to IFN- γ secretion in the absence of PD-1	56
6.1.11 PD-1 deficiency does not induce overt motor disturbances in PLPtg mice.....	57
6.2 Role of PD-1 in the PNS.....	58
6.2.1 CD8 ⁺ T- lymphocytes, but not macrophages, are significantly elevated in PD-1 deficient P0 ^{+/-} bone marrow chimeras (BMCs)	59
6.2.2 Pathological features are enhanced in P0 ^{+/-} /RAG-1 ^{-/-} BMC PD-1 ^{-/-}	61
6.2.3 Electrophysiological investigations reveal features indicative of increased axonopathy and myelin damage in P0 ^{+/-} /RAG-1 ^{-/-} BMC PD-1 ^{-/-} mice.....	64
6.2.4 Altered gait test and reduced sensitivity in behavioural testing in P0 ^{+/-} /RAG-1 ^{-/-} BMC PD-1 ^{-/-} mice.....	66
6.2.4.1 Rotarod.....	66
6.2.4.2 Gait test.....	67
6.2.4.3 Thermal sensitivity.....	67
6.2.4.4 Mechanical sensitivity.....	68
6.2.5 Isolated PNS derived T- cells show features indicative of activated effector cells, but do not show evidence of clonal expansions...	69
6.2.6 PNS derived T- cells are prone to IFN- γ secretion in P0 ^{+/-} mice....	70
7. Discussion.....	72
7.1 Presence and influence of inflammation in neurological diseases.....	72

7.2 Myelinopathies and corresponding animal models.....	73
7.3 Role of immune cells in peripheral and central myelinopathies.....	74
7.3.1 Granzyme B is pathogenetically relevant PLPtg mice.....	75
7.3.2 Immune modulation by the coinhibitory molecule PD-1.....	76
7.3.2.1 Increased number of immune cells in the CNS in the absence of PD-1.....	77
7.3.2.2 Increased number of immune cells in the PNS in the absence of PD-1.....	78
7.3.2.3 Worsened myelin damage in PD-1 deficient CNS myelin mutants.....	79
7.3.2.4 Worsened myelin damage in PD-1 deficient PNS myelin mutants.....	79
7.3.2.5 Deteriorated electrophysiology, motor and sensory abilities in PD-1 deficient P0+/- mutants.....	80
7.3.2.6 Absence of PD-1 favours clonal expansion	81
7.3.2.7 Increased IFN- γ production in the absence of PD-1.....	82
7.4 Synopsis.....	83
8. Literature.....	86
9. Acknowledgements.....	106
10. Appendices.....	107
10.1 Appendix 1: Reagents and consumables.....	107
10.1.1 Reagents.....	107
10.1.2 Consumables.....	108
10.2 Appendix 2: Equipment.....	110
10.3 Appendix 3: Media, buffers and solutions.....	111
10.3.1 Cell culture media.....	111
10.3.2 Buffers and solutions.....	111
10.4 Appendix 4: List of antibodies.....	113
10.4.1 Primary antibodies.....	113
10.4.2 Secondary antibodies.....	114
11. Abbreviations.....	115
12. Curriculum vitae.....	117
13. List of publications.....	119
13.1 Publications in peer-reviewed international journals.....	119
13.2 Reviews.....	122

13.3 Oral presentations.....	122
13.4 Posters.....	123

1. Abstract

Myelin mutations in the central and peripheral nervous system lead to severely disabling, currently untreatable diseases. In this study, we used transgenic PLP overexpressing mice (PLPtg) as a model for central inherited myelinopathies, such as leukodystrophies, and heterozygously P0 deficient (P0+/-) mice as models for peripheral hereditary polyneuropathies. Both models are characterized by low grade nervous tissue inflammation. Macrophages and CD8+ T- lymphocytes contribute to the myelin pathology as shown by crossbreeding experiments with immunodeficient mice.

Having shown the relevance of CD8+ T- lymphocytes in PLPtg mice, we investigated the influence of one major cytotoxic molecule (granzyme B) on neural damage. By generation of granzyme B deficient PLPtg bone marrow chimeras, we could demonstrate a reduction of myelin pathology and oligodendrocyte death. Taken together, granzyme B is at least partly responsible for the cytotoxicity induced neural damage in PLPtg mice.

To further explore the role of immune modulation, we focussed on the influence of the coinhibitory molecule PD-1, a CD28-related receptor expressed on activated T- and B- lymphocytes.

By investigating myelin mutants of the CNS and PNS (PLPtg and P0+/-) with an additional PD-1 deficiency, induced by crossbreeding or bone marrow chimerization, we found a significant increase of CD8+ T- lymphocytes and massive increase of the myelin pathology in both the CNS and PNS model.

In PLPtg mice, absence of PD-1 increased oligodendrocyte apoptosis, clonal expansions and a higher propensity of CNS but not peripheral CD8+ T- cells to secrete proinflammatory cytokines. In P0+/- mice, absence of PD-1 lead to moderate motor and sensory disturbances, confirming the important role of PD-1 in immune homeostasis.

Taken together, we identified granzyme B as an important effector agent of cytotoxic T- lymphocytes in PLPtg mice and PD-1 as a crucial player in regulating the effector cells in our models of central and peripheral myelinopathy. Alterations of this regulatory pathway lead to overt neuroinflammation of high pathogenetic impact. These results might help to understand mechanisms responsible for high clinical variability of polygenic or even monogenic disorders of the nervous system.

2. Zusammenfassung

Myelinmutationen des zentralen und peripheren Nervensystems verursachen erheblich behindernde und bislang nicht heilbare Erkrankungen. In dieser Arbeit verwendeten wir transgene PLP überexprimierende Mäuse (PLPtg) als Modell für zentrale Myelinopathien und heterozygot P0 defiziente (P0+/-) Mäuse als Modell für hereditäre Neuropathien des peripheren Nervensystems. Beide Modelle zeigen eine niedriggradige Inflammation des Nervengewebes. Durch Verpaarung mit immundefizienten Mausstämmen konnten wir die Relevanz von Makrophagen und T- Lymphozyten in der Entstehung der Myelinpathologie zeigen. Nachdem wir beweisen konnten, dass CD8+ T- Lymphozyten maßgeblich zur Pathologie in PLPtg Mäusen beitragen untersuchten wir den Einfluss eines wichtigen zytotoxischen Moleküls, Granzym B, auf den neuralen Schaden. Durch Generierung von Granzym B defizienten PLPtg Knochenmarkschimären konnten wir eine deutliche Reduktion des glialen Schadens und der Oligodendrozytenapoptose nachweisen. Granzym B ist also zumindest teilweise verantwortlich für die Schädigung, die durch T- Lymphozyten hervorgerufen wird.

Um die zusätzliche Informationen über die Rolle der Immunmodulation in unseren Modellen zu gewinnen, untersuchten wir das koinhibitorische Molekül PD-1, einen CD-28 verwandten Rezeptor, der auf B- und T- Lymphozyten exprimiert wird.

Bei der Untersuchung von Myelinmutanten des ZNS und PNS (PLPtg und P0+/-), die zusätzlich PD-1 defizient waren, konnten wir einen signifikanten Anstieg von CD8+ T- Lymphozyten und eine deutliche Verschlechterung des glialen Schadens beobachten. In PLPtg Mäusen induzierte die Abwesenheit von PD-1 verstärkte Oligodendrozytenapoptose und klonale Expansion. Außerdem neigen ZNS- Lymphozyten aber nicht periphere CD8+ T- Zellen zur verstärkten Sekretion von proinflammatorischen Zytokinen. In P0+/- Mäusen führt Abwesenheit von PD-1 zu moderaten motorischen und sensorischen Störungen, was die wichtige Rolle von PD-1 in immunologischen Regulationsmechanismen unterstreicht. Zusammenfassend kann man festhalten, daß Granzym B ein wichtiges Effektormolekül zytotoxischer T- Zellen in PLPtg Mäusen ist. PD-1 spielt eine wichtige Rolle in der Regulation von Effektorzellen in unseren Modellen für zentrale und periphere Myelinopathien. Veränderungen dieser Regulation können deutliche Neuroinflammation mit starker Myelinpathologie hervorrufen. Diese Ergebnisse können dazu beitragen, die starke klinische Variabilität von polygenen und sogar monogenen neurologischen Erkrankungen zu erklären.

3. Introduction

3.1 Nerve conduction

The nervous system bilaterally transduces messages between the periphery of an organism and the central nervous system. To allow a fast and reliable delivery, a complex tissue structure is required. Glial cells provide structural and trophic support of axons and are essential for rapid nerve conduction. Action potentials in non-myelinated axons are dependent on the axon caliber and range from 1 m/s up to 18 m/s in squid giant axons with a caliber of 1 mm (Rosenthal et al., 2000). Saltatory conduction of action potentials in myelinated axons is less space consuming: It can be as fast as 150 m/s in a 15 μm axon.

To allow saltatory propagation of action potentials, axons with a caliber $> 1 \mu\text{m}$ are covered with myelin sheaths which reach extensions of up to 1.5 mm and are called internodes (Kandel et al., 2000). Axons are myelinated by consecutive Schwann cells in the peripheral nervous system (PNS), where Schwann cells myelinate only one axon, or oligodendrocytes in the central nervous system (CNS), which are able to myelinate more than one axon each.

3.2 Nodes of Ranvier

The unmyelinated parts of the axons are called nodes of Ranvier. In these regions the insulation is missing, so an ion exchange can take part to maintain the action potential. Nodes of Ranvier consist of nodal, paranodal and juxtaparanodal regions (Poliak et al., 2003).

Voltage gated Na^+ channels, which are essential for depolarisation and thereby generation of the action potential, are located within the nodal region of the axolemma. The nodal concentration of Na^+ channels is mediated by the cytoskeletal proteins ankyrin-G and spectrin. Ankyrin G was shown to interact not only with the Na^+ channels and the cytoplasmic domains of neurofascin 186 and Nr-CAM (NCAM related cell adhesion molecule), but also with spectrin, thereby providing a link between the spectrin cytoskeleton and the other components. Neurofascin and Nr-CAM might interact with other cell adhesion molecules located on the microvilli of the Schwann cells (Arroyo et al., 2000).

The paranodal region is characterized by uncompacted myelin. Typical examples of this are periaxonal collars, paranodal loops, which contain Schwann cell cytoplasm, and Schmidt-Lanterman incisures. Ultrastructural analyses show septate junctions between the paranodal axolemma and the paranodal loops, where they serve as diffusion barriers for small molecules and ions. These domains consist of the marker molecule of this area, a complex built by contactin and the contactin-associated protein (Caspr-1), which interacts with Neurofascin 155 from the Schwann cell membrane. The juxtaparanodal region consists of voltage gated K^+ channels and Caspr-2. K^+ most likely serves to buffer cations which are set free during neuronal activity (Arroyo et al., 2000).

3.3 Composition of myelin and role of myelin related proteins

Myelin consists of lipids, glycolipids and a defined set of myelin proteins. Important myelin proteins of uncompact myelin are E-cadherin, which is present in adherens junctions and links different myelin layers (Scherer, 1997) and the gap junction protein Connexin 32 (Cx32). Cx32 is mainly found in uncompact myelin domains, paranodal loops and Schmidt-Lanterman incisures (Martini, 1997; Scherer et al., 1995) where it might form gap junctions between myelin leaflets, thereby enabling a direct diffusion pathway which would shorten the diffusion distance as much as 1000 fold (Scherer et al., 1995).

A myelin protein present in non compact parts of both peripheral and central myelin is myelin associated glycoprotein (MAG) which is expressed on periaxonal Schwann cell and oligodendrocyte membranes (Quarles, 2007), but also in membranes of Schmidt-Lanterman incisures and the inner and outer mesaxon (Trapp et al., 1982). Furthermore, it could be detected in PNS and most CNS paranodes. The 100 kDa protein is composed of five immunoglobulin like domains, one transmembrane domain and two isoforms of a cytoplasmic domain. MAG is involved in axon glia interactions and mediates differentiation, maintenance and survival of both oligodendrocytes and myelinated axons. *In vitro*, MAG was shown to increase expression and phosphorylation of neurofilament subunits, suggesting a role in a signalling pathway that directly affects the axon (Quarles, 2007). Importantly, MAG is also one of the white matter inhibitors of axonal regeneration like Nogo, and oligodendrocyte-myelin glycoprotein (OMgp), which all interact with the Nogo receptor (Filbin, 2006).

With 0.05 %, myelin oligodendrocyte glycoprotein (MOG) is a minor component of the CNS myelin. The highly conserved 28 kDa protein is located on outer lamellae of myelin sheaths (Brunner et al., 1989). The *MOG* gene maps to the MHC region (6p21.3-p22) in rodents and humans (Pham-Dinh et al., 1995). MOG has strong immunogenic property and reactions towards MOG induce demyelinating disease (Johns et al., 1999). It is a member of the immunoglobulin superfamily and it might have functions as an adhesion molecule or a stabilizer of oligodendrocyte microtubules (Lazzarini et al., 2004).

Proteolipidprotein (PLP) is the most abundant myelin protein of the CNS. Together with MBP it makes up 90 % of the CNS myelin. The *p/p* gene is localized on the X chromosome and consists of 7 exons with a transcriptional unit over 17kB (Griffiths et al., 1998a). PLP is a strongly hydrophobic protein with four transmembrane domains and a molecular weight of 30 kDa. The amino acid sequences of human and murine PLP share 100% identity with minor differences in the coding sequence. PLP is identical to the splice variant DM-20, from which it might have developed, except for 105 nucleotides, coding for 35 amino acids within the cytoplasmic loop (Griffiths et al., 1998a). The internal splice donor site for DM-20 is located in exon 3 (Nave et al., 1987). In the CNS, DM-20 is expressed during development (Dickinson et al., 1996; Fanarraga et al., 1996) but is later only a minor component compared to PLP.

Interestingly, DM-20 is also expressed in Schwann cells, where it is mainly found in paranodal loops and Schmidt-Lanterman incisures (Griffiths et al., 1998a; Griffiths et al., 1995a).

Myelin basic protein (MBP) is frequently present in compact myelin of both PNS and CNS. The *mbp* gene can be mapped to chromosome 18 (Roach et al., 1985). Different isoforms have been described for human and murine MBP. Human MBP appears at 17.2, 18.5, 20.2 and 21.5 kDa (Kamholz et al., 1986; Roth et al., 1987), while murine MBP is 14.2, 17.2, 18.5 or 21.5 kDa large (Barbarese et al., 1977; Barbarese et al., 1983). Additional isoforms have been described on mRNA level. The main function of MBP is maintenance of the myelin sheaths structure (Lazzarini et al., 2004).

Compact myelin, as present in the internode, is formed by wrapping of Schwann cell processes around the axon. During this process, cytoplasm is squeezed out leading to a very compact and dense myelin structure which is stabilized by different myelin proteins (Kettenmann and Ransom, 2005). A typical protein of the compact myelin is myelin protein zero (MPZ or P0), the most abundant myelin protein in the PNS, where it is exclusively expressed (Greenfield et al., 1973). Approximately 50 % of myelin expressed by Schwann cells is composed of P0 (Greenfield et al., 1973) which is essential for normal myelin function and structure (Giese et al., 1992). P0 is a highly conserved member of the immunoglobulin superfamily (Lai et al., 1987) which is made up of one extracellular domain, one transmembrane domain and a cytoplasmic domain (Lemke et al., 1988; Shy, 2006).

The extracellular domain forms homotetramers which interact with tetramers from the opposing myelin membrane to form the intraperiod line (Filbin et al., 1993; Shapiro et al., 1996). The basic intracellular domain is involved in mediating adhesion properties and might interact with phospholipids of the neighbouring Schwann cell membrane leaflet forming the major dense line (D'Urso et al., 1990; Martini, 1997; Shy, 2006). Both P0 and myelin basic protein (MBP) are involved in the formation of the major dense line. In P0 / MBP doubly deficient mice, the major dense line is absent while the lack of either one of these proteins results in a normal intracellular compaction (Martini et al., 1995a). The importance of an intact intracellular domain of P0 is demonstrated by the dominant negative loss of adhesion *in vitro* when this domain is truncated (Xu et al., 2001; Shy, 2006).

Another important protein of the compact peripheral myelin is peripheral myelin protein (PMP) 22. It is composed of four transmembrane domains and plays an important role in growth and differentiation of Schwann cells. Furthermore, PMP22 forms complexes with P0 (D'Urso et al., 1998; Muller, 2000) and is closely linked with $\beta 4$ integrin levels (Amici et al., 2007). Nevertheless, the exact role of PMP22 remains to be clarified.

3.4 Human hereditary myelinopathies

Hereditary diseases of the CNS which affect the white matter and induce its progressive degeneration are frequently storage disorders. Members of this group of so called leukodystrophies are, among others, metachromatic leukodystrophy, X-linked adrenoleukodystrophy, Krabbe disease and Pelizaeus Merzbacher disease (PMD).

Metachromatic leukodystrophy is a lysosomal storage disorder where a defective desulfation of lipids leads to accumulation of sulfatide (galactosylceramide 3-sulfate) in some cell types, mainly in the white matter but also in the kidneys. The most frequently affected gene is *ASA*, encoding the enzyme arylsulfatase A. In rare cases, the disease can alternatively be caused by saposin B deficiency. Metachromatic leukodystrophy appears as infantile, juvenile and adult form with clinical symptoms varying by age. Children usually show ataxia and spasticity which later progresses to a decerebrate state. Adults mostly present with behavioural disturbances and dementia (Eichler et al., 2007).

X-linked adrenoleukodystrophy (X-ALD) is a disorder with a disturbed ability to degrade very long chain fatty acids which results in accumulation and pathology in the adrenal cortex and CNS myelin. The responsible gene, *ABCD1*, is located on the X-chromosome (Xq28) and codes for a peroxisomal membrane protein which is a member of the adenosine triphosphate binding cassette (ABC) transporter superfamily (Moser et al., 2004). A large variety of mutations in the *ABCD1* gene has been described, to date without a clear association between the kind of mutation and disease severity. X-ALD manifests in two distinct categories, the adrenomyeloneuropathy and the cerebral forms (Moser, 1997). While the former is a non-inflammatory axonopathy which affects spinal cord and also peripheral nerves, the latter is a highly inflammatory disease which results in a progressive myelinopathy mainly of the occipital regions (Moser et al., 2004). As in metachromatic leukodystrophy, different ages of disease onset have been described. Patients displaying the childhood form develop dementia and progressive neurological disturbances leading to death. Other patients develop the first symptoms in early adulthood and suffer from a slowly progressing paraparesis. A subgroup of these patients develops a fatal rapidly progressive demyelination (Eichler et al., 2007; van Geel et al., 2001). Due to the localization on the X-chromosome, usually hemizygous male persons are affected. Approximately 15 % of the heterozygous female carriers are symptomatic but show the milder manifestation (adrenomyeloneuropathy) while only very few of them present with inflammatory brain disease (Moser et al., 1991).

Krabbe disease, also called globoid cell leukodystrophy, is an autosomal recessive disorder which could be mapped to chromosome 14q25-31. It is caused by the absence or dysfunction of the lysosomal enzyme galactocerebrosidase (GALC). GALC is responsible for the hydrolysis of galactolipids (Wenger et al., 2000). In the absence of this enzyme,

galactosylceramide accumulates and forms the so called “globoid cells” which are microglial cells and macrophages which contain PAS (Period acid – Schiff) positive material. Hallmarks of this disease are demyelination and gliosis of the CNS, but also segmental demyelination, endoneurial fibrosis, proliferation of fibroblasts and macrophage infiltration (Moser, 2006). The infantile form of Krabbe disease shows an early onset before six months of age with arrest of development, spasticity and temperature elevation, later leading to a decerebrate condition and death before the age of two. In a smaller percentage of the cases, later onset with blindness or progressive neuropathy has been described (Wenger et al., 1997).

Another leukodystrophy is caused by a CNS myelin mutation. The dysmyelinating Pelizaeus Merzbacher disease (PMD), which was mapped to Xq22, a locus encoding the myelin proteins PLP and DM20 as spliced isoforms. PMD patients suffer from early childhood onset motor disabilities, loss of myelin sheaths in the CNS and additional neurological symptoms like nystagmus, choreotactic movements, ataxia and pyramidal tract signs. Typically, motor abilities ameliorate slightly, reaching a plateau at 10-20 years followed by deterioration and signs of cortical atrophy. In a very severely affected subgroup, patients show extended psychomotor impairment and frequently die during the first decade of life. The most frequent mutation is a complete duplication of PLP (Sistermans et al., 1998; Mimault et al., 1999; Regis et al., 2008), other mutations cause 10- 25 % of cases. Further mutations include missense mutations, which cause more severe phenotypes, deletions and splice site mutations, which result in milder phenotypes. The most severe outcome is detected in patients with single amino acid exchanges within highly conserved regions (Cailloux et al., 2000). Missense mutations might have toxic effect, possibly due to accumulation of protein in the endoplasmatic reticulum (Scherer, 1997). *In vitro*, severe mutations detain PLP from reaching the cell surface (Gow et al., 1996).

PLP mutations have also been related with X-linked spastic paraplegia 2, which is defined by gait difficulties, sometimes accompanied by nystagmus, ataxia and mental retardation. The diseases vary in the motor development, being almost normal in SPG2 patients in contrast to PMD.

Not only in the CNS but also in the peripheral nervous system, many disorders, namely peripheral neuropathies, can disturb the normal function. Besides multiple external causes like diabetes or influence of toxic substances, myelin mutations can evoke neuropathies. These hereditary peripheral neuropathies are subdivided into characteristic groups of hereditary motor and sensory neuropathies (HMSN) and also exclusively motor or sensory subforms, e.g. the hereditary sensory and autonomic neuropathy (HSAN).

HMSN I corresponds to Charcot-Marie-Tooth (CMT) disease type 1 and 4, while HMSN II is used synonymously for CMT type 2. CMT was first described in 1886 by Jean Martin

Charcot, Pierre Marie and Howard Tooth. HMSN III includes, among others, the Dejerine-Sottas Syndrome (DSS).

The demyelinating, autosomal dominant HMSN I is the most frequent subform (1:2500; Suter et al., 1995) of hereditary polyneuropathies. Demyelinating diseases can be regarded as myelin degenerative diseases, while dysmyelination represents developmental disturbances. HMSN I characterized by a disease onset between five and 20 years of age. Patients suffer from slowly progressive, symmetric, distally pronounced muscle weakness, muscle atrophy, typical steppage gait and foot deformities. Sensory deficits are also present but less pronounced. The histopathology is characterized by segmental de- and remyelination, secondary axonal degeneration and supernumerary Schwann cells, also termed onion bulb formations (Suter et al., 2003).

Onion bulb formations are different layers of Schwann cells with their processes which express molecules typical for immature Schwann cells (Guenard et al., 1996) which might be indicative for a compensatory remyelination. CMT1 can be diagnosed electrophysiologically by a reduction of nerve conduction velocity (< 38 m/s; Harding et al., 1980).

In the last years, many gene loci and gene mutations responsible for CMT1 were identified: CMT1A could be linked to chromosome 17q11.2 (Vance et al., 1989) and is most frequently caused by a 1.5 megabase duplication (Lupski et al., 1991; Raeymaekers et al., 1991) which also contains the *pmp22* gene (Suter et al., 1995; Timmerman et al., 1992). Approximately 70-80 % of CMT1 patients carry this duplication (Huxley et al., 1996). Alternatively, CMT1A can be evoked by a variety of point mutations. Of special interest are mutations which can also be detected in the murine *pmp22* gene where they cause the TremblerJ phenotype, which will be explained when discussing animal models for hereditary neuropathies (Martini, 1997). Other mutations induce additional symptoms like deafness e.g. a mutation in the second exon of *pmp22*, leading to an alanine to proline substitution in the second transmembrane domain of PMP22 (Kovach et al., 1999).

Interestingly, a deletion of the chromosome 17p11.2-p12 is linked with the autosomal dominant hereditary neuropathy with liability to develop pressure palsies (HNPP; Chance et al., 1993). Clinically, HNPP patients develop recurrent pareses after application of pressure or minor trauma. This neuropathy is histopathologically characterized by focal hypermyelination with the formation of myelin tomacula and demyelination and can also be linked to frameshift null mutations in *pmp22* (Nicholson et al., 1994; Young et al., 1997; Martini, 1997).

CMT1B is also transmitted autosomal dominantly but is caused by different mutations. It was first linked to the duffy blood group locus at 1q22-23 (Bird et al., 1982), before the mutated gene could be identified as P0 (Hayasaka et al., 1993b; Hayasaka et al., 1993c; Hayasaka et

al., 1993d). To date, more than 120 mutations are described within P0 (Shy, 2006), as summarized at <http://www.molgen.ua.ac.be/CMTMutations/>.

Another gene responsible for a subform of CMT, CMTX, was mapped to Xq13.1 (Gal et al., 1985) and identified as the gap junction protein Connexin 32 (Cx32; Bergoffen et al., 1993; Suter et al., 1995; Scherer, 1997). To date, more than 300 mutations within this gene have been detected (<http://www.molgen.ua.ac.be/CMTMutations/>). Some mutations lead to a functional disruption of the gap junctions, resulting in a blockade of the diffusion pathway (Martini, 1997). Mutations described in Cx32 are mainly loss of function and not dominant negative mutations and mostly cause a rather homogenous phenotype.

CMT4 is a group of autosomal recessive disorders. Clinically, it resembles CMT1 but shows an earlier onset and more severe disease course. Causative mutations include, among others, mutations in ganglioside-induced differentiation-associated protein-1 (GDAP1; Baxter et al., 2002) and the SET binding factor 2 (SBF2), which might be involved in phosphoinositide-mediated signalling (Senderek et al., 2003). Further affected proteins are myotubularin related protein (MTMR2; Bolino et al., 2000) and the early growth response gene (EGR2), also known as Krox20 (Warner et al., 1998), which is a regulator of cellular proliferation, the latter being also described to be mutated in CMT1 families (Werner et al., 1998). The crucial role of the zinc finger protein Krox20 is demonstrated by a complete block in Schwann cell differentiation in deficient mice (Topilko et al., 1994).

HMSN II or CMT2, in contrast, is designated by mainly axonal damage. Electrophysiology reveals normal to only slightly reduced nerve conduction velocity. Clinically, CMT2 is represented by distal muscle weakness accompanied by frequent ulcerations and infections of the feet. CMT2 is usually transmitted autosomal dominant. Mutations related to CMT2 include the microtubule kinesin family gene (*Kif1B β* ; Zuchner et al., 2004) which apparently results in reduced mitochondrial transport and thereby axonal depletion of energy. Other mutations alter the regulation of vesicular transport as with RAB7, a member of the Rab family of Ras- related GTP-ases (Verhoeven et al., 2003) or affect NF-L, the Neurofilament light gene (Mersiyanova et al., 2000) and different heat shock proteins (Tang et al., 2005; Evgrafov et al., 2004).

Interestingly, also different point mutations in P0 are described to cause CMT2 (Marrosu et al., 1998; De Jonghe et al., 1999), but patients with one of those mutations can not be clearly attributed to CMT1 or CMT2 due to nerve conduction velocities (De Jonghe et al., 1999).

HMSN III, also known as Dejerine- Sottas syndrome (DSS), is a very severe hereditary polyneuropathy. Its characteristics are onset of disease in the first decade of life, delayed motor development and motor and sensory disturbances. Nerve conduction velocities are usually below 10 m/s and the histopathology shows dysmyelination within the peripheral

nerves (Suter et al., 2003). DSS can be either caused by dominant mutations, e.g. in P0, PMP22, Cx32 or by recessive mutations in MTMR2 and Periaxin (Suter et al., 2003).

Interestingly, CMT patients display a large interindividual variability of disease severity between no or hardly any neurological symptoms to wheel chair bound (Birouk et al., 1997). This is even noticed in patients with identical mutations like identical twins (Garcia et al., 1995) and most likely due to other modifying factors like other genetic or environmental factors (Meyer zu Horste et al., 2006).

3.5 Animal models for hereditary myelinopathies

Several animal models exist and are useful tools to investigate hereditary myelinopathies.

For the most abundant myelin protein in the CNS, PLP, there are several models for different mutations, like *Jimpy* mice, which have a point mutation in the X- chromosomal *plp* gene resulting in defective splicing. The resulting protein has only three transmembrane domains and thereby not only loses its normal function but also, most likely, develops a dominant negative effect. In these mice, more than 90 % of oligodendrocytes are lost due to cell death (Skoff, 1995). The mutation *Jimpy*^{msd} is characterized by a point mutation resulting in an amino acid substitution of alanine to valine. Both genotypes suffer from ataxia and tremor beginning at the age of 2 weeks and tonic seizures which eventually kill the mice around 4 weeks of age. The CNS of these animals is nearly devoid of myelin because of massive oligodendrocyte apoptosis (Cerghet et al., 2001). The *rumpshaker* mutation, which is also a PLP missense mutation, results in a far milder phenotype with better myelination and a normal lifespan (Griffiths et al., 1990; Griffiths et al., 1995b; Werner et al., 1998). This mutation was described in a patient with X-linked spastic paraplegia (Werner et al., 1998). The severe phenotypes described above most likely result from “toxicity” caused by the mutation and not from the absence of PLP. The phenotype of *jimpy* mice could not be rescued by transgenic expression of wildtype PLP in these mice, underlining the probability of a dominant negative effect (Schneider et al., 1995). Furthermore, PLP deficient mice, which are hemizygous males or homozygous females, show an overall healthy phenotype, normal fertility and lifespan.

Functional tests revealed reduced activity on the rotarod and in the open field test and a reduced nerve conduction velocity in the optic nerve. Histopathologically, the mice show poor compaction of myelin with lack of intraperiod line (Boison et al., 1994; Klugmann et al., 1997) and, in higher ages, signs of neurodegenerative disease with axonal swellings and Wallerian degeneration. These axonal swellings are also a sign of impaired axonal transport, where mitochondria, membranous dense bodies and neurofilament accumulated mainly at the distal paranode (Griffiths et al., 1998b).

To investigate the influence of PLP gene dosage on myelination, PLP overexpressing mice were produced (Readhead et al., 1994; Kagawa et al., 1994). PLP overexpression results in arrested maturation of oligodendrocytes depending on the extent of overexpression and oligodendrocyte cell death (Anderson et al., 1998). Homozygous overexpression of PLP leads to lethal dysmyelination. Heterozygosity results in a less severe phenotype with demyelination only at higher ages (Readhead et al., 1994). Similarly, mice expressing 70 copies of human DM-20 develop demyelination accompanied by inflammation (Johnson et al., 1995; Mastronardi et al., 1993; Werner et al., 1998). These findings underline the usefulness of these mice as models for Pelizaeus Merzbacher and related diseases.

Mouse models have also been established for other leukodystrophies. Arylsulfatase A deficient mice show storage of sphingolipid cerebroside-3-sulfate in neuronal and non-neuronal tissues which was reminiscent to metachromatic leukodystrophy, but no white matter abnormalities occurred (Hess et al., 1996). In spite of a more recent study describing moderate behavioral alterations (Stroobants et al., 2008), this mouse model does not convincingly reflect the human disease.

Similarly, mice with inactivated *ABCD1* gene were generated as a model for X-linked adrenoleukodystrophy (Lu et al., 1997). In young and adult mice, no CNS phenotype was detectable. Only very old mice (15- 20 months) showed behavioral abnormalities and myelin pathology in the spinal cord and sciatic nerve, but not in the brain (Pujol et al., 2002), thereby being a suitable model for adrenomyeloneuropathy, the milder form of the disease.

The mouse model for galactosylceramidase deficiency (Krabbe disease), the twitcher mouse, is a naturally occurring mutant which displays very similar clinical and biochemical features as the patients (Duchen et al., 1980). The symptoms begin approximately at the age of three weeks and include “twitching”, weight loss and pareses. Bone marrow transplantation in twitcher mice resulted in a longer lifespan but only minimal, if any, neuropathological improvement (Wenger et al., 2000; Yeager et al., 1984).

Strictly spoken, the mouse mutants introduced next, the MBP deficient shiverer mouse and the MAG deficient mouse, can not be denoted as a model because the respective mutations have not been described in humans. Nevertheless, the mice provide interesting information about the role of MBP and MAG.

Shiverer mice lack MBP due to a naturally occurring null allele (Werner et al., 1998). It is an autosomal recessive mutation of the *mbp* gene on chromosome 18 (Jacobs, 2005). Homozygous mice are characterized by severe hypomyelination. The remaining myelin wraps are uncompacted and do not contain a major dense line (Rosenbluth, 1980). Heterozygous shiverer mice appear healthy, which is in contrast to patients with a heterozygous deletion of MBP: In a rare disorder, the 18q syndrome, patients lack one allele of the *mbp* gene, among other genes, due to a deletion of parts of chromosome 18. Those

patients show a broad variety of symptoms, including mental retardation and hypomyelination of the CNS (Werner et al., 1998; Gay et al., 1997).

In shiverer mice, the phenotype can be partly corrected by the expression of a wildtype MBP transgene (Readhead et al., 1987). Interestingly, the PNS is largely unaffected by the lack of MBP (Kaplan et al., 1997; Privat et al., 1979), where P0 most likely compensates for its absence. The only abnormality in the PNS of shiverer mice is a strong increase the frequency of Schmidt-Lanterman incisures and a slight reduction of the axon diameter (Gould et al., 1995).

Another example in which compensation might play an important role is MAG deficiency, which does not result in striking abnormalities and is also no model which is based on a human disease. At the ultrastructural level, redundant myelin loops and periaxonal collars are detectable (Montag et al., 1994; Li et al., 1994). Nevertheless, at higher ages, these mice display a mild peripheral neuropathy with onion bulb formations, tomacula and degenerating axons (Fruttiger et al., 1995; Guenard et al., 1996; Martini et al., 1997).

But also for disease relevant PNS myelin protein mutations, a large variety of animal models has been established. PMP22 as a frequently affected protein in CMT has been studied intensively: PMP22 deficient mice (Adlkofer et al., 1995) display hypermyelination, delayed myelination and formation of myelin tomacula which disappear at higher age by degeneration, together with degeneration and myelin loss. The role of PMP22 can therefore be defined as regulation of myelin thickness and initiation of myelin formation. Less affected heterozygously deficient mice are a useful model of HNPP for the case that one allele is preserved (Adlkofer et al., 1997; Martini, 1997; Martini et al., 1997). Some pathological features, but not all, present in the mouse model resemble the histopathology found in HNPP patients (Martini, 1997).

As most cases of CMT1A are due to a PMP22 duplication, resulting in three copies of the gene, PMP22 overexpressing rats were produced (Sereda et al., 1996). Clinical signs are muscle atrophy and reduced nerve conduction velocity, but also de- and remyelination and onion bulb formations as described in CMT1A patients (Gabreels-Festen et al., 1992; Thomas et al., 1996). Interestingly, mainly motor axons are affected in this and other animal models (Adlkofer et al., 1995; Adlkofer et al., 1997; Carenini et al., 1997; Martini et al., 1995b), which is in contrast to severely affected human sural nerve biopsies, the sural nerve being a sensory nerve (Martini, 1997). PMP22 transgenic mice with 16-30 extra copies of PMP22 display lack of myelin formation and a severe affection (Magyar et al., 1996), while transgenic mice with 8 additional copies are less severely affected (Huxley et al., 1996)- similar to patients carrying 4 copies of PMP22, a duplication on both chromosomes (De Jonghe et al., 1997; Martini, 1997).

PMP22 point mutations are represented in mice carrying spontaneous mutations: Trembler mice share a mutation with CMT1A patients (Suter et al., 1992a), while Trembler mice carry the same mutation that was detected in DSS patients (Suter et al., 1992b; Ionasescu et al., 1997; Martini, 1997). Interestingly, the mutations resulted in similar histological findings in humans and mice (Martini, 1997).

Mice with P0 mutations serve as models of CMT1B. Disruption of P0 (Giese et al., 1992) leads to severe hypomyelination and significantly reduced nerve conduction velocities (Zielasek et al., 1996). The peripheral nerves show different abnormal features, like axon Schwann cell units which are devoid of myelin, incomplete compaction or widened intraperiod spaces (Martini et al., 1995b; Martini, 1997). In older mice, the number of myelinating Schwann cells is reduced and onion bulb formations as well as macrophages laden with myelin debris appear (Martini et al., 1995b; Giese et al., 1992), indicating a role of P0 in myelination and maintenance of myelin integrity (Martini, 1997). In contrast to P0^{-/-} mice, patients with comparable histopathological features are all heterozygous carriers of the mutant gene (Hayasaka et al., 1993a; Hayasaka et al., 1993b; Hayasaka et al., 1993d; Martini, 1997). Mice heterozygously deficient for P0 (P0^{+/-}) show signs of myelin degeneration, onion bulb formation and remyelination earliest at 4 months of age with only a mild alteration of electrophysiology (Martini et al., 1995b). The differences between the situation in human disease and the mouse model can be explained by a dominant negative effect in CMT patients differing from a mere reduction of dose (Martini, 1997). Nevertheless, patients have been described with a mild CMT1B phenotype due to a heterozygous loss of function mutation in P0 (comparable to the situation in P0^{+/-} mice) whose children were homozygous carriers of the mutation and more severely affected (DSS phenotype; Warner et al., 1996), thereby confirming the importance of P0^{+/-} and P0^{-/-} mice as models for CMT1B and DSS (Martini, 1997). Interestingly, a severe chronic idiopathic demyelinating polyneuropathy (CIDP) – like demyelination was described in the same P0^{+/-} mouse model (Shy et al., 1997). This can serve as an example how epigenetic and environmental factors can influence the phenotype of mice with identical mutations when kept under different conditions. There are further CMT1B mouse models with point mutations within the P0 gene, representing a dominant negative effect with altered ultrastructure, de- or dysmyelination and reduced nerve conduction velocities (Runker et al., 2004; Wrabetz et al., 2006).

P0 mutations result in completely different forms of appearance. While the heterozygous loss of P0 induces a loss of function characterized by myelin decompaction and degeneration, other point mutations cause a dominant negative gain of function. This is impressively shown in the Ile106Leu substitution (P0_{sub}) mouse where the missense mutation leads to hypermyelination, frequent presence of onion bulb formations and tomacula as well as functional impairment (Runker et al., 2004).

Absence of Cx32 does not interfere with myelin formation but leads to a progressive demyelination of motor branches of the PNS (Nelles et al., 1996). Cx32^{-/-} mice are characterized by a high number of onion bulb formations, thinly myelinated axons and thick periaxonal collars (Anzini et al., 1997) which are also frequently found in CMTX patients. Furthermore, mice show axonal loss, if less frequent as found in patient biopsies.

3.6 Role of immune cells in myelin mutants

In PLP transgenic mice, immune related cells increase in the CNS during aging. In this mouse model, a constant low grade immune activation takes place, defined by an increase of CD11b⁺ macrophages / microglial cells in several parts of the CNS (optic nerve, corpus callosum, cerebellum and spinal cord) over the lifespan of the mice with a peak at 12 months, which is significantly elevated compared to wildtype mice (Ip et al., 2006a). Likewise, the number of CD8⁺ T- cells in the CNS also increases, while CD4⁺ T- cells are scarce and B-lymphocytes are never detectable. In higher ages, these mice display demyelination and axonal loss.

By cross breeding with recombination activation gene 1 (RAG-1) deficient mice, which lack mature B- and T- lymphocytes, the pathogenetic relevance of T- cells was verified: In the absence of lymphocytes, the demyelination is significantly ameliorated. By bone marrow chimerization experiments and investigation of the ventricular size by MRI (magnetic resonance imaging), it could be shown that CD8⁺ lymphocytes are the main pathogenic cells in this model. The role of macrophage/ microglia like cells in PLP^{tg} mice was defined by cross breeding PLP^{tg} mice with Sialoadhesin (Siglec-1, Sn) deficient mice, which lack a cell surface adhesion molecule which is most likely essential for the activation of T- cells by macrophages. These mice exhibit a reduction of CD8⁺ T- cells to the wildtype level with normal numbers of CD11b⁺ cells and an ameliorated pathology (Ip et al., 2007). Despite having shown the relevant pathogenic influence of immune cells in induction of myelin damage in different models of hereditary myelinopathies, the exact mechanisms of immune cell activation and regulation are not completely clear.

The involvement of the immune system in myelinopathies is not an isolated murine phenomenon. Warshawsky and colleagues reported a case of a woman carrying a PLP mutation, who developed a late onset primary progressive multiple sclerosis (MS), while her son, as a hemizygous carrier of the mutant allele, suffered from Pelizaeus Merzbacher disease (Warshawsky et al., 2005). Similarly, a ten year old boy with steroid responsive MS like relapses was diagnosed with an exonal mutation in the PLP gene (Gorman et al., 2007). Immune related cells also influence the disease course in other leukodystrophy models. As the X-ALD mouse is a suitable model for the non-inflammatory adrenomyeloneuropathy, influence of inflammation is also not reported for this mouse model. Nevertheless, the human

cerebral form of X-ALD is characterized by strong inflammation with CD8+ T- lymphocytes as the most prominent cell population (Ito et al., 2001).

In the mouse model for Krabbe disease, the twitcher mouse, a marked increase of microglial cells was detected (Ohno et al., 1993). Importantly, the absence of MHC-II led to reduced inflammation, but also to reduced demyelination and functional amelioration (Matsushima et al., 1994). Bone marrow transplantation ameliorates the disease course of twitcher mutants (Yeager et al., 1984). In general, hematopoietic stem cells invade the CNS and mostly differentiate as microglial cells (Simard et al., 2004; Ip et al., 2008). In twitcher mice, stem cells predominantly invade the most demyelinated parts of the CNS but might be endangered by the increased production of TNF- α by twitcher microglia (Pellegatta et al., 2006).

Compared to the CNS myelin mutants, a very similar age dependent increase of immune related cells could be detected in the PNS of mice carrying mutations in the peripheral myelin proteins, in P0^{-/-} or P0^{+/-}, Cx32^{-/-} and PMP22 transgenic mice. P0^{+/-} mice, as a model for CMT1B, show an age dependent increase of both F4/80⁺ macrophages and CD8⁺ T-lymphocytes compared to wildtype mice in the quadriceps nerve, the mainly motor part of the femoral nerve. Interestingly, CD4⁺ lymphocytes are scarce and B- lymphocytes have not been detected (Schmid et al., 2000). Comparable results are found in Cx32^{-/-} mice, the model for CMTX (Kobsar et al., 2002). The phenotype in both mouse models can be significantly ameliorated by cross breeding with RAG-1 deficient mice, paralleling the findings in the CNS myelinopathy (Schmid et al., 2000; Kobsar et al., 2003). The confirmation that immune cells are indeed pathogenetically relevant is provided by the reversion of the RAG-1^{-/-} rescue effect after reconstitution with wildtype bone marrow (Maurer et al., 2001). P0^{+/-} mice have been also crossbred with MCSF^{-/-} (op/op) macrophage mutants, leading also to an ameliorated phenotype and thereby proving the pathogenetic influence of macrophages in this model (Carenini et al., 2001). Similarly, when crossbreeding P0^{+/-} mice with Sialoadhesin deficient mice, the animals show a reduced number of macrophages and lymphocytes in the peripheral nerve, together with an ameliorated phenotype (Kobsar et al., 2006).

P0^{-/-} mice as a model of the severe DSS disease also show an increase of CD8⁺ T-lymphocytes and macrophages in the peripheral nervous tissue. While T- cells accumulate with age, the macrophage number is most pronounced at the age of three months and later declines. Interestingly and in contrast to other myelin mutants investigated, the immune system has a protective role in P0^{-/-} mice. In RAG-1 deficient double mutants, the macrophage number does not decline after three months and there is no rescue of the myelination status, in contrary, P0^{-/-}/RAG-1^{-/-} mice suffer from a more pronounced loss of axons in the plantar nerve (Berghoff et al., 2005).

PMP22tg mice also show an increase of macrophages in the peripheral nervous tissue with no difference between motor and sensory nerves (Kobsar et al., 2005). The influence of immune cells in these mice is currently under investigation.

Not only in PMD but also in CMT patients, an influence of immune cells has been described: A subgroup of CMT1 patients was reported to respond to anti-inflammatory treatment. Their nerve biopsies show inflammatory infiltrates and edema and they frequently suffer from progression with relation to infections, paresthesia and pain (Martini et al., 2004). In CNS myelin mutations, immune cells are described to play a role in the disease.

As immune cells clearly contribute to development and extend of hereditary myelinopathies, it becomes increasingly important to regard the immune system as an important modulator of these diseases. One of the most demanding issues still is to find out the reasons for the high interindividual variability between patients and which factors are involved in the modulation of the disease. Regarding the data concerning inflammation in myelin mutants, modulatory factors within the immune system might play an important role.

3.7 Activation and modulation of the adaptive immune system

For the activation of naïve T- cells, several signals are required. A specific signal derived by presentation of an antigen to the specific T- cell receptor (TCR) in context of a major histocompatibility complex (MHC) molecule. The presentation is performed by an antigen presenting cell (APC). The second signal is a costimulatory signal. The best described molecules of this group are CD28, which is expressed on T- lymphocytes and its ligands CD80 (B7-1) and CD86 (B7-2) on antigen presenting cells. Ligation in presence of the first signal induces activation and proliferation of T- cells as well as interleukin (IL) - 2 production (Linsley et al., 1991; Gimmi et al., 1991; Zang et al., 2007). The third signal required is the secretion of cytokines and chemokines. Costimulatory and coinhibitory molecules are frequently members of the B7/ CD28 family, like CTLA-4, which shares the ligands with CD28 but, in contrast to CD28, is upregulated during the effector phase and strongly inhibits and thereby terminates the immune response.

Other inhibitory members of this family are programmed death-1 (PD-1, CD279) with its ligands PD-L1 (B7-H1, CD274) and PD-L2 (B7-DC, CD273). PD-1 received its name because it was first isolated from apoptotic T- cell hybridoma (Ishida et al., 1992). It is a 55 kDa transmembrane protein and a member of the Ig superfamily (Agata et al., 1996). In humans, the *pdcd1* gene is located on chromosome 2q37.3 (Shinohara et al., 1994). PD-1 is expressed on a small proportion of thymocytes, T- and B- lymphocytes and on myeloid cells. In the resting state, it is hardly detectable but is strongly induced upon stimulation (Agata et al., 1996; Nishimura et al., 1996). In its cytoplasmic domain, PD-1 contains an immunoreceptor tyrosine based inhibitory motif (ITIM) which is involved in negative

regulation of signalling and an immunoreceptor tyrosine switch motif (ITSM). Both motifs interact with SHP-2 (Sheppard et al., 2004; Okazaki et al., 2001) resulting in an attenuation of CD3 ξ chain and ZAP70 phosphorylation (Sheppard et al., 2004). The inhibitory action of PD-1 is transmitted by direct inhibition of early activation events that are mediated by CD28 induced activation of PI3K (Parry et al., 2005; Greenwald et al., 2005) or indirectly through IL-2 (Keir et al., 2008), when PD-1 induced reduction of IL-2 results in a dramatically reduced cell proliferation (Carter et al., 2002).

The ligands of PD-1 are differentially expressed. B7-H1 is expressed on CD4+CD25+ cells, on antigen presenting cells and on a broad variety of tissues, indicating a role in regulation of immune responses in the peripheral tissues. B7-DC, in contrast, is only expressed on macrophages and dendritic cells (Greenwald et al., 2005).

PD-1 deficient mice show a mild splenomegaly and an increased number of B- cells and myeloid cells, thus proving the role of PD-1 in inhibition of proliferation, differentiation and class switching in B-cells (Nishimura et al., 1998). Interestingly, PD-1 deficiency (Nishimura et al., 1998) induces a diversity of autoimmune diseases depending on the genetic background, like lupus like nephritis and arthritis in BL/6 mice (Nishimura et al., 1999) or cardiomyopathy in BALB/c mice (Nishimura et al., 2001b). A polymorphisms in the human PD-1 (PD-1.3) is associated with susceptibility to systemic lupus erythematosus (SLE; Prokunina et al., 2002), type I diabetes (Nielsen et al., 2003) and rheumatoid arthritis (Lin et al., 2004). We could recently show that this polymorphism is associated with a progressive disease course of multiple sclerosis (MS; Kroner et al., 2005).

Taken together, PD-1 plays a crucial role in modulation of lymphocyte responses and in the induction and maintenance of tolerance and is therefore an interesting target to investigate as an immune modulator in our myelin mutants.

4. Aim of the study

Earlier studies identified CD8+ cells as culprit cells in proteolipidprotein (PLP) overexpressing mice, so it was an important question which cytotoxic molecules are involved in the pathology of PLPtg mice. For this, we investigated the influence of granzyme B on myelin damage and oligodendrocyte apoptosis.

Furthermore, we were interested in the modulation of T- cell responses in myelin mutants of the CNS and PNS and therefore focussed on the influence of the coinhibitory molecule PD-1 in PLPtg and P0+/- mice. We sought to investigate immune cells in the target tissue, their contribution to the myelin damage and the general characteristics of immune responses and subsets in the investigated mice.

5. Materials and methods

5.1 Reagents, chemicals, media, buffers, equipment

Reagents and consumables (Appendix 1), equipment (Appendix 2), media, buffers and solutions (Appendix 3) as well as antibodies (Appendix 4) are listed in detail in the appendices.

5.2 Methods

5.2.1 DNA Purification

Genomic DNA was purified from tail biopsies using the DNeasy blood & tissue kit (Qiagen, Hilden, Germany) according to the manufacturer's instructions.

5.2.2 PCR (Polymerase chain reaction)

Amplification of DNA fragments was performed by PCR. For this method, specific oligomers or "primers" are designed which bind to defined regions of the genomic DNA with antiparallel orientation. Addition of Taq polymerase (a thermostable DNA polymerase) combined with dNTPs (nucleotide components of DNA) induces polymerisation of complementary DNA strands. To achieve large amounts of the amplicon, this process is repeated for several times. For this, DNA double strands are first separated by melting (94°C), then the temperature is reduced to values suitable for binding of the primers ("annealing temperature", usually between 50°C and 60°C). A completion of the new complementary strands is best performed at 72°C for approximately 1 min per 1kB. Usually, this cycle is repeated for 35-40 times.

5.2.3 Animals and determination of Genotypes

All investigated mice were bred on a C57/ B6 background for more than 10 generations.

All mouse strains used in this study were kept under barrier conditions at the department of neurology, University of Wuerzburg. Animal experiments were approved by the local authorities (Regierung von Unterfranken).

The following mouse strains were used in this study:

5.2.3.1 PLP transgenic mice

PLP transgenic mice (Readhead et al., 1994) were bred and genotyped as described previously (Ip et al., 2006a) In short, presence of the transgene was displayed by PCR amplification with the primer set 5'-CAGGTGTTGAGTCTGATCTACACAAG-3' and 5'-GCATAATACGACTCACTATAGGGATC-3'. The PCR was performed following a standard protocol with an annealing temperature of 55°C and an elongation time of 45 seconds at 72°C.

5.2.3.2 P0+/- mice

Genotypes of P0-mutants were determined by conventional PCR using the oligonucleotides 5'-TCAGTTCCTTGTCCCCGCTCTC-3', 5'-GGCTGCAGGGTCGCTCGGTGTTTC-3' and 5'-ACTTGTCTCTTCTGGGTAATCAA-3' leading to a 334bp product for the P0 null allele and 500 bp for the wildtype allele, respectively (Schmid et al., 2000).

5.2.3.3 RAG-1-/- mice

The recombinaase activating gene-1 (RAG-1) deficiency was confirmed either by flow cytometric analysis of tail vein blood with CD4- and CD8- specific antibodies as previously described (Schmid et al., 2000; Kobsar et al., 2003; Ip et al., 2006a) or PCR as provided by Jackson Lab (www.jax.org) using the primers 5' TGGATGTGGAATGTGTGCGAG 3', 5' GAGGTTCCGCTACGACTCTG 3' and 5' CCGGACAAGTTTTTCATCGT 3' with an annealing temperature of 58°C and an elongation time of 45 seconds at 72°C. On an agarose gel, the wildtype band could be detected at 474bp and the knockout band was located at 530bp.

5.2.3.4 Granzyme B-/- mice

Granzyme B deficient mice were obtained from Charles River Laboratories and genotyped according to the companies PCR recommendations (www.jax.org). Briefly, PCR was performed with the primers 5'TGAAGATCCTCCTGCTACTGC3' and 5'TCCTGAGAAAGACCTCTGCC 3' (to detect the wildtype allele) and the primer pair 5'CTTGGGTGGAGAGGCTATTC 3' and 5'AGGTGAGATGACAGGAGATC 3' for the null allele. Amplification was performed with an annealing temperature of 65°C and an elongation time of 1 minute at 72°C. On an agarose gel, the wildtype band could be detected at 130bp and the knockout band was located at 280bp.

5.2.3.5 PD-1-/- mice

Absence of PD-1 in PD-1-/- mice (Nishimura et al., 1998) was also confirmed by PCR genotyping. For this, the wildtype allele was amplified using the primer pair 5' CCGCCTTCTGTAATGGTTTG 3' and 5' TGTTGAGCAGAAGACAGCTAGG 3' with an annealing temperature of 54°C and an elongation time of 45 seconds. Additionally, the Neo Cassette inside the knockout allele was detected using the primer pair 5' GCCCGGTTCTTTTTGTCAA GACCGA 3' and 5' ATCCTCGCCGTCGGGCATGCGCGCC 3' with an annealing temperature of 60°C and an elongation time of 45 seconds. PCR products were visualized on an agarose gel with the wildtype allele at 690bp and the knockout allele at 400bp. Agarose gels were always prepared with 1% agarose in TBE Buffer.

5.2.3.6 Double mutants

Double mutants (PLPtg/RAG-1^{-/-}, P0^{+/-}/RAG-1^{-/-} and PLPtg/PD-1^{-/-}) were obtained by cross breeding either PLPtg or P0^{+/-} mice with RAG-1^{-/-} mice or PD-1^{-/-} mice respectively. The offsprings in the F1 generation were tested for the presence of the PLP transgene or the heterozygous absence of P0, all being heterozygously deficient for RAG-1 or PD-1. Offsprings from the first generation (F1) were crossbred with RAG-1^{-/-} or PD-1^{-/-} mice which resulted in P0^{+/-}/RAG-1^{-/-}, PLPtg/RAG-1^{-/-} or PD-1^{-/-} mice (among other genotypes) in the F2 generation. To receive a higher number of the desired genotypes, PLPtg/RAG-1^{-/-} or PLPtg/PD-1^{-/-} mice could be crossbred with either RAG-1^{-/-} or PD-1^{-/-} mice in the following generations. Genotyping was performed the same way as in single mutants.

5.2.4 Bone marrow chimerization

Granzyme B^{-/-} or wildtype bone marrow was transplanted at the age of 6-8 weeks into PLPtg/RAG-1^{-/-} mice. Experiments including these mice were performed in collaboration with Chi Wang Ip. Likewise, PD-1^{-/-} or wildtype bone marrow was transplanted into either PLPtg/RAG-1^{-/-} or P0^{+/-}/RAG-1^{-/-} recipients with PLPwt/RAG-1^{-/-} as controls, or into PLPtg mice with PLPwt mice as controls, which were irradiated with 5 Gy. Transplantation was performed as described before (Maurer et al., 2001; Ip et al., 2006a). Briefly, bone marrow from donor mice was isolated by flushing out femoral bone marrow with sterile PBS, washed and filtered through a mesh with 70 µm pore size to remove debris. Afterwards, cells were resuspended in 500 µl PBS and approximately 2×10^7 cells were injected intravenously into recipient mice. Successful transplantation was confirmed by flow cytometry for CD4 and CD8 as described for definition of the RAG-1^{-/-} status. Animals were kept under frequent controls until the age of 10 months and then transcardially perfused, followed by tissue preparation as described below.

5.2.5 Purification of mononuclear cells

5.2.5.1 Splenocytes

Splenocytes were extracted by passing the tissue through a 70 µm cell strainer (BD Biosciences Pharmingen, San Jose, CA, USA) with a plunger and washed with PBS. Erythrocyte lysis was performed for 5 minutes at room temperature with a lysis buffer. Cells were then washed once and processed as indicated for the respective experiments.

5.2.5.2 CNS lymphocytes

Mice were killed with CO₂ and transcardially perfused with cold 0.1 M PBS. The brains were prepared and spinal cords flushed out with PBS by hydrostatic pressure. CNS tissue was homogenized and cells were isolated from the interface of a 30 to 50% Percoll gradient as

described above. Mononuclear cells were washed, counted and used for subsequent experiments.

5.2.5.3 PNS immune cells

Mice were killed with CO₂ and transcardially perfused with cold 0.1 M PBS. Sciatic, plantar and femoral nerves were prepared as well as ventral roots.

PNS tissue was homogenized and cells were isolated from the interface of a 30 to 50% Percoll gradient. Mononuclear cells were washed, counted and used for subsequent experiments.

5.2.6 Flow cytometry

Flow cytometry allows surface and intracellular detection of marker molecules in living cells. For flow cytometry, splenocytes and CNS or PNS lymphocytes were stained with the following directly labelled antibodies for 30 min at 4 °C in FACS buffer: CD4-PerCP, CD8-FITC, CD8-PE, B220-PE, CD11b-PerCP, CD62L-APC, CD44-FITC, CD69-FITC and PD-1-PE. Afterwards, cells were washed once, diluted in the desired volume and measured by flow cytometry. Specific staining was assessed by application of isotype control antibodies. Analysis was performed using CellQuestPro software.

5.2.7 Tissue preparation and immunohistochemistry

For F4/80, T- lymphocyte (CD4 or CD8) and MBP staining, the animals were perfused with 0.1 M phosphate buffered saline (PBS) only and the tissue was snap frozen immediately after dissection. For identification of CD11b+ macrophage-like cells, mice were transcardially perfused with 4% paraformaldehyde in 0.1 M cacodylate buffer. Tissue was dissected, postfixed in the same fixative for 2 hours and cryoprotected in 30 % sucrose overnight.

For investigation of the PNS, femoral, sciatic and plantar nerves were obtained, for investigation of the CNS spinal cord and optic nerve were used. After snap freezing in O.C.T. matrix, 10 µm thick transverse sections of respective tissues were cut. Immunohistochemical stainings were performed as described before (Carenini et al., 2001; Ip et al., 2006a; Ip et al., 2007).

For MBP staining cross sections of the optic nerve at the region of 1200-1400 µm caudal to the retinal pigment epithelium were used. Sections were frozen in liquid nitrogen and thawed again.

For cleaved caspase-3 staining (pre-apoptotic cells), sections from PBS rinsed mice were preincubated with 4 % paraformaldehyde while sections from 4 % paraformaldehyde perfused mice were fixed with acetone. Unspecific binding was blocked for 30 min in 5 % BSA/PBS and then incubated with the primary antibodies, diluted in 1 % normal bovine

serum, containing 2 % DMSO (caspase-3, PFA perfused) or 0.3 % Triton-X (caspase-3, PBS perfused) overnight at 4°C.

Activated macrophage-like cells in the CNS were detected with rat- anti mouse CD11b (Serotec, Oxford, UK) or rat- anti mouse CD169 (anti- Sialoadhesin, Serotec, Oxford, UK); in the PNS macrophages were detected using rat- anti mouse F4/80 antibody. Rat- anti mouse CD4 (Serotec, Oxford, UK) and rat- anti mouse CD8 (Chemicon, Temecula, CA, USA) antibodies were used for the identification of T- lymphocytes, MBP staining was performed with rabbit- anti mouse MBP (MBL, Woburn, MA, USA), cleaved caspase-3 expression was detected with a rabbit- anti human cleaved caspase-3 antibody (5A1, Cell Signaling, Danvers, MA, USA), which cross reacts with murine tissue.

After washing three times with PBS, detection of primary antibodies was achieved by using a biotinylated secondary antibody to rat immunoglobulins (Igs), for macrophage-like cells or T- cells, or to rabbit Igs for MBP and cleaved caspase-3 for 1 hour.

Colorimetric stainings were finalised with StreptABComplex kit (Dako, Hamburg, Germany) which contains horseradish peroxidase. Substrate visualization was performed using Diaminobenzidine (DAB; 1mg / ml) substituted with 0.02 % H₂O₂. DAB stainings were mounted with Aquatex (Merck, Darmstadt, Germany) whereas fluorescence stainings were mounted with DABCO and kept dark at -20°C. The specificity was controlled by omission of the primary antibodies.

5.2.8 Assessment of demyelination and axonal damage

5.2.8.1 Analysis of semithin sections

For the investigation of semithin or ultrathin sections, optic nerves, femoral and sciatic nerves and spinal roots were used. These tissues were processed for light microscopy of semithin sections as recently reported for the CNS and the PNS (Carenini et al., 2001; Ip et al., 2006a). Mice were transcardially perfused with 4% paraformaldehyde and 2% glutaraldehyde in 0.1 M cacodylate buffer. The tissue was postfixed in the same fixative overnight, followed by osmification with 2 % osmiumtetroxide in 0.1 M cacodylate buffer for two hours, dehydration in acetone and embedding in Spurr's medium. 0.5 µm thick semithin sections were cut for light microscopic analysis, and stained with alkaline methylene blue. Tissue damage was assessed by quantification of axonopathic vacuoles > 6 µm in optic nerve cross sections. In peripheral nerves, nerve damage was assessed by ranking nerves with regard of myelin loss.

5.2.8.2 Electron microscopy

Ultrathin sections (100 nm) were contrasted with lead citrate and analysed using a ProScan Slow Scan CCD camera mounted to a Leo 906 E electron microscope (Zeiss) and

corresponding software iTEM (Soft Imaging System). All sections were analysed by the investigator being not aware of the genotype.

5.2.8.3 Analysis of myelin status by MBP- immunohistochemistry

Myelin damage in optic nerve cross sections was assessed and rated as described before (Ip et al., 2007) by a blinded semi quantitative approach of MBP distribution. Score 1 depicts homogeneous MBP distribution, score 5 massive myelin loss.

5.2.9 Quantification of immune cells and apoptotic oligodendrocytes

Longitudinal sections of the optic nerve of non diseased wildtype, PD-1^{-/-}, PLPtg and PLPtg/PD-1^{-/-} mice at the age of 2, 6 and 12 months were examined. Optic nerves of bone marrow chimeras were investigated at the age of 10 months. Quantification was performed as described before (Ip et al., 2006a). Briefly, quantification of CD11b⁺ and Siglec-1⁺ cells was performed in the rostral region, covering the rostral 800 - 1500 μm of the optic nerve using a light microscope (Olympus BH2, Olympus, Hamburg, Germany) with a final magnification of 600x using the ocular grid (0.0256 mm^2). The cell number of macrophage-like cells was calculated per mm^2 . Caspase-3 positive profiles were quantified in the rostral part of the optic nerve and calculated per mm^2 . Only profiles which were morphologically consistent with oligodendrocytes were counted. In addition, CD4⁺ and CD8⁺ T- cells were quantified in longitudinal sections of the complete optic nerve using a Zeiss Axiophot2 microscope at a final magnification of 300x. The area was measured using digital images acquired via a CCD- camera and ImagePro 4.0 software. Cell density was calculated per mm^2 .

In the peripheral nerve, quantification of F4/80⁺ macrophages and CD4⁺ or CD8⁺ T- lymphocytes was performed as described before (Carenini et al., 2001; Fischer et al., 2008b) on cross sections of the femoral nerve, regarding both quadriceps and saphenous branch. In general, quantification was performed by investigators being blinded regarding the genotype of the investigated animals.

5.2.10 CDR3 Spectratyping

The CDR3 spectratyping with the corresponding primers was performed as described previously (Pannetier et al., 1995) on cells derived from CNS or PNS lymphocyte preparations and spleens. Briefly, 500 ng of leukocyte mRNA were transcribed into cDNA and then used in PCRs with a C β specific reverse primer and 24 V β specific forward primers. The PCR steps were as follows: 94°C, 1min; 94°C, 1m in 10s; 60°C, 1min; 72°C, 4 min (40 steps); 72°C, 10min. Each V β -C β PCR product was labelled during PCRs, using 13 fluorescence-labelled reverse primers (12 J β , 1 C β). The PCR steps were: 94°C, 2min, 60°C,

1min, 72°C, 15min (5 steps). The labelled PCR products (V β -J β , V β -C β) were analysed on an ABI Prism 3130 capillary sequencer (Applied Biosystems) to determine their length and distribution, using a module for fragment-analysis. As an internal length standard, 500-ROX (Applied Biosystems) was used in every sample. This part of the study was performed in collaboration with Nicholas Schwab.

5.2.11 Investigation of urine glucose and protein

To exclude lupus like effects and nephritis which were described to occur occasionally in aged PD-1^{-/-} mice, urine samples were investigated for protein and glucose by using CombiScreen® urine tests (Biocon Diagnostik, Voehl-Marienhagen, Germany).

5.2.12 Phagocytosis rate of peritoneal macrophages

Mice were killed by CO₂, peritoneal macrophages were obtained by injection of 5 ml of ice cold PBS into the peritoneal cavity and the fluid containing peritoneal macrophages was extracted. The peritoneal fluid was centrifuged, cells were counted and taken into culture (Medium: RPMI with 10 % FCS , 1 % Penicillin and Streptomycin, 1 % Glutamate (all from Gibco, Invitrogen, Karlsruhe, Germany)) in a concentration of 1x 10⁶ cells/ml and incubated for 24 hours at 37°C in a humidified atmosphere with 5 % CO₂/ 95 % air.

For examination of phagocytosis rate, fluorescent polystyrene latex beads (Fluoresbrite® YG Microspheres 2.00 μ m, Polysciences Inc., Warrington, PA, USA) were first incubated with 1% BSA for 30 minutes, then medium was added and the mixture was added to macrophages in a tenfold concentration and incubated for 30 minutes in the dark.

Afterwards, cells were washed five times with ice cold PBS, then detached using EDTA Trypsin (Gibco, Invitrogen, Karlsruhe, Germany) for five minutes. Cells were washed once more in FACS buffer (0.1 M PBS containing 0.1% BSA and 0.1 % Sodiumazide) and analysed by flow cytometry. Positive labelling was visualized in the F1 channel, ingestion of more than one fluorescent bead resulted in proportional increase of fluorescence intensity.

In all flow cytometry experiments, cells were measured and analyzed using a FACSCalibur (BD Biosciences Pharmingen, San Jose, CA USA) with CellQuest software and FlowJo7 software (Tree Star Inc., Ashland, OR, USA).

5.2.13 Apoptosis in cultured splenocytes

3 x 10⁶ Splenocytes were cultured in splenocyte complete medium (10 mM HEPES, 25 μ g/ml Gentamicin, 50 μ M Mercaptoethanol, 5 % FCS, 2 mM Glutamine, 1 % NEAA, all from Sigma, Schnelldorf, Germany) with maximal stimulation (Concanavalin A (ConA) 5 μ g/ml (Sigma, Schnelldorf, Germany)) or 3 x 10⁶ CD3/CD28 microspheres (Dynal, Karlsruhe, Germany) for 48 hours. Afterwards, cells were washed in the permeabilization buffer (1 mM HEPES, 150

mM NaCl, 5 mM KCl, 1 mM MgCl₂, 0.18 mM CaCl₂, all from Sigma, Schnelldorf, Germany) and stained with FITC labelled Annexin V (Roche, Mannheim, Germany) and 50 µg/ml Propidium Iodide (Calbiochem, Merck, Nottingham, UK). Analysis was performed by flow cytometry.

5.2.14 Detection of cytokines

5.2.14.1 ELISPOT assays

IFN- γ production in CNS, PNS and splenic lymphocytes was investigated as follows:

CNS or PNS lymphocytes or splenocytes were incubated for 24 hours in provided 96-well-plates, unstimulated or stimulated with either phorbol myristate acetate (PMA; 20 ng/ml) / ionomycin (500ng/ml, both Sigma, Munich, Germany), and in case of CNS lymphocytes, four mixed class I PLP peptides (VCGSNLLSI, AATYNFAVL, ATYNFAVL, NYQDYEYL), four mixed class I MOG peptides (LIICYNWL, VGLVFLFL, SPGKNATGA, FYWVNPGVL) or one MBP peptide (ADPGNRPHL, all peptides from Genscript Corp, Piscataway, NJ, USA, used at 200 nM; Leder et al., 2007). ELISPOT assays were performed according to the manufacturer's instructions (BD Pharmingen, San Diego, CA, USA). Additionally, Granzyme B expression was analysed in CNS lymphocytes and splenocytes with and without stimulation with PMA / ionomycin as described above, also following the manufacturer's instructions (R & D Systems, Minneapolis, MN, USA). Spots were quantified by CTL Europe (Aalen, Germany) using ImmunoSpot 4.0.17.

5.2.14.2 ELISA

Investigation of cytokine production, namely IFN- γ , IL-2 and IL-10 was performed by ELISA of cell culture supernatants. For this, splenocytes were purified as described above, diluted to a concentration of 1×10^6 /ml and cultured unstimulated or stimulated with ConA (2 µg/ml, Sigma, Schnelldorf, Germany) or the 1×10^6 CD3/CD28 coated microspheres as cells (DynaL, Invitrogen, Karlsruhe, Germany) in splenocyte complete medium. After 48 hours, supernatant was harvested and stored at -20°C until further use. ELISA for IFN- γ , IL-2 or IL-10 (all R&D Systems, Minneapolis, MN, USA) was performed according to the manufacturer's instructions.

5.2.15 Electrophysiology

Sciatic nerve conduction properties from P0+ $+/RAG-1^{-/-}$ and P0+ $^{-/}RAG-1^{-/-}$ mice which were either transplanted with wildtype or PD-1 $^{-/-}$ bone marrow were determined at the age of 10 months by established electrophysiological methods as previously described (Samsam et al., 2003; Zielasek et al., 1996). Briefly, mice were anaesthetized with Hypnorm (diluted 1:1 in Aqua dest.) and electrodes were placed. For motor response, two electrodes were applied

into the foot muscle. For distal stimulation, two electrodes were placed behind the ankle and one more electrode pair was placed at the sciatic notch for proximal stimulation. Distal and proximal stimulation were performed with increasing strength until supramaximal stimulation with maximal motor response. Based on these measurements, latencies (including F-wave latency) and amplitudes could be defined.

This part of the study was performed with Carsten Wessig, who was not aware of the genotype or treatment of the mice.

5.2.16 Behavioral Testing

5.2.16.1 Rotarod

To determine muscle weakness and balance, 10 months old P0+/-/RAG-1-/- wt and PD-1-/- bone marrow chimeras (BMCs) as well as 1 year old wt, PLPtg, PD-1-/- and PLPtg/PD-1-/- mice were tested on the rotarod (Ugo Basile, Comerico, Italy) as described before (Grohmann et al., 2004). For that, mice were placed on an accelerating rotarod for 4 times on two consecutive days. Before testing, mice were allowed to adapt to the movement. Each trial was finished after 5 minutes.

5.2.16.2 Sensitivity to mechanical stimuli

Sensitivity to mechanical impulses was tested by von Frey hair test (Chaplan et al., 1994). Here, the threshold is defined as earliest paw withdrawal response when paws are touched with filaments of defined strength. Briefly, mice were placed on wire mesh in Plexiglas cages without bottom. When all four paws were placed on the wire, the plantar surface of one hind paw was touched with a von Frey monofilament. Hair values were beginning at 0.69 g, where pressure was administered for 5 sec with a slightly bent filament. Withdrawal of the hind paw was defined as threshold, than the next finer von Frey hair was applied. If the animal did not react, the next stronger monofilament was used. The range of von Frey monofilament strength used was 0.07-1.20 g. Each hind paw was tested six times consecutively. The 50% withdrawal threshold (i.e., force of the von Frey hair to which an animal reacts in 50% of the administrations) was recorded as described before (Uceyler et al., 2006).

5.2.16.3 Sensitivity to thermal stimuli

Heat sensitivity was measured by assessment of paw withdrawal latency as described earlier (Hargreaves et al., 1988; Uceyler et al., 2006) by using a standard Ugo Basile Algesiometer (Comerio, Italy). Mice were placed in cages on a glass surface. A heat source was positioned under one hind paw and the time until a withdrawal reaction occurred was measured. To avoid burn damage, the maximal time for heat application was 15 sec. Each hind paw was

tested three times. To avoid adaptation, an interval of 2 min was kept between the measurements.

5.2.16.4 Gait studies

Subtle motor disturbances were investigated by gait studies as described previously (Kunkel-Bagden et al., 1993; Uceyler et al., 2006). For this, the hind paws were painted with ink and the mice animals were allowed to walk through a cardboard tunnel placed over two pieces of paper. Three consecutive footprint pairs were analysed regarding distinct gait parameters like stride width (distance between feet), stride length on the right and left sides, and limb rotation. The average values were calculated for each parameter. To rule out an influence of animal size, mice were weighed before the procedure.

5.2.17 Statistical analysis

The unpaired two-tailed students' t-test was used for comparison of quantified profiles. It may be used for parametric distributions. Scores and percentages were analyzed by using the nonparametric Mann-Whitney-U test and the Kruskal-Wallis test.

6. Results

6.1 Role of immune cells in the CNS

In recent studies, we could show that in PLP overexpressing mice (PLPtg), CD8⁺ T- cells and CD11b⁺ macrophage-like cells accumulate in different parts of the CNS in an age-dependent manner. Differences between wildtype and PLPtg mice were detected in corpus callosum, cerebellum, spinal cord and optic nerve to a similar extent. CD4⁺ cells were only scarcely present while B-cells were never detected within the CNS (Ip et al., 2006a). PLPtg mice were crossbred with lymphocyte deficient RAG-1^{-/-} mice. Myelin damage was assessed by the amount of axonopathic vacuoles inside the optic nerve which reached a certain size (> 6 µm) and was significantly reduced in the absence of lymphocytes, thus proving the pathogenetic impact of these cells (Ip et al., 2006a). Bone marrow reconstitution experiments with CD4^{-/-} or CD8^{-/-} bone marrow revealed that CD8⁺ T- lymphocytes are the major culprit cells in tissue destruction in this myelin mutant (Ip et al., 2006a).

Another relevant molecule in PLPtg mutants is sialoadhesin (Sn; also designated Siglec-1), which is a macrophage restricted molecule playing a role in macrophage T- cell interaction. Interestingly, it is expressed on a high percentage of CD11b⁺ cells in PLPtg mice but only rarely on wildtype macrophage-like cells. In a recent paper we could show that absence of sialoadhesin in PLPtg mice reduced the amount of CD8⁺ T- cells to wildtype level and also significantly reduced the myelin pathology (Ip et al., 2007).

In the present study, we investigated the molecular mechanisms of cytotoxicity in this model and the mechanisms underlying regulation of cytotoxic T- lymphocytes and tissue homeostasis.

6.1.1 Granzyme B is involved in the tissue damage of PLPtg mice

Based on the fact that CD8⁺ but not CD4⁺ T- lymphocytes accumulate in the CNS of PLPtg mice and on experiments showing the major contribution of CD8⁺ cells to the myelin pathology, we started to investigate the effector mechanisms of CD8⁺ lymphocytes in our model. Cytotoxic T- lymphocytes contain modified lysosomes, so called lytic granules, which comprise effector molecules. These molecules, granzymes and perforin, act together in the induction of apoptosis via the induction of caspase-3. The serine protease granzyme B enters the target cell where it contributes to induction of caspases-dependent apoptosis (Bots et al., 2006). The way granzyme B enters the target cell is still a matter of discussion. Perforin is critically involved in this process (Bolitho et al., 2007). It is able to form membrane pores, but if granzyme B is indeed able to enter the target cell through these pores is not entirely clear. Alternatively, these pores might function as ion channels that destabilize the membrane. Internalization of perforin and granzymes could take place during the following

membrane repair process (Keefe et al., 2005). To investigate the contribution of one major cytotoxic factor of CD8+ T- lymphocytes, granzyme B, to the pathogenesis in PLPtransgenic (PLPtg) mice, we transplanted PLPtg/RAG-1^{-/-} mice with either wildtype or granzyme B deficient bone marrow (**Figure 1**).

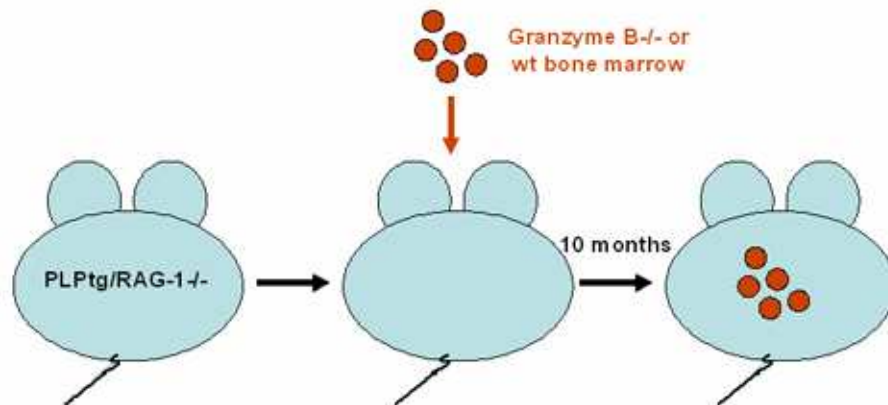


Figure 1: Experimental setup for granzyme B^{-/-} bone marrow transplantation in PLPtg mice

PLPtg mice which lack mature B- or T- lymphocytes (RAG-1^{-/-}) were transplanted with wt or granzyme B^{-/-} bone marrow and investigated 10 months later.

At the age of 12 months, mice were perfused and optic nerve sections were investigated. Determination of neural damage was performed by ranking in a blinded manner by Rudolf Martini and Chi Wang Ip with special attention to vacuolization and demyelination. Vacuoles represent an axonopathic situation with degenerating and shrinking axons and are frequently localized in the close vicinity of macrophage-like cells containing myelin debris. In addition, quantification of axonopathic vacuoles > 6 μm was performed on semithin cross sections through the optic nerve. This method was previously described and is an established method to detect and quantify neural damage in this model, because especially large axonopathic vacuoles seem to reflect the myelin damage (Ip et al., 2006a; Ip et al., 2007; **Figure 2**). Both methods revealed a strong tendency towards a milder phenotype in PLPtg/RAG-1^{-/-} BMC granzyme B^{-/-} compared to wt transplanted mice (data not shown).

After entering the target cell, granzyme B cleaves and thereby activates caspases, especially the main target caspase, caspase-3 (Chowdhury et al., 2008) which then cleaves further caspases, thereby inducing apoptosis (Adrain et al., 2005). Since caspase-3 is a relevant molecule in the granzyme B mediated apoptosis pathway, we quantified the number of pre-apoptotic cleaved caspase-3+ profiles displaying morphological features of oligodendrocytes. Oligodendrocytes are typically organised in rows following the longitudinal extension of the optic nerve.

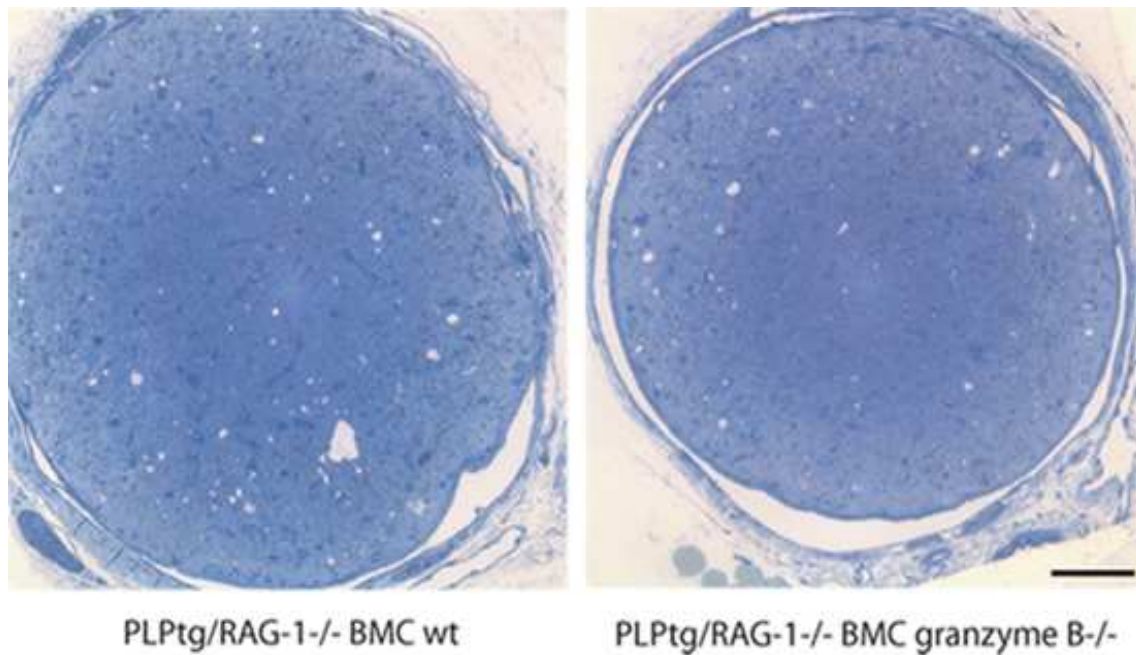


Figure 2: Granzyme B deficiency reduces myelin damage in PLPtg mice

Semithin cross sections through the optic nerve of 12 months old PLPtg/RAG-1-/- BMC wt and granzyme B-/- mice. Note the large amount of axonopathic vacuoles in wt transplanted mice. Scale bar: 50 μ m.

We quantified the amount of pre-apoptotic oligodendrocytes by counting caspases-3+ profiles which were colocalized with the typical oligodendrocyte nuclei in the optic nerve. Interestingly, the highest amount of these profiles was detected in the rostral region of the optic nerve, where also the highest amount of CD11b+ macrophages and the strongest damage are detected. The amount of caspase-3+ oligodendrocytic profiles was significantly reduced in PLPtg/RAG-1-/- BMC granzyme B-/- compared to PLPtg/RAG-1-/- BMC wt (**Figure 3**), indicating that the damage in PLPtg mice is, at least partly, mediated by oligodendrocyte apoptosis mediated by granzyme B.

This is underlined by the fact that PLPwt mice showed hardly any caspase-3+ profiles (not shown). Thus, granzyme B is clearly involved in oligodendrocyte apoptosis and, thereby, in the demyelinating and axonopathic neuropathy of PLPtg mice.

Taken together, damage in PLPtg mice is mediated by CD8+ T- lymphocytes (Ip et al., 2006a). Absence of the cytotoxic molecule granzyme B alleviated the myelin damage and reduced the amount of caspase-3+ oligodendrocyte in our model of CNS demyelination.

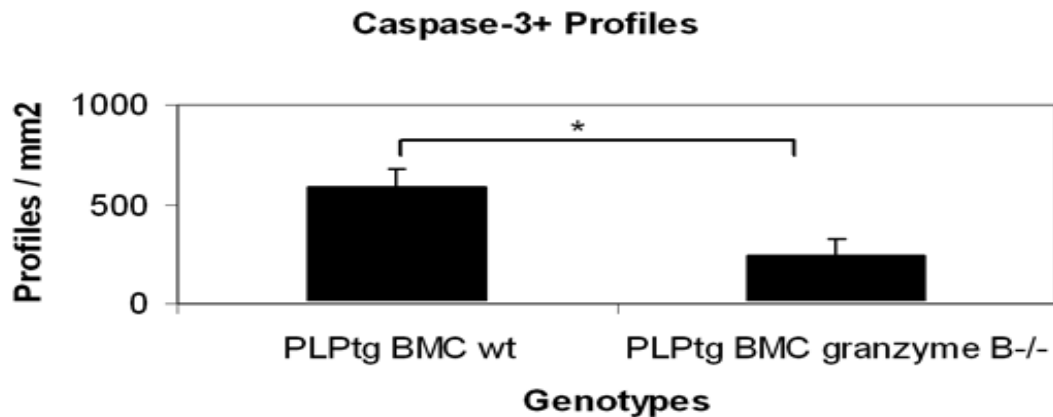


Figure 3: Granzyme B deficiency reduces caspase-3+ oligodendrocytes in PLPtg mice

Quantification of caspase-3+ oligodendrocytes in the rostral part of the optic nerve from 12 months old PLPtg/RAG-1^{-/-} BMC wt and granzyme B^{-/-} mice. * = p-values < 0.05. Error bars represent standard deviations.

6.1.2 CD8+ T- lymphocytes in the CNS express PD-1

To obtain myelin mutants with inactivated PD-1 function, two strategies have been chosen. First, double mutants have been generated in analogy to previous experiments (Ip et al., 2006a; Ip et al., 2007) by crossbreeding the corresponding single mutants. This strategy has the advantage that all cells of the organism lack PD-1. As a complementary and alternative strategy, bone marrow chimeric mutants have been generated using either irradiated or RAG-1-deficient PLPtg mice as recipients and PD-1^{-/-} mice as donors (Ip et al., 2006a; Maurer et al., 2001). The latter strategy has the advantage that unexpected side effects or influences of the systemic PD-1-inactivation (e.g. influences of PD-1 deficiency on thymic maturation or neonatal tolerance) can be circumvented.

To gain further information about regulation of the inflammatory processes in our myelin mutants, we investigated the impact of PD-1, an immune modulatory molecule, on the regulation of cytotoxic CD8+ T- lymphocytes, similar to experiments performed in a model for hereditary myelinopathy in the PNS (P0^{+/-}). To first demonstrate PD-1 expression on CNS T- lymphocytes, we pooled CNS from three mice of each group of wildtype (wt), PLPtg and PD-1 deficient mice (PD-1^{-/-}), isolated the lymphocytes and performed flow cytometry with a staining for CD8 and PD-1. Cells were gated on CD8+ cells, which are the most frequent T- lymphocytes present in the CNS of the mutants (Ip et al., 2006a). In 6 months old mice, wildtype and PLPtg CD8+ lymphocytes expressed PD-1, while it was absent in PD-1^{-/-} (Figure 4).

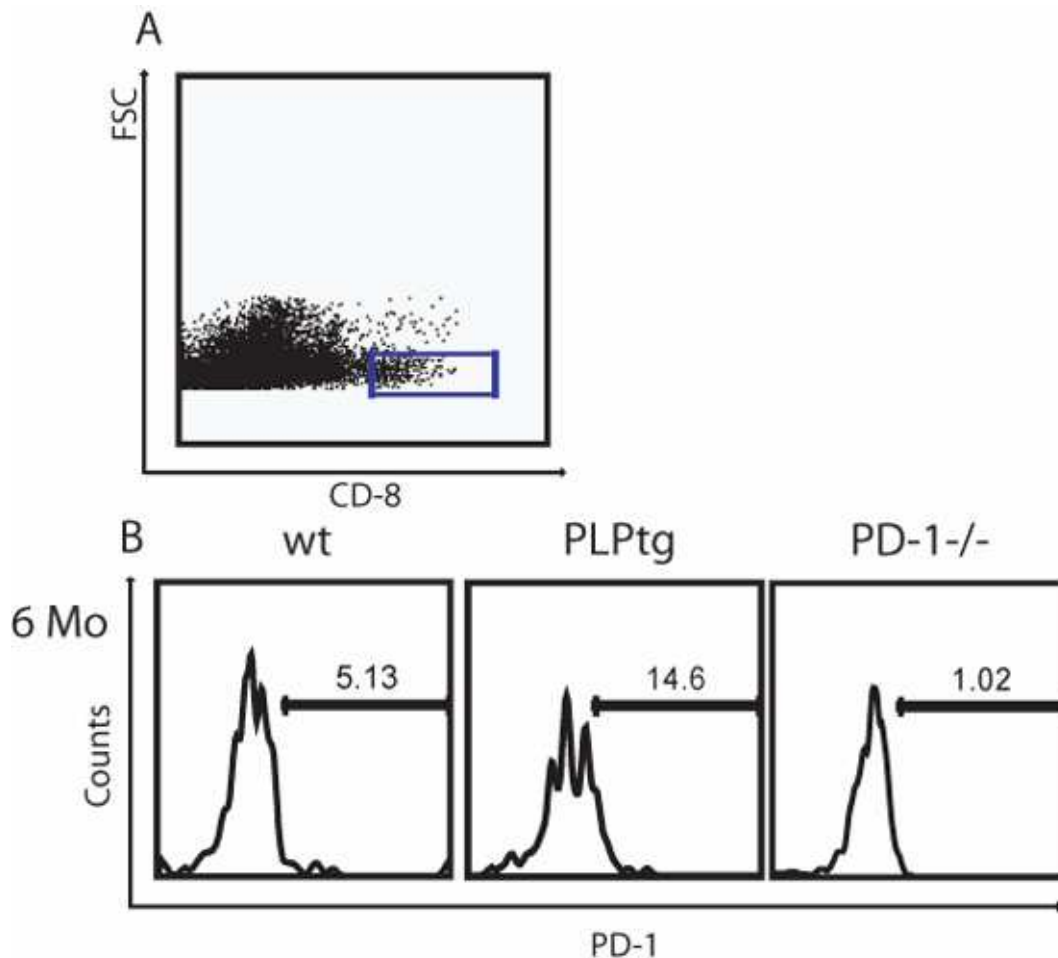


Figure 4: Expression of PD-1 on brain derived lymphocytes

This figure shows the expression of PD-1 on CNS derived lymphocytes of wildtype (wt), PLPtg and PD-1^{-/-} mice as a negative control. A. shows the FSC (forward scatter) and a staining for CD8⁺ cells. The forward sideward scatter plots cells by size on the Y- axis while CD8 positivity is visible on the X- axis. The gate (blue square) was set on CD8⁺ cells. B. Shows histograms for PD-1 staining with the gate set from A. Note that brain derived lymphocytes from wt and PLPtg mice express PD-1 which is not present in PD-1^{-/-} mice.

6.1.3 Numbers of CNS immune cells are significantly elevated in PLPtg/PD-1^{-/-} double mutants

PLPtg/PD-1^{-/-} double mutants and their respective controls (wt, PD-1^{-/-} and PLPtg mice), were examined at the age of 2, 6 and 12 months (n = 3-7). To quantify immune cells in the CNS, we focussed on longitudinal sections of the optic nerve, an already established read out technique for the scoring of inflammation in PLP mutant CNS (Ip et al., 2006a; Ip et al., 2007). To verify that the results were comparable also in other CNS regions, quantification was repeated in spinal cord cross sections.

6.1.3.1 Elevation of lymphocytes in PLPtg/PD-1^{-/-} mice compared to PLPtg mice

At the age of two months, there was no significant difference between wt, PD-1^{-/-}, PLPtg and PLPtg/PD-1^{-/-} mice. At 6 months, however, there was a slight elevation of CD8⁺ T- cells in the optic nerve of PLPtg mice in comparison to wildtype mice, consistent with our previous observations (Ip et al., 2006a). PD-1^{-/-} also showed a mild elevation, whereas PLPtg/PD-1^{-/-} double mutant mice exhibited a robust upregulation of CD8⁺ T- cells in optic nerve sections (approximately 35-fold increase compared to wildtype mice and a more than 8-fold increase in comparison to PLPtg mice; **Figure 5 A**). In 12 months old mice, the numbers of CD8⁺ lymphocytes in optic nerves were similar in the different genotypes, but proportions had shifted a little: wt and PD-1^{-/-} mice were now at similar levels (with no marked increase of profiles in PD-1^{-/-} mice compared to the 6 months old group), and PLPtg mice displayed significantly more CD8⁺ profiles than the former two genotypes. Strikingly, these CD8⁺ T- lymphocytes were again clearly outnumbered by those from PLPtg/PD-1^{-/-} mice (**Figure 5 B, C**).

CD4⁺ T- lymphocytes are rarely present in the CNS of PLPtg and wt mice (Ip et al., 2006a). At the age of two months, no differences were detectable in all investigated groups. In parallel to CD8⁺ lymphocytes, at the age of 6 months a significant elevation of CD4⁺ lymphocytes was already visible in PLPtg/PD-1^{-/-} compared to wt, PD-1^{-/-} and PLPtg mice and there was no marked increase until the age of 12 months (**Figure 5 D**). Taken together, few CD4⁺ cells were detectable in the CNS, but clearly elevated in the double mutants. Numbers of CD4⁺ T- cells were always lower than 10 % of the CD8⁺ lymphocytes of the corresponding genotypes. Importantly, the significant increase of cells was not only found in the optic nerve but also in the spinal cord (not shown).

6.1.3.2 No elevation of macrophages in PLPtg/PD-1^{-/-} mice compared to PLPtg mice

To investigate not only T- lymphocytes but also the largest group of immune-related cells present in the CNS, we quantified the CD11b⁺ macrophage-like / microglial cells in the optic nerve. We did not detect significant differences at the age of 2 or 6 months, although a trend of increased numbers was already detectable in PLPtg mice and PLPtg/PD-1^{-/-} double mutants compared to wildtype mice at the age of 6 months. In 12 months old mice, however, a significant difference was detectable. While wt and PD-1^{-/-} mice showed a common low level of cells, both PLPtg, as expected due to earlier studies (Ip et al., 2006a) and PLPtg/PD-1^{-/-} mice had significantly higher numbers of CD11b⁺ cells but did not differ significantly from each other (**Figure 6 A**).

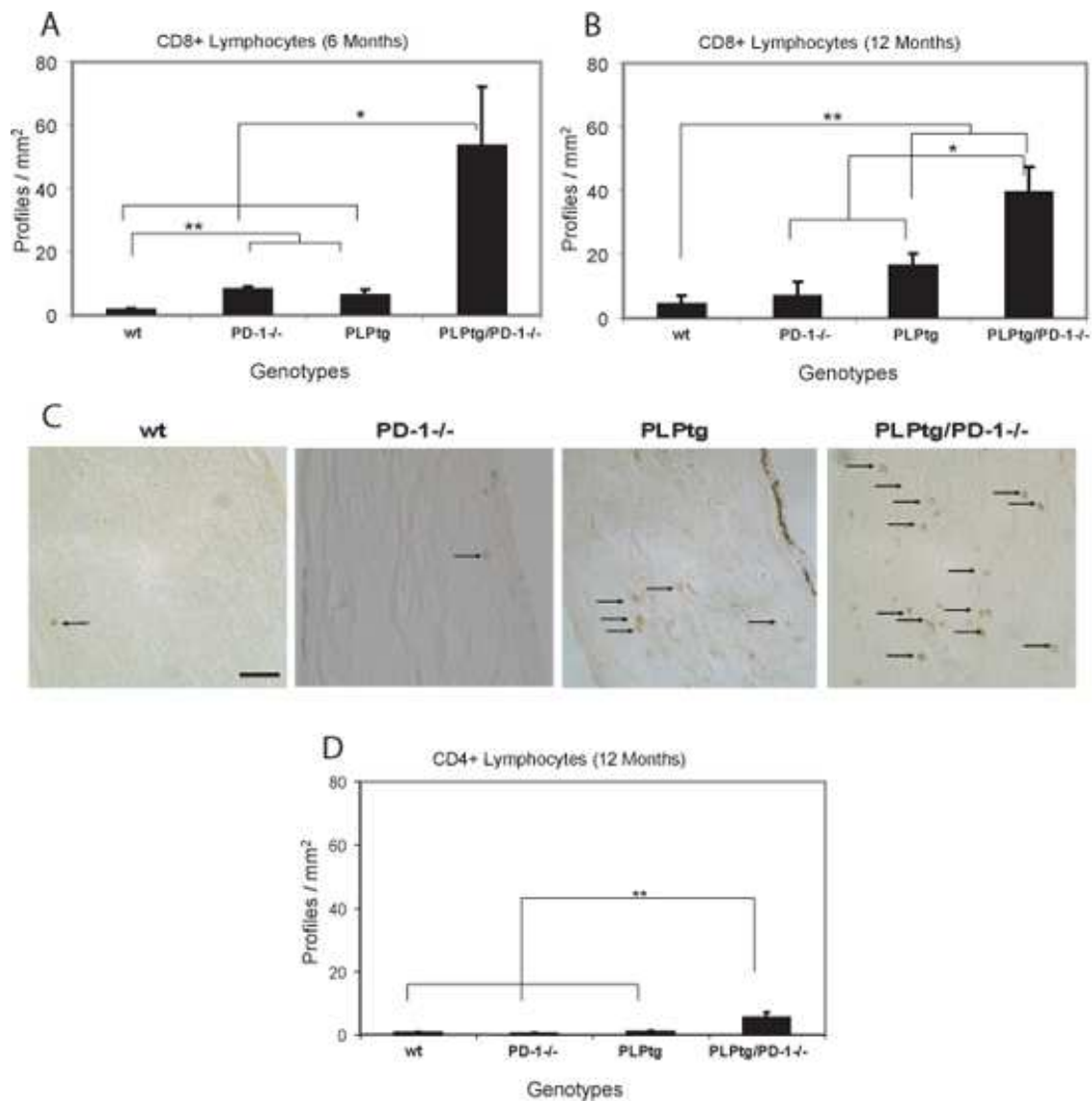


Figure 5: Quantification of CNS lymphocytes in wt, PD-1^{-/-}, PLPtg and PLPtg/PD-1^{-/-} mice

A, B: Quantification of CD8+ T- lymphocytes in longitudinal sections of optic nerves from 6 months old (A) and 12 months old (B) mice. C: Immunohistochemistry for CD8 in longitudinal sections of the optic nerves of 12 months old animals. Arrows indicate positively labelled CD8+ lymphocytes. Note the morphologically typical, rounded structure of these cells. D: Quantification of CD4+ lymphocytes in optic nerves of 12 months old mice. Note that in the myelin mutants, both CD8+ and the generally scarce CD4+ lymphocytes are substantially increased in the absence of PD-1. Error bars represent standard deviations. * = p - value < 0.05, ** = p - value ≤ 0.01. Scale Bar: 50 μm.

We also investigated the number of Sn expressing macrophage-like cells in 12 months old PLPtg/PD-1^{-/-} mice and detected a very low amount of positive profiles in both wildtype and PD-1^{-/-} mice. In PLPtg as well as PLPtg/PD-1^{-/-} mice, a more than 10-fold increase was detectable, as expected from earlier studies in PLPtg mice (Ip et al., 2007), but there was no difference between the latter two groups (**Figure 6 B**).

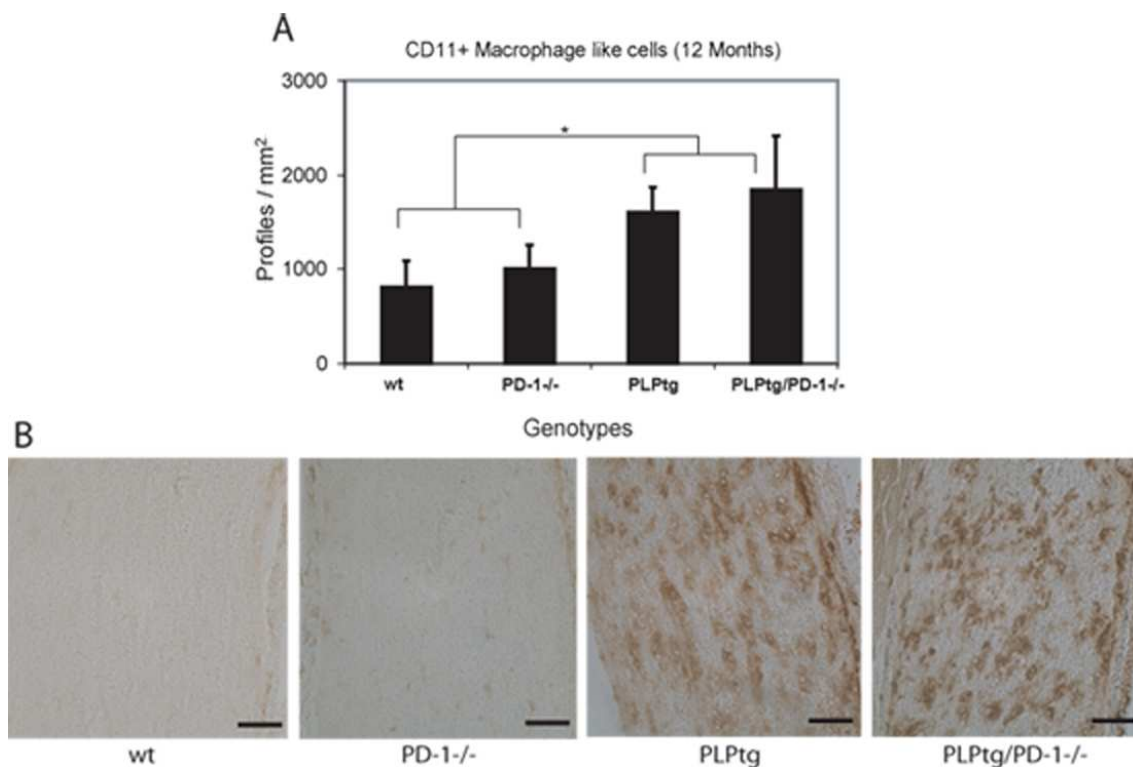


Figure 6: No differences in macrophage-like cells in PLPtg and PLPtg/PD-1^{-/-} mice

A. Quantification of CD11b⁺ macrophage-like cells in the optic nerves of 12 months old mice. B. Immunohistochemistry of Siglec- 1 (Sialoadhesin) in the different groups. Note the large, rounded macrophage-like cells in the myelin mutants (PLPtg and PLPtg/PD-1^{-/-}) and the rare, small and ramified cells in wt and PD-1^{-/-} mice. Error bars represent standard deviations. * = p- value < 0.05. Scale Bar: 50 μ m.

6.1.4 Numbers of immune cells are significantly elevated in PLPtg PD-1^{-/-} transplanted bone marrow chimeras (BMCs)

Another strategy to investigate the role of PD-1 in PLPtg mice was to examine PLPtg mice which were transplanted with bone marrow from either PD-1^{-/-} mice (PLPtg BMC PD-1^{-/-}) or wildtype mice (PLPtg BMC wt). Wildtype mice which were transplanted with either wildtype or PD-1^{-/-} bone marrow served as controls. These animals never displayed myelin pathology or CNS inflammation in any experiment.

Two strategies to generate bone marrow chimera were performed (**Figure 7**): In one group, the recipients were sublethally irradiated (5 Gy) to avoid allograft rejection, while the other group was deficient for the recombination activating gene (RAG)-1 (RAG-1^{-/-}). The bone marrow chimeras were transplanted at the age of 6-8 weeks and investigated at the age of 10 months (n = 8-9).

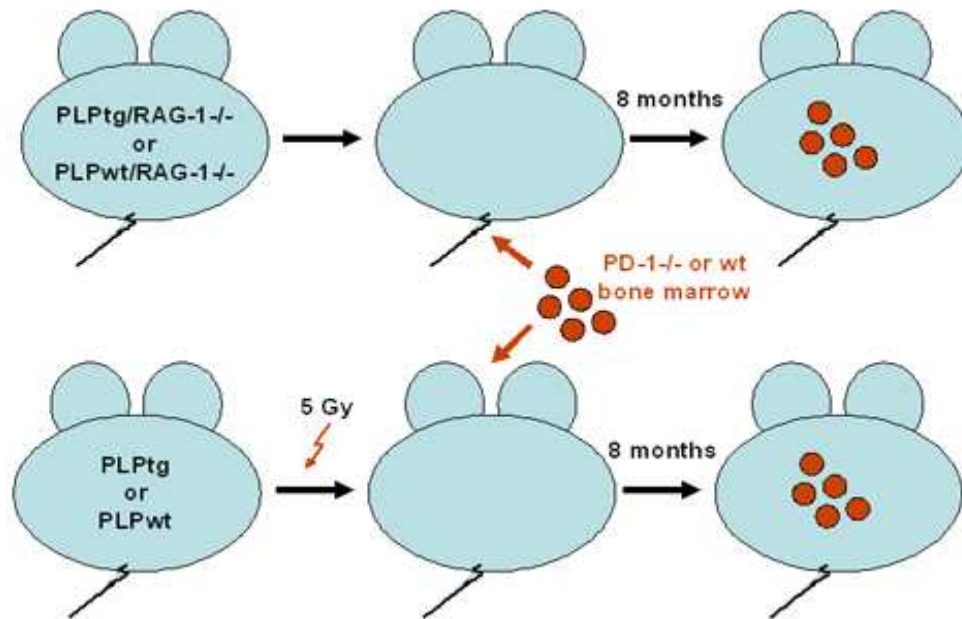


Figure 7: Two strategies for bone marrow chimerization of PLP_{tg} myelin mutants

PLP_{tg} or PLP_{wt} mice which were either RAG-1 deficient (upper row) or immunocompetent (lower row) were transplanted with wt or PD-1^{-/-} bone marrow and investigated 8 months later. Immunocompetent bone marrow recipients (lower row) were irradiated with 5 Gy to prevent allograft rejection.

With regard of the CNS lymphocyte counts, the bone marrow chimeric mice faithfully reflect the findings described for the double mutants. For example, both irradiated and PLP_{tg}/RAG-1^{-/-} recipients showed a robust upregulation of CD8⁺ lymphocytes, when bone marrow was derived from PD-1^{-/-} mice (**Figure 8 A**). Similar observations were made for the low but significantly elevated amount CD4⁺ cells (**Figure 8 B**). Increased elevation of CD8⁺ and CD4⁺ cells in the absence of PD-1 was significant both in irradiated and in RAG-1-deficient PLP_{tg} mice. Analysis of CD11b⁺ macrophage-like cells also depicted a significant increase in PLP_{tg} PD-1^{-/-} transplanted chimeras compared to recipients that received bone marrow from wildtype mice (data not shown). In the irradiated PLP_{tg} mice statistical significance was reached, while the PLP_{tg}/RAG-1^{-/-} mice showed a trend into the same direction but did not reach the level of significance ($p = 0.06$), thereby nicely reflecting the results seen in PLP_{tg}/PD-1^{-/-} double mutants.

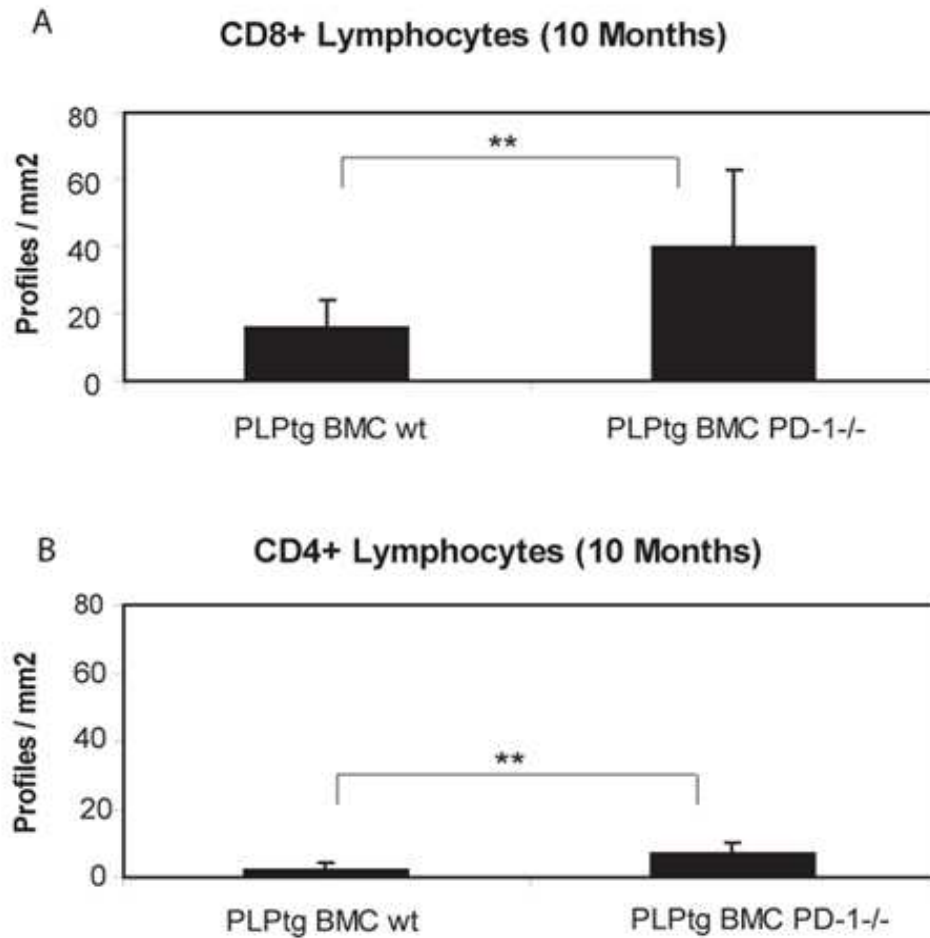


Figure 8: Significantly higher numbers of lymphocytes in PLPtg BMC PD-1^{-/-} mice

Quantification of CD8⁺ (A) and CD4⁺ (B) lymphocytes in the optic nerves of 10 months old mice bone marrow chimeras. Note the significant increase of both cell types in myelin mutants which received PD-1^{-/-} bone marrow and the generally scarce presence of CD4⁺ lymphocytes. ** = p-value < 0.01. Error bars represent standard deviations.

6.1.5 PD-1 deficiency leads to an increase of granzyme B⁺ T- lymphocytes and pre-apoptotic profiles in oligodendropathy-induced neuroinflammation

After having shown that CD8⁺ immune cells are elevated in PD-1-deficient PLPtg myelin mutants, we investigated whether this elevation also comprises an elevation of cytotoxic granzyme B⁺ cells. We, therefore, quantified by ELISPOT assay the CNS derived granzyme B⁺ cells from PLPtg and PLPtg/PD-1^{-/-} mice. For this equal numbers of CNS derived lymphocytes were unspecifically stimulated with the PKC-activator PMA and the Ca⁺⁺ ionophore ionomycin. Afterwards, the ELISPOT assay was developed and the number of single dots, representing granzyme B⁺ cells, was analysed. A small, but significant number of granzyme B⁺ cells were detectable among CNS immune cells from PLPtg mice (**Figure 9 A**). In the absence of PD-1, however, a 3 – 4 fold increase of granzyme B⁺ cells was

detectable (**Figure 9 A**). Thus, PD-1 not only regulates CD8+ cells in general but also the cytotoxic granzyme B+ population involved in the neuropathology of the PLPtg mutants. We also quantified pre-apoptotic cells represented by caspase-3+ profiles in the optic nerves of 12 months old wt, PD-1^{-/-}, PLPtg and PLPtg/PD-1^{-/-} mice. No pre-apoptotic profiles were detectable in the optic nerves of wt and PD-1^{-/-} mice. A substantial amount of pre-apoptotic cells were detected in PLPtg mice, with values similar to those detected in PLPtg BMCs (see **Figure 3**). Most interestingly, a robust increase in pre-apoptotic cells was found in PLPtg/PD-1^{-/-} mice (**Figure 9B**).

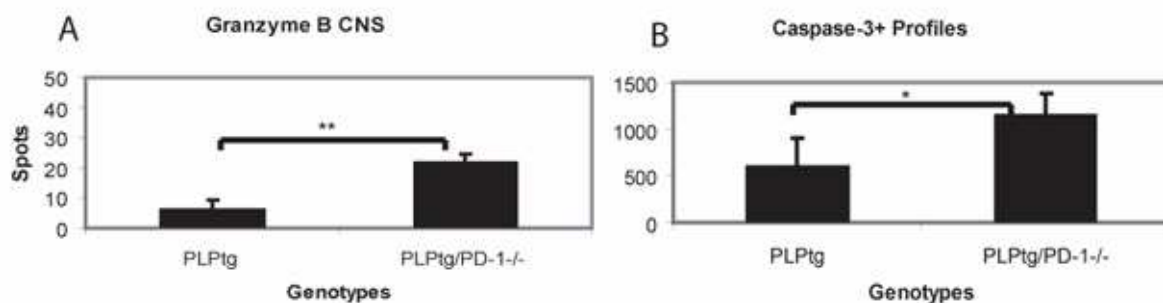


Figure 9: Increase of granzyme B+ cells and caspase-3+ oligodendrocytes in PLPtg/PD-1^{-/-} mice

A. Quantification of granzyme B+ CNS derived lymphocytes from PLPtg and PLPtg/PD-1^{-/-} mice by ELISPOT assay after stimulation with PMA/ ionomycin. Note elevated spot numbers in CNS T-lymphocytes taken from PLPtg/PD-1^{-/-} mice in comparison to PLPtg mice. B. Significant elevation of caspase-3+ profiles in the rostral part of the optic nerve in PLPtg/PD-1^{-/-} compared to PLPtg mice representing an activation of the apoptotic pathway in the absence of PD-1. Error bars represent standard deviations. * = p - value < 0.05, ** = p - value ≤ 0.01.

6.1.6 Pathological features are enhanced in PLPtg/PD-1^{-/-} double mutated mice

To make sure that the increase of immune cells was not an isolated phenomenon without any impact on the myelin status, we next assessed the pathological damage in the double mutants. The myelin damage was rated in the CNS by an investigation of myelin basic protein (MBP) distribution in optic nerve cross sections.

To ensure a comparable situation in all investigated animals, consecutive cross sections were collected beginning at retinal level, but only sections of the rostral area of the optic nerve (1000 – 1500 μm proximal to the retina) were used for the analysis.

MBP stainings on the cross sections were ranked according to the distribution of MBP. MBP-scoring revealed that, in clear correlation with numbers of CD8+ T- cells, wildtype and PD-1^{-/-} mice always showed a homogeneous distribution of myelin, indicating intact and healthy myelin, while PLPtg mice displayed a more patchy and inhomogeneous MBP

staining in line with moderate myelin loss. Compared to that, PLPtg/PD-1^{-/-} mice showed an even less homogeneous MBP distribution, reflecting extensive myelin loss (**Figure 10 A**).

MBP distribution was quantified by scoring, with score 1 depicting homogeneous distribution of myelin and score 5 depicting extensive myelin loss (**Figure 10 B**). Generally, the persons investigating the histopathological features (Antje Kroner, Rudolf Martini) were blinded regarding the genotypes of the mice. Similar to these results in double mutant mice, 10 months old PLPtg BMCs reconstituted with PD-1^{-/-} bone marrow showed a more disrupted state of MBP distribution than PLPtg mice transplanted with BMCs from wt mice (data not shown).

As another morphological parameter for pathological features we investigated periaxonal vacuoles, which reflect vacuoles surrounding degenerating axons, in semithin cross sections of the optic nerve (age of 12 months in double mutants, age of 10 months in bone marrow chimeras). Axonopathic vacuoles > 6 µm were previously shown to be a reliable marker of myelin and axonal pathology (Ip et al., 2006a; Ip et al., 2007).

PLPtg/PD-1^{-/-} double mutants, compared to PLPtg mice, showed a clear trend of increased vacuole numbers (13.3 ± 7.9 versus 7.95 ± 3.6), while wildtype and PD-1^{-/-} mice never displayed any vacuoles.

PLPtg BMCs transplanted with wt bone marrow showed 2.6 ± 0.57 vacuoles per cross section, while PLPtg BMCs transplanted with PD-1^{-/-} bone marrow contained 8.3 ± 3.7 vacuoles/ section, which represented a highly significant increase of axonal damage in PD-1^{-/-} myelin mutants (**Figure 10 C, D, E**). In the optic nerves of wildtype mice, we never detected any vacuoles, regardless what kind of bone marrow had been transplanted.

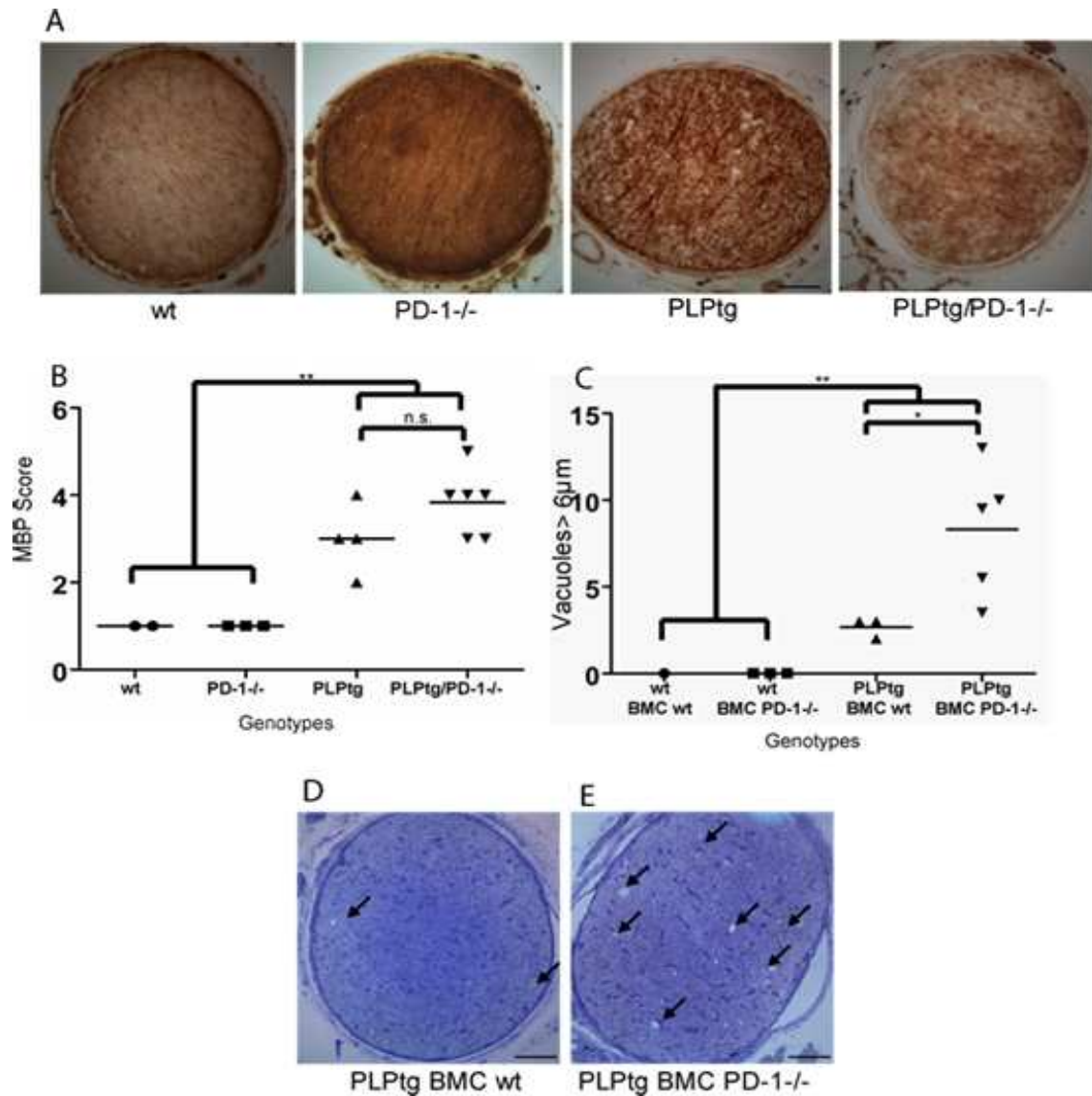


Figure 10: Pathological features in myelin mutants are enhanced in the absence of PD-1

A. MBP immunohistochemistry of optic nerve cross sections of 12 months old wt, PD-1^{-/-}, PLPtg and PLPtg/PD-1^{-/-} mice. Note homogenous MBP distribution in wt and PD-1^{-/-} mice compared to more disrupted myelin in PLPtg and, even more pronounced, PLPtg/PD-1^{-/-} mice. B. Semiquantitative ranking of MBP loss (Score 1: homogenous myelin distribution, Score 5: severe myelin disruption). PD-1-deficiency leads to the highest MBP loss in the myelin mutants and the most seriously affected mutants belong to the PD-1-deficient group. C. Quantification of vacuoles > 6 µm in bone marrow chimeras. PD-1-deficiency leads to the most robust histopathological alterations in the myelin mutants and the most seriously affected mutants belong to the PD-1-deficient group. D, E. Semithin cross sections through the optic nerve of 10 months old PLPtg mice which were transplanted with either wt (D) or PD-1^{-/-} (E) bone marrow. Arrows indicate periaxonal vacuoles. * = p-value < 0.05, ** = p-value ≤ 0.01. Scale bars: 50 µm

Interestingly, in one PLPtg/PD-1^{-/-} optic nerve we observed an extended and sharply confined area of MBP-loss, reminiscent of a demyelinated lesion common to active or

inactive MS plaques (**Figure 11 A**). This lesion was associated with an accumulation of CD8+ lymphocytes (**Figure 11 B**) and hematoxylin-stained cells of probably inflammatory character (**Figure 11 C**).

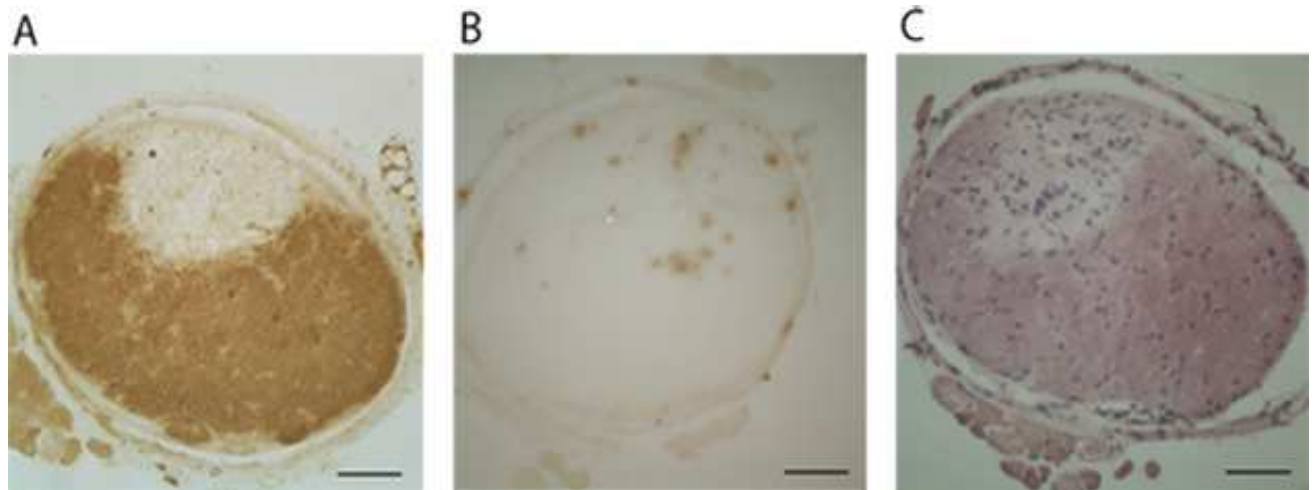


Figure 11: “MS- like” plaque in one PLPtg/PD-1^{-/-} mouse

Immunohistochemistry of optic nerve cross sections of one 12 months PLPtg/PD-1^{-/-} mouse. Detection of A. MBP, B. CD8+ T- cells, C. hematoxylin eosin staining in a plaque like demyelinating lesion. Note the sharply defined lesion (A.) with accumulated T- cells (B.) and other, probably inflammatory, cell nuclei (C.) Scale bars: 50 μ m.

6.1.7 T- cell CDR3 spectratyping analysis: robust clonal expansions in the CNS of PD-1^{-/-} and PLPtg/PD-1^{-/-} mice

CNS and peripheral T- lymphocytes were subjected to T- cell receptor (TCR) CDR3- spectratyping to analyze the T- cell repertoire in mutated mice. The CDR3 spectratyping was performed as described previously (Pannetier et al., 1995; Leder et al., 2007) on cells derived from CNS lymphocyte preparations and spleens. Briefly, T- cell receptors, which are composed of several subunits, are investigated to detect accumulation of cells carrying the same receptor which would be indicative for reactivity towards the same antigen.

With this method, the V and J regions of the TCR β -chain are amplified by PCR and the resulting products are analysed regarding their lengths. Unusually high amounts of CDR3 regions of the same length result in a peak, which is frequently a sign for clonal expansion.

Single clonal expansions of CD8+ T- cells were found in the CNS of PLPtg mice (Leder et al., 2007). Evidence for monoclonal T- cell expansions as revealed by single V β -J β peaks in the corresponding PCR-diagrams could be detected (one V β peak per animal) in PLPtg mice corroborating these previous findings (Leder et al., 2007). Corresponding expansions could not be detected in spectratyping analyses from lymphocytes of wildtype mice. Spleens of the

same animals displayed the expected Gaussian distribution of V β profiles (Leder et al., 2007) (Figure 12).

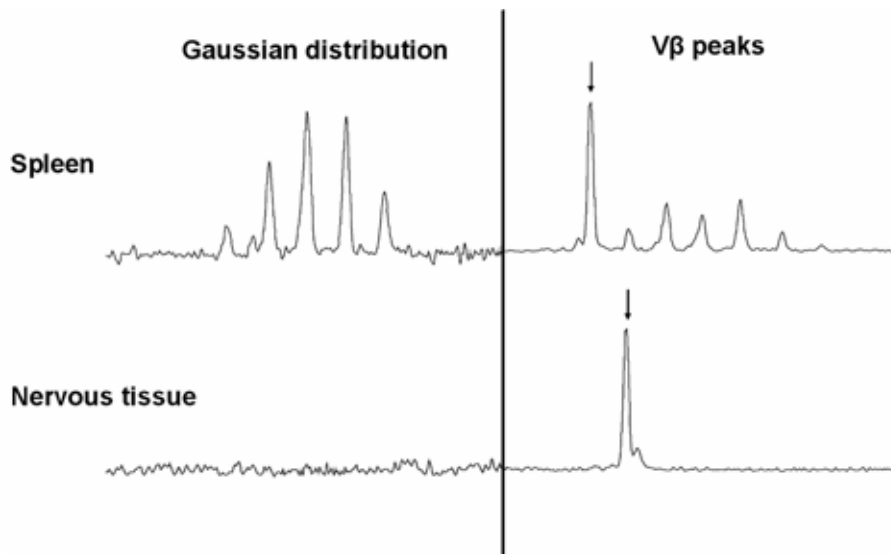


Figure 12: CDR3 spectratyping analysis with spleen and CNS derived lymphocytes

Representative example of spectratyping analysis on spleen derived (upper row) and nervous tissue derived (lower row) lymphocytes. On the left side, a normal, Gaussian distribution without peaks is shown while the right side shows typical V β peaks (arrows). The different size of profiles in spleens and nervous tissue can be explained by the difference in cell numbers.

CDR3 spectratyping in PD-1^{-/-} mice (n= 7) showed more than one V β peak (Figure 13).

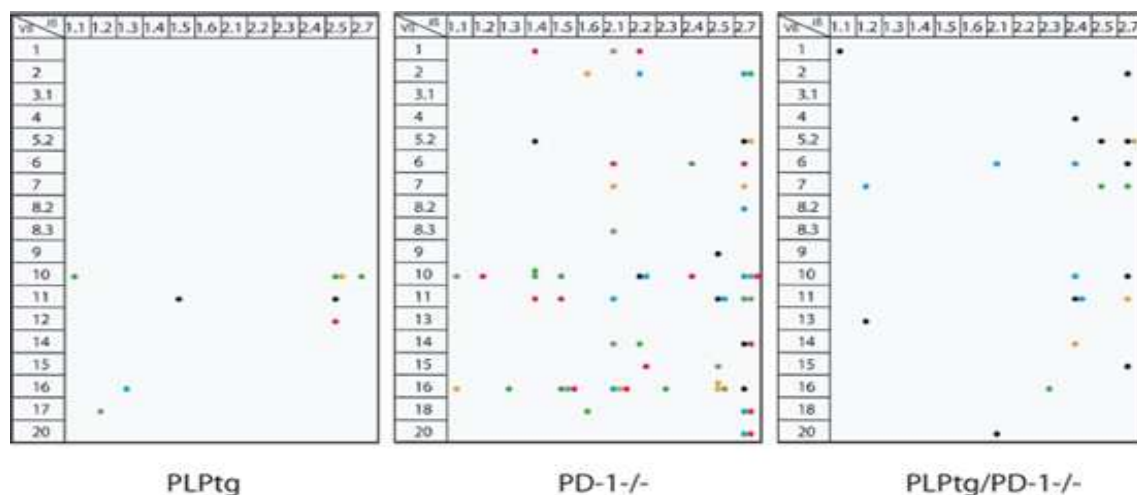


Figure 13: CDR3 Spectratyping of CNS derived lymphocytes and splenocytes

CDR 3 regions of lymphocytes from the CNS of 12 months old PLPtg (as adopted from (Leder et al., 2007), PD-1^{-/-}, and PLPtg/PD-1^{-/-} mice were analysed by spectratyping. Clonal expansions (visible as single peaks in the fragment analysis) are shown as colored dots (different colors indicate individual animals). The expanded T- cells are characterized by their V β - and J β -chains (V β : rows / J β : columns). The clonal expansions occurred widely distributed over different V β and J β regions, although some domains seemed to be prone for clonal expansions in different mutant mice. Note that different numbers of experimental mice contribute to the different numbers of dots.

Similarly, multiple V β peaks were visible in the CNS of PLPtg/PD-1^{-/-} double mutants (n = 3; **Figure 13**), as well as in 10 months old PLPtg/PD-1^{-/-} BMCs (n = 5).

The clonal expansions occurred widely distributed over different V β and J β regions, although some domains seemed to be prone for clonal expansions in different mutant mice. Notably, approximately 30 % of the individual clonal expansions were detected in both spleen and brain, 70 % of the expansions were exclusively present in CNS tissue.

6.1.8 Urinary protein and glucose are not elevated in the absence of PD-1

To exclude unspecific influence of autoimmune lupus like nephritis, which is frequent in older PD-1^{-/-} mice, we investigated the amount of glucose and protein in PD-1^{+/+} and PD-1^{-/-} myelin mutants by testing urine with a test stripe. While glucose was never detectable in the urine of these mice, protein was detectable but to a comparable amount in the presence and absence of PD-1. This indicates that in our model systemic autoimmune disease, as described for PD-1^{-/-} BL/6 mice, does not play a role (**Figure 14**).

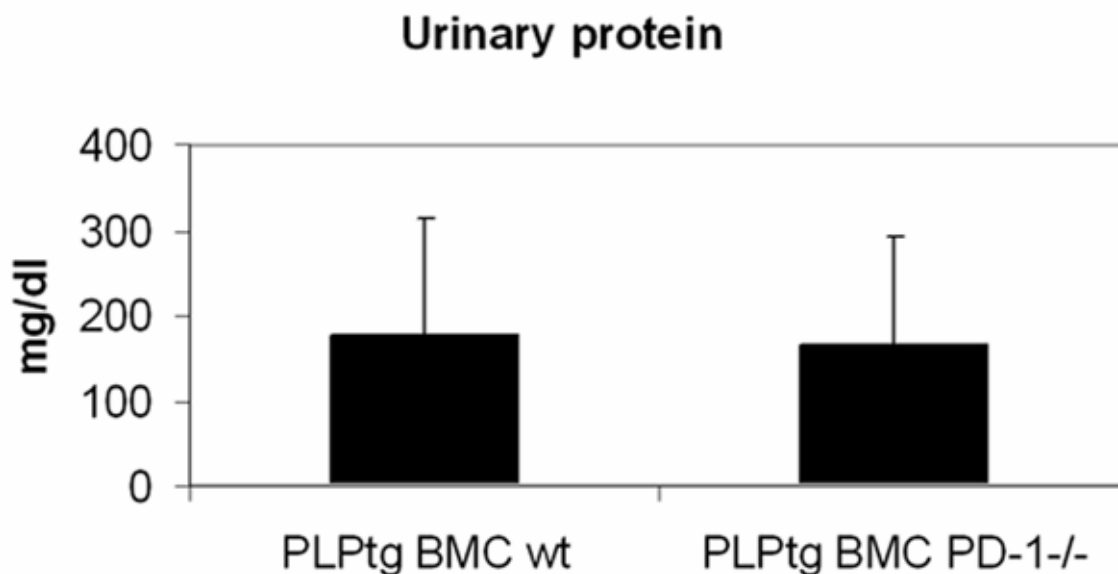


Figure 14: Measurement of urinary protein as a marker of autoimmune nephritis

This figure demonstrates measurement of urinary protein levels in PLPtg bone marrow chimeric mice which were either transplanted with wildtype or PD-1^{-/-} bone marrow. No differences in protein levels could be detected. Error bars represent standard deviations.

6.1.9 Peripheral immune parameters do not differ between mutant mouse strains

In order to exclude that peripheral immune parameters in the mutant mouse strains could account for the different numbers of immune cells and the different pathological features in

the nervous tissue of double mutated mice, we analyzed different features of the peripheral immune system in the different groups (wt, PD-1^{-/-}, PLPtg, PLPtg/PD-1^{-/-}) by analyzing Immune cell subset distribution (CD4⁺, CD8⁺, CD11b⁺, B220), phagocytic capability of macrophages, inducibility and rate of stimulation-induced apoptosis, and levels of stimulation induced IL-2.

6.1.9.1 Immune cell subsets

Immune cell subsets of CD4⁺ and CD8⁺ T- lymphocytes, B220⁺ B- lymphocytes and CD11b⁺ macrophages were analyzed by flow cytometry and did not differ significantly between splenocytes obtained from the different genotypes (**Figure 15**).

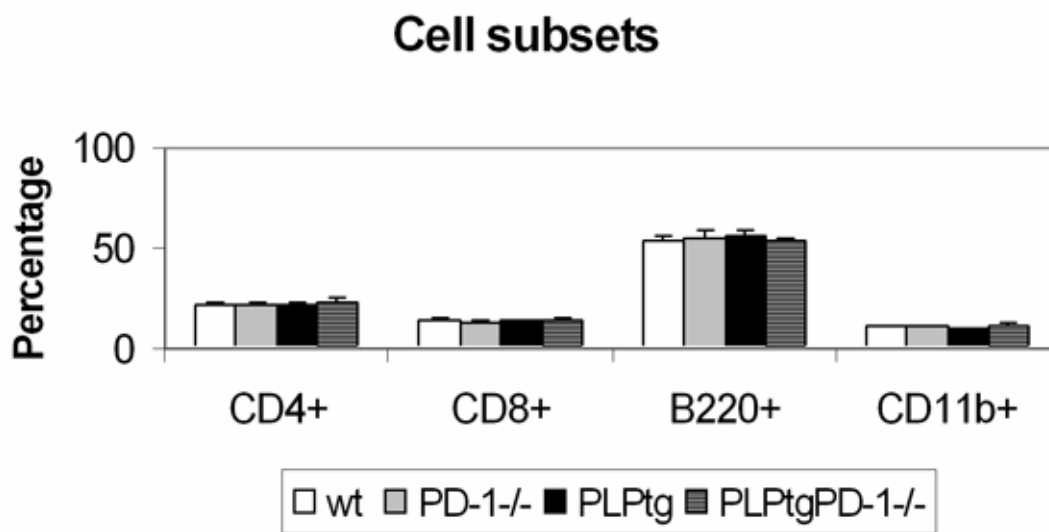


Figure 15: No difference in splenocytic cell subsets

This figure shows the characterization of cell subsets of CD4⁺ and CD8⁺ T- lymphocytes, B220⁺ B- lymphocytes and CD11b⁺ macrophages obtained from the spleen of wt, PD-1^{-/-}, PLPtg and PLPtg/PD-1^{-/-} mice. Note the similar amounts in all investigated groups. Error bars represent standard deviation.

6.1.9.2 Phagocytic activity of macrophages

Next, we ruled out differences in the general phagocytic capability of macrophages from the different genotypes. For this, peritoneal macrophages from the investigated genotypes were collected and confronted with fluorescent latex beads which then were quantified by flow cytometry. Also in this case, no differences between the groups were detected (**Figure 16**).

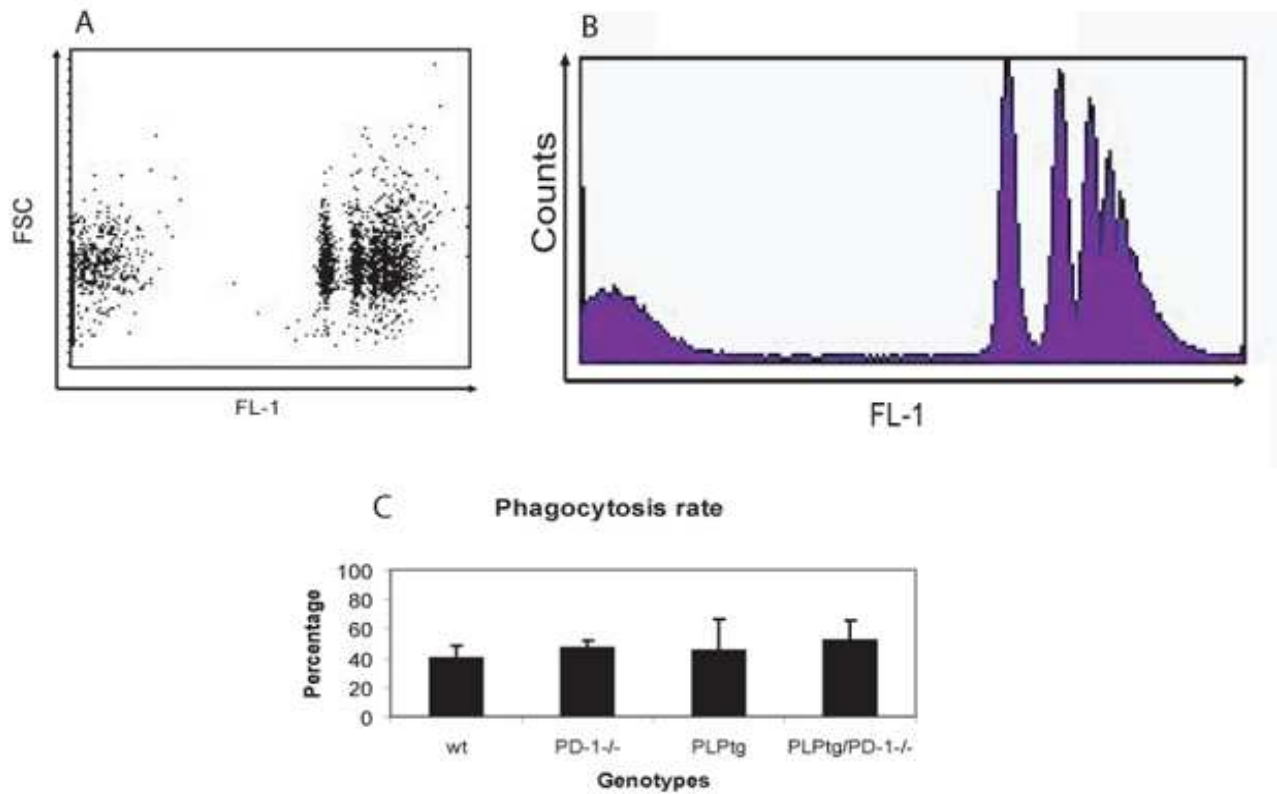


Figure 16: No difference in phagocytosis rate

Phagocytosis rate of peritoneal macrophages was determined by ingestion of FITC-fluorescent latex beads. A. Flow cytometry of one representative example. FSC (forward sideward scatter) and FL-1 (FITC- fluorescence). B. Histogram picture of A: The population on the very left represents cells which did not ingest any beads, each peak on the right represents cells which took up the same amount of beads. C. Phagocytosis rate of wt, PD-1^{-/-}, PLPtg and PLPtg/PD-1^{-/-} mice, which ingested one or more fluorescent beads. Error bars represent standard deviation.

6.1.9.3 Stimulation induced apoptosis

To detect differences in the inducibility and rate of stimulation induced apoptosis, splenocytes were supramaximally stimulated and apoptotic cells were detected by flow cytometry. Again, no differences were present between the different genotypes (**Figure 17**).

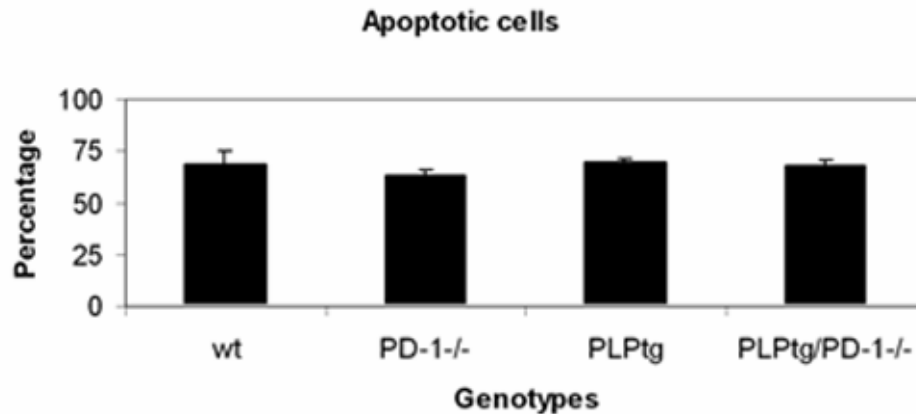


Figure 17: No difference in splenocyte apoptosis

This figure shows the percentage of preapoptotic and apoptotic splenocytes from wt, PD-1^{-/-}, PLPtg and PLPtg/PD-1^{-/-} mice after maximal stimulation. Error bars represent standard deviation.

6.1.9.4 Cytokine levels

To rule out crude differences in the peripheral production of proinflammatory cytokines, we performed ELISA analysis on cell culture supernatants. Levels of IFN- γ and IL-2 production did not between the different groups (**Figure 18**).

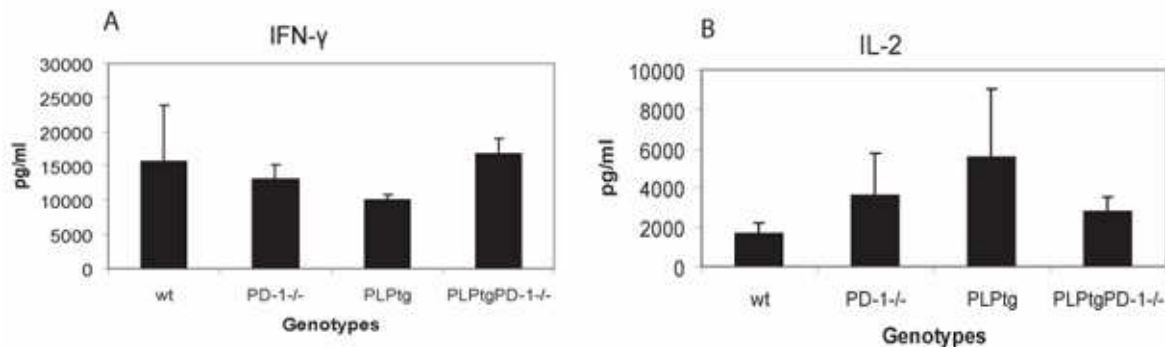


Figure 18: No difference in proinflammatory cytokine levels measured on splenocyte supernatant of the different genotypes

The production of proinflammatory cytokines was quantified in the supernatants of splenocytes from wt, PD-1^{-/-}, PLPtg and PLPtg/PD-1^{-/-} mice. A. IFN- γ , B. IL-2. No significant differences were detected between the groups. Error bars represent standard deviation.

6.1.10 CNS T- cells are prone to IFN- γ secretion in the absence of PD-1

Polyclonal immune responses in the periphery do not differ between mouse mutants. We therefore tested whether CNS cells show altered production of inflammatory cytokines upon stimulation. Functional immune responses (IFN- γ secretion) of CNS-derived T- lymphocytes thus were measured after addition of PMA/ ionomycin or upon antigenic stimulation.

CNS lymphocytes from wt, PD-1^{-/-}, PLPtg and PLPtg/PD-1^{-/-} mice were isolated, stimulated with PMA/ ionomycin and analysed by ELISPOT assay. Interestingly, CNS lymphocytes of PD-1^{-/-} and PLPtg/PD-1^{-/-} mice showed strong IFN- γ secretion upon PMA/ ionomycin challenge, while CNS T- cells from PLPtg mice or wt showed only minimal or no cytokine production (**Figure 19 A**). Of note, such differences have not been observed in T- lymphocytes derived from spleen (**Figure 19 B**). As expected, in the absence of a stimulus, no IFN- γ secretion was detected in any of the groups. Antigenic stimulation with a number of MHC class I related myelin peptides (Leder et al., 2007) did not lead to IFN- γ production of CNS T- cells under any condition in the ELISPOT (data not shown). This suggests that there were no T- cells present which were specific for the investigated myelin peptides.

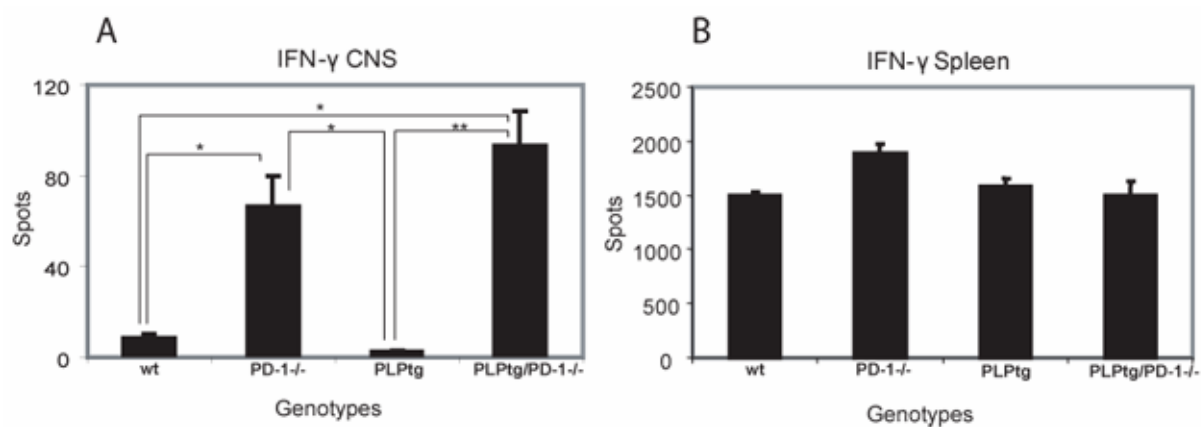


Figure 19: IFN- γ ELISPOT reveals higher susceptibility to activation in the absence of PD-1

IFN- γ ELISPOT assay after stimulation with PMA/ ionomycin on CNS derived lymphocytes (A) and splenocytes (B) from wt, PD-1^{-/-}, PLPtg and PLPtg/PD-1^{-/-} mice. Note elevated spot numbers in CNS T- lymphocytes taken from PLPtg/PD-1^{-/-} mice in comparison to wt and PLPtg mice, reflecting a higher susceptibility to activation. Error bars represent standard deviations. * = p - value < 0.05, ** = p - value \leq 0.01.

6.1.11 PD-1 deficiency does not induce overt motor disturbances in PLPtg mice

To investigate the functional consequences of PD-1 deficiency on PLPtg mouse mutants, we performed rotarod tests with 12 months old PD-1^{-/-}, PLPtg and PLPtg/PD-1^{-/-} mice. The test was performed as described above by placing mice on an accelerating, rotating rod. Each test run ended when the mice fell of the rod or, alternatively, after 300 seconds, which is considered the wildtype level of performance. The investigation revealed no significant differences between the groups and no difference to the wildtype level (**Figure 20**).

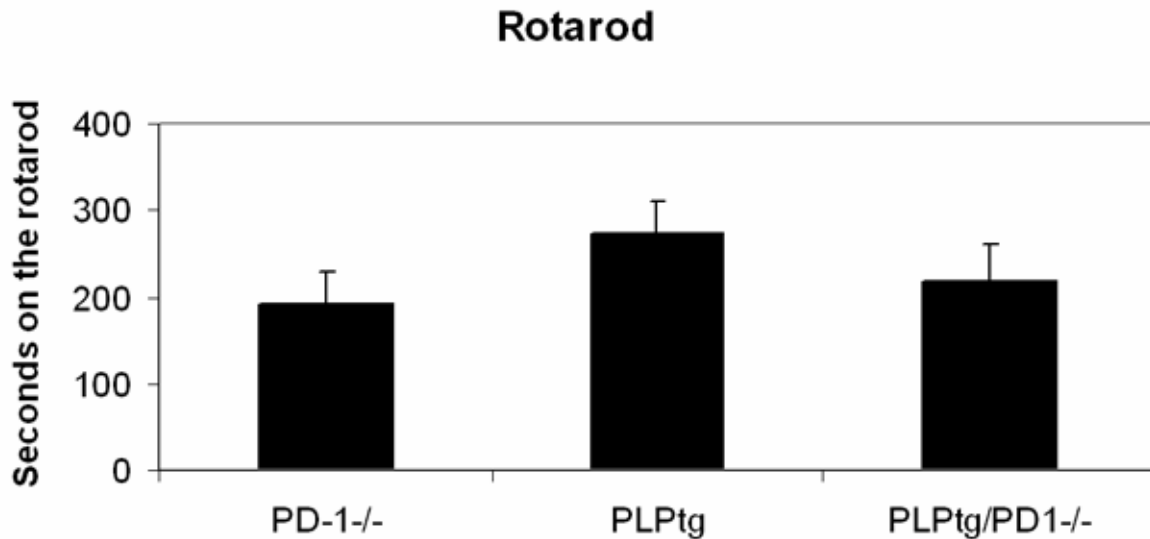


Figure 20: No overt motor disturbances in PLPtg/PD-1^{-/-} mice

The motor and coordinative abilities of 12 months old PD-1^{-/-}, PLPtg, PLPtg/PD-1^{-/-} were tested on a rotarod. Average seconds on the rod were quantified with a maximum of 300 seconds. Error bars represent standard deviation.

In this study, we investigated the influence of the coinhibitory molecule PD-1 in PLPtg mice. Absence of PD-1 induces a significant increase of both CD4⁺ and CD8⁺ CNS lymphocytes and granzyme B expressing cells. Furthermore, myelin damage and apoptotic oligodendrocytes increased. PD-1 deficiency induced higher susceptibility towards activation and clonal expansions independent from the myelin status. Importantly, the absence of PD-1 alone is not sufficient to induce neural damage in mice.

6.2 Role of PD-1 in the PNS

In earlier studies, we have shown that numbers of immune-related cells, namely F4/80⁺ macrophages and CD8⁺ T- lymphocytes increase in the peripheral nerve of P0^{+/-} mutants (Schmid et al., 2000), which serve as a model for CMT1B. As mentioned above, the pathogenetic impact of immune cells has been proven by crossbreeding myelin mutants with mutants lacking lymphocytes (RAG-1^{-/-}; Schmid et al., 2000) or macrophage colony stimulating factor (MCSF = MCSF^{-/-}; Carenini et al., 2001). A major inexplicit point in CMT disease is the fact that the same mutation, e.g. in the same family, may accounts for diverging disease courses. It is possible that differences within the immune system might influence disease outcome, possibly by altered coinhibition, like PD-1 deficiency, where lymphocytes show a “hyperactive” phenotype.

To analyse the pathogenetic impact of PD-1 deficiency in P0+/- mutants, we performed bone marrow chimerization experiments using wildtype (wt) or PD-1-deficient mutants (Nishimura et al., 1998) as bone marrow donors and P0+/- or P0+/- mice devoid of mature T- and B-lymphocytes (RAG-1-/- mice) as recipients (**Figure 21**). This approach enabled us to avoid irradiation of the recipients. Of note, PD-1 deficiency *per se* on a wildtype C57/BL6 background showed no alterations in the peripheral nerves, as also described above for the investigations in the CNS. The resulting bone marrow chimeras (BMCs), P0+/-/RAG-1-/- BMC wt and P0+/-/RAG-1-/- BMC PD-1-/-, were investigated at the age of 10 months (8 months after transplantation). To control the impact of PD-1 deficiency in mice with normal myelin, we additionally investigated P0+/-/RAG-1-/- BMC PD-1-/- and P0+/-/RAG-1-/- BMC wt mice. In all transplanted mice investigated, the success in transplantation was controlled by flow cytometry of the peripheral blood and splenocytes of BMCs. Only individuals with normal amounts of CD4+ and CD8+ T- lymphocytes were included in the study.

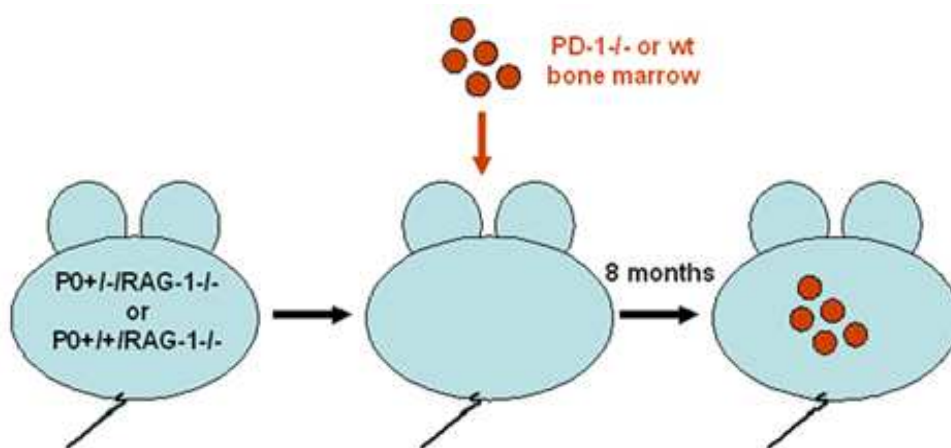


Figure 21: Experimental setup for bone marrow chimerization of PNS myelin mutants

P0+/- or P0+/- mice which lack mature B- or T- lymphocytes (RAG-1-/-) were transplanted with wt or PD-1-/- bone marrow and investigated 8 months later.

6.2.1 CD8+ T- lymphocytes, but not macrophages, are significantly elevated in PD-1 deficient P0+/- bone marrow chimeras (BMCs)

We performed immunohistochemistry for F4/80+ macrophages, CD4+ and CD8+ T-lymphocytes and B-lymphocytes on frozen cross sections of the femoral nerve of myelin mutant and wildtype mice in the presence and absence of PD-1. CD8+ T-lymphocytes were elevated in the mainly motor part of the femoral nerve, the quadriceps nerve, in P0+/-/RAG-1-/- BMC wt mice compared to P0+/-/RAG-1-/- BMC (wt or PD-1-/-) mice ($p = 0.002$), as expected from earlier investigations (Schmid et al., 2000).

In P0+/-/RAG-1-/- BMC PD-1-/- mice, however, there was a significant increase of CD8+ cells compared to P0+/-/RAG-1-/- BMCs wt ($p = 0.01$; **Figure 22 A**). As reported previously,

CD4⁺ T- lymphocytes were only scarcely present in the sections with no significant differences between the wildtypes and both groups of transplanted myelin mutants (data not shown). B220⁺ B-lymphocytes were not detectable in peripheral nerves in either of the mice investigated (data not shown).

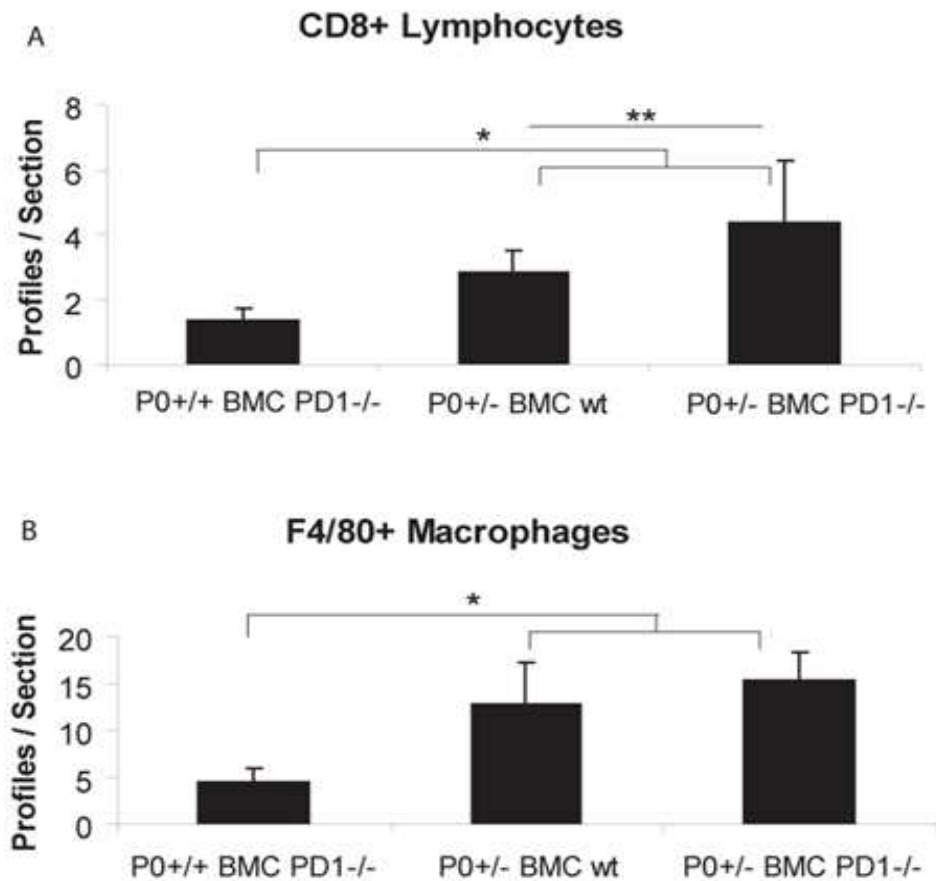


Figure 22: Elevation of CD8⁺ T- lymphocytes, but not macrophages, in P0+/-/RAG-1-/- BMC PD-1-/- mice compared to P0+/-/RAG-1-/- BMC wt mice

A. Quantification of CD8⁺ lymphocytes in the quadriceps part of the femoral nerve in P0+/-/RAG-1-/- and P0+/-/RAG-1-/- bone marrow chimeras transplanted with either wt or PD-1-/- bone marrow. Note elevation in myelin mutants compared to wildtype mice and further elevation in the absence of PD-1.

B. Quantification of F4/80⁺ macrophages in the quadriceps part of the femoral nerve in P0+/-/RAG-1-/- and P0+/-/RAG-1-/- bone marrow chimeras transplanted with either wildtype or PD-1-/- bone marrow. No significant difference was detected between P0+/-/RAG-1-/- mice which received wt or PD-1-/- bone marrow. In this and the subsequent figures, RAG-1 deficiency is not mentioned explicitly for lack of space but, if applicable, is always referred to in the figure legends. Error bars represent standard deviation. * = p- value \leq 0.05, ** = p- value \leq 0.01.

F4/80+ macrophages were significantly elevated in the mainly motor part of the femoral nerve, the quadriceps nerve, in P0+/-/RAG-1-/- BMC wt mice compared to P0+/-/RAG-1-/- BMC (wt or PD-1-/-) mice ($p = 0.002$), as expected from earlier publications (Schmid et al., 2000). Neither in P0+/-/RAG-1-/- BMC nor in P0+/-/RAG-1-/- BMC the absence of PD-1 caused an increased number of macrophages. In the saphenous nerve, which is the mainly sensory part of the femoral nerve, macrophage numbers were not significantly altered in either of the groups investigated (**Figure 22B**).

As expected from earlier publications (Schmid et al., 2000), the number of F4/80+ macrophages in the saphenous nerve, which is the mainly sensory part of the femoral nerve, did not differ significantly between P0+/-/RAG-1-/- and P0+/-/RAG-1-/- mice independent from the bone marrow they had received (data not shown).

Remarkably, in one P0+/-/RAG-1-/- BMC PD-1-/- mouse we detected abnormally high numbers of CD4+ (32 cells/section), CD8+ (41 cells/section) and F4/80+ (121 cells/section) profiles. Correspondingly, this animal also displayed robust myelin degeneration and axonopathic changes in the peripheral nerves. Since this was a unique case, we excluded this mutant from statistical analysis (**Figure 23**).

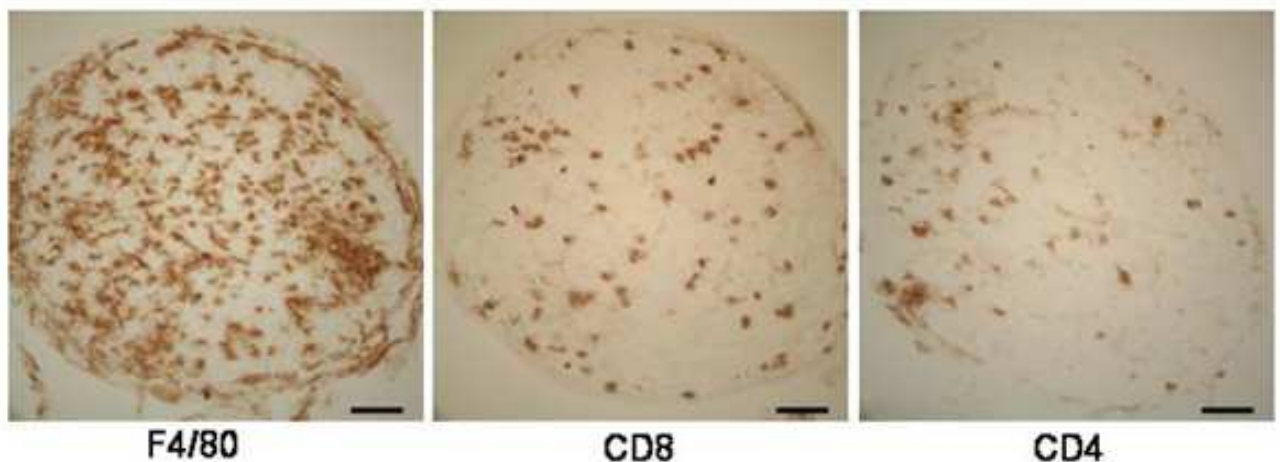


Figure 23: Massive amounts of immune cells in one myelin mutant in the absence of PD-1

Cross sections through the femoral quadriceps nerve of one P0+/-/RAG-1-/- BMC PD-1-/- mouse with immunohistochemistry of F4/80, CD8 and CD4. Note the large amount of profiles in all stainings. Scale bar: 50 μ m.

6.2.2 Pathological features are enhanced in P0+/-/RAG-1-/- BMC PD-1-/-

We investigated semithin sections of ventral roots, sciatic and femoral nerves of P0+/-/RAG-1-/- BMC PD-1-/- compared to P0+/-/RAG-1-/- BMC wt. The myelin damage visible in semithin sections was ranked by two blinded investigators (Antje Kroner and Rudolf Martini)

with a scoring system from 1, representing a completely healthy myelin status, to 5, characterizing nerves with massive demyelination. This ranking already revealed a significantly more pronounced damage in sciatic nerves of P0+/-/RAG-1-/- BMC PD-1-/- than in wildtype transplanted animals ($p = 0.03$; **Figure 24**). Ranking of ventral roots showed a similar result (data not shown).

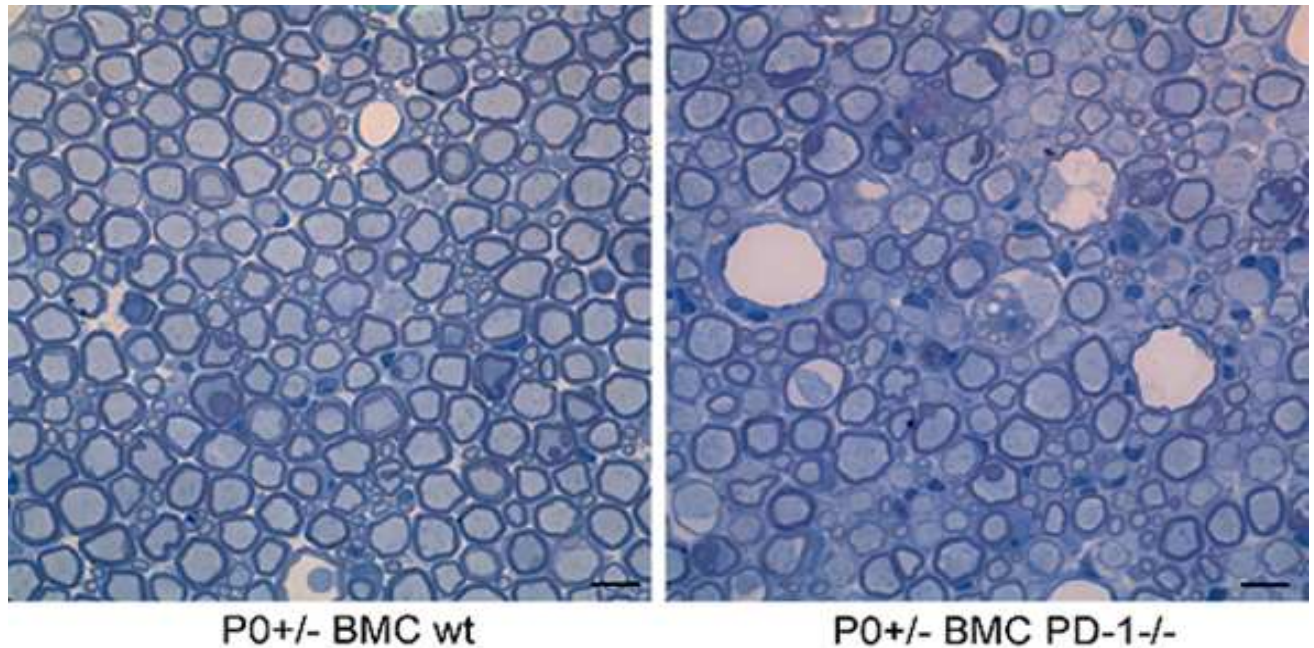


Figure 24: Increase of myelin damage in the absence of PD-1

Representative semithin sections through ventral roots of P0+/-/RAG-1-/- BMC wt and PD-1-/-. Note the higher number of pathologically myelinated axons and axonopathic vacuoles in P0+/-/RAG-1-/- BMC PD-1-/-. Scale bar: 10 μm .

To confirm these observations on a quantitative level, we determined pathological alterations by ultrastructural analyses. Ventral roots from both P0+/-/RAG-1-/- BMC wt and PD-1-/- displayed a normal phenotype, with only 0.1 % abnormally myelinated axons.

In ventral roots from P0+/-/RAG-1-/- BMC PD-1-/-, there were significantly more abnormally myelinated axons (completely demyelinated and thinly myelinated axons) than in P0+/-/RAG-1-/- BMC wt ($p = 0.04$; **Figure 25 A**). There were also significantly more total pathological profiles like, in addition to thinly myelinated and totally demyelinated axons, degenerating axons and axonopathic vacuoles ($p = 0.04$).

Analysis of the quadriceps nerve as the mainly motor part of the femoral nerve also showed a significant elevation of thinly myelinated axons in P0+/-/RAG-1-/- BMC PD-1-/- compared to P0+/-/RAG-1-/- BMC wt mice. The number of completely demyelinated nerves was also higher in PD-1-/- BMCs with an average of 10 % of all myelinated axons versus 0.6 % in the

wt transplanted mice, but due to high interindividual differences, no statistical significance was reached. Similarly, the overall pathology affected 5 % of all myelinated axons in wt BMCs compared to 22 % in PD-1^{-/-} BMCs (**Figure 25 B**).

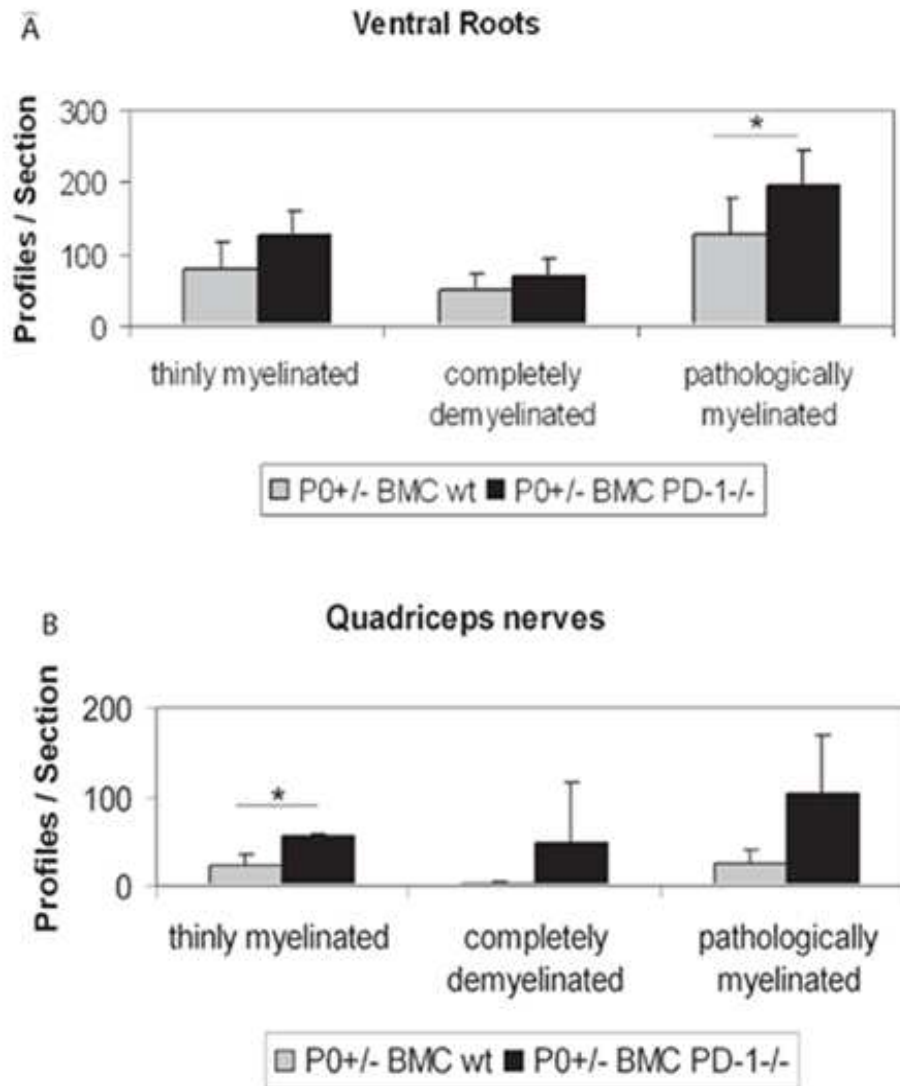


Figure 25: Increased myelin damage in the absence of PD-1

Electron micrograph analysis of ventral roots (A) and quadriceps nerves (B) of P0^{+/-}/RAG-1^{-/-} BMC wt and PD-1^{-/-} mice. Thinly myelinated axons and completely demyelinated axons were quantified. Pathologically myelinated axons are the sum of these quantifications. Error bars represent standard deviations, * = p-value < 0.05.

Previous studies on P0^{+/-} mice had shown an affection of mainly motor axons like in ventral roots and in the quadriceps part of the femoral nerve. Predominantly sensory parts of the peripheral nervous system, such as dorsal roots and saphenous nerves, were much less affected and particularly profiles indicative of myelin degeneration were lacking.

Since absence of PD-1 leads to increased pathological alterations, we investigated whether under such disease-aggravating conditions the sensory parts of the PNS are still preserved from myelin degeneration. For this purpose, we selected the dorsal spinal roots, which, at this segmental level, contain approximately 2000 myelinated axons of predominantly smaller size, and a large number of unmyelinated axons in association with non-myelinating Schwann cells, so called Remak bundles.

There was a trend towards higher amounts of pathologically altered profiles in the dorsal roots of P0+/-/RAG-1-/- BMC PD-1-/- compared to wildtype mice, but statistical significance was not reached, possibly due to high individual variations (**Table 1**). In spite of this mild increase in pathological profiles in the absence of PD-1, they were far less frequent than in ventral roots or femoral nerves of these mutants.

	thinly myelinated axons	completely demyelinated axons	pathologically altered axons (without thinly myelinated axons)	degenerated axons and axonopathic vacuoles
P0+/-/RAG-1-/- BMC wt	2.6 +/- 0.65	1.2 +/- 0.50	1.8 +/- 0.72	0.54 +/- 0.27
P0+/-/RAG-1-/- BMC PD-1-/-	2.2 +/- 1.14	2.1 +/- 1.41	3.37 +/- 2.34	1.13 +/- 0.83

Table 1: Myelin damage in dorsal roots of the PNS is not significantly increased

Ultrastructural quantification of pathological profiles in the dorsal roots of P0+/-/RAG-1-/- BMC wt (n = 5) and P0+/-/RAG-1-/- BMC PD-1-/- (n = 7) mice. All numbers represent pathological profiles as a percentage of the total number of myelinated axons. Analyzed pathological profiles include thinly myelinated, completely demyelinated and degenerating axons and axonopathic vacuoles.

6.2.3 Electrophysiological investigations reveal features indicative of increased axonopathy and myelin damage in P0+/-/RAG-1-/- BMC PD-1-/- mice

To investigate the functional consequences of the increased pathological alterations in P0+/-/RAG-1-/- BMC PD-1-/- mice, we performed electrophysiological investigations in 10 months old P0+/-/RAG-1-/- BMC wt (n = 10) and P0+/-/RAG-1-/- BMC PD-1-/- (n = 12) mice. In 5 P0+/-/RAG-1-/- BMC wt and 4 P0+/-/RAG-1-/- BMC PD-1-/-, both sides were investigated.

In brief, sciatic nerves were stimulated at the level of the sciatic notch (proximal stimulation) or above the ankle (distal stimulation) and compound muscle action potentials were recorded from the small foot muscles as previously described (**Figure 26**).

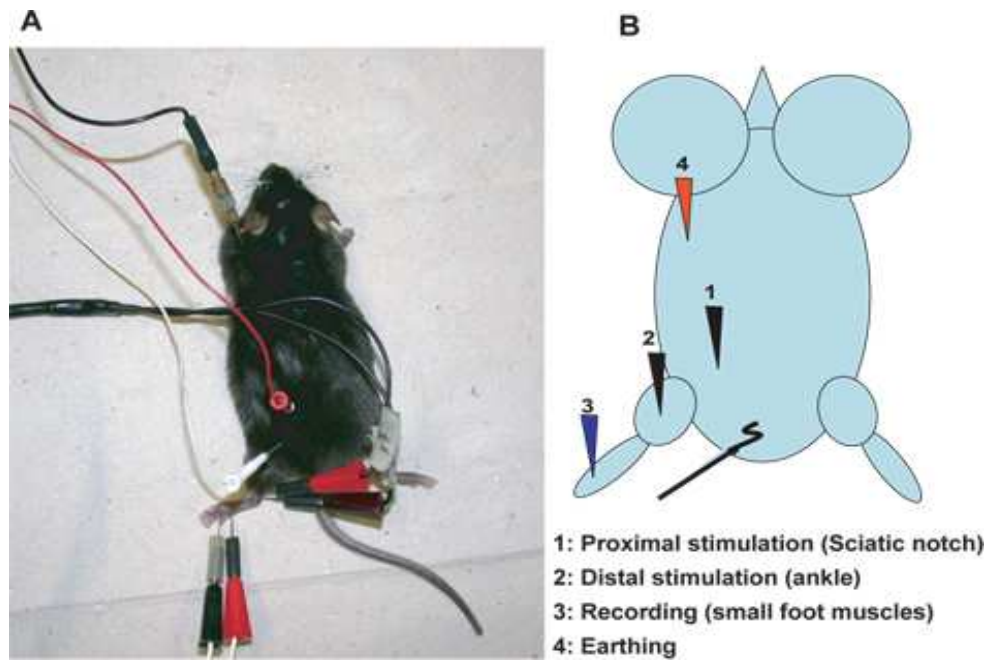


Figure 26: Experimental setup for electrophysiology of the sciatic nerve

Representative example (A) and schematic view (B) of experimental setup for electrophysiological recordings. Mice were anesthetized and electrodes were placed at the sciatic notch (1) for proximal stimulation, above the ankle (2) for distal stimulation and in the small foot muscles (3) for recording. Additionally, another electrode was applied for grounding (4).

Analyses include distal and proximal stimulation with results in compound action potentials (CMAP) with the amplitude as a measure for axonal integrity, duration and nerve conduction velocity (NCV) as a marker for myelin damage and F- wave latency and persistence. The F-wave results from the fact that upon electrophysiological stimulation, the signal spreads out in both directions of the nerve. It spreads out distally towards the muscle, also known as orthodromic signal and proximally towards the motor neurons, alternatively described as antidromic signal. An orthodromic signal induces a compound muscle action potential and, in the electrophysiological measurement, a so called M- wave. The antidromic signal, in contrast, reaches the motor neuronal cell bodies which react with a backfire and another orthodromic wave is generated and induces a smaller muscle contraction, termed F-wave.

The present recordings in the largest group analyzed together with five P0+/-/RAG-1-/- BMC wt and four P0+/-/RAG-1-/- BMC PD-1-/- mice revealed showed reduced distal amplitudes as well as significantly delayed F- wave latency in and P0+/-/RAG-1-/- BMC PD-1-/- versus P0+/-/RAG-1-/- BMC wt, reflecting increased axonopathy and myelin damage, respectively.

The F- wave was not persistent in one P0+/-/RAG-1-/- BMC PD-1-/- mouse. Paradoxically, the nerve conduction velocity (NCV) appeared shorter in P0+/-/RAG-1-/- BMC PD-1-/- mice. At this point is important to mention that the NCV is not as reliable to assess myelin damage, especially in small animals, as the F- wave latency (**Table 2**). Interestingly, bilateral

electrophysiological measurement of both sides always showed minor differences between the investigated sides, independent of the bone marrow they had received.

When all electrophysiological investigations (also from different sessions) were analysed together, there was only a significantly reduced distal amplitude (5.11 ± 2.18 mV versus 3.74 ± 1.54 mV) in P0+/-RAG-1-/- BMC PD-1-/- mice (p-value = 0.02). Nevertheless, it is also difficult to combine data obtained at different time points due to varying external parameters.

	P0+/-RAG-1-/- BMC wt	P0+/-RAG-1-/- BMC PD-1-/-	p- value
Amplitude (distal)	6.32 ± 1.89 mV	4.04 ± 2.27 mV	0.03
Latency (distal)	0.94 ± 0.09 ms	0.91 ± 0.11 ms	n.s.
Amplitude (proximal)	4.71 ± 1.5 mV	3.38 ± 2.27 mV	n.s.
Latency (proximal)	1.56 ± 0.09 ms	1.6 ± 0.1 ms	n.s.
F- wave latency	5.76 ± 0.67 ms	6.54 ± 0.54 ms	0.02
NCV	31.77 ± 5.83 m/s	27.16 ± 1.84 m/s	0.048

Table 2: Impaired amplitudes and delayed F- wave latencies in the absence of PD-1

P0+/-RAG-1-/- BMC wt (n = 5) and P0+/-RAG-1-/- BMC PD-1-/- (n = 4) mice were bilaterally electrophysiologically investigated. Distal and proximal amplitude (in mV), latencies (in ms), F- wave latencies (in ms) and nerve conduction velocities (NCV, in m/s) were analysed. Note decrease in amplitudes of compound muscle action potentials and increased F-wave latencies and nerve conduction velocities in the absence of PD-1. p- values < 0.05 are considered significant, n.s. = not significant

6.2.4 Altered gait test and reduced sensitivity in behavioural testing in P0+/-RAG-1-/- BMC PD-1-/- mice

6.2.4.1 Rotarod

To test the motor abilities of P0+/-RAG-1-/- BMC wt and PD-1-/- mice, a rotarod test was performed. For this, 10 months old P0+/-RAG-1-/- BMC wt and PD-1-/- mice had to walk and balance on a rotating, accelerating rod and the time was measured until the mice dropped off. Before the actual measurements took place, mice were allowed several test runs to accommodate with the task. This rotarod test did not reveal a difference between P0+/-RAG-1-/- BMC wt and PD-1-/- mice (**Figure 27**).

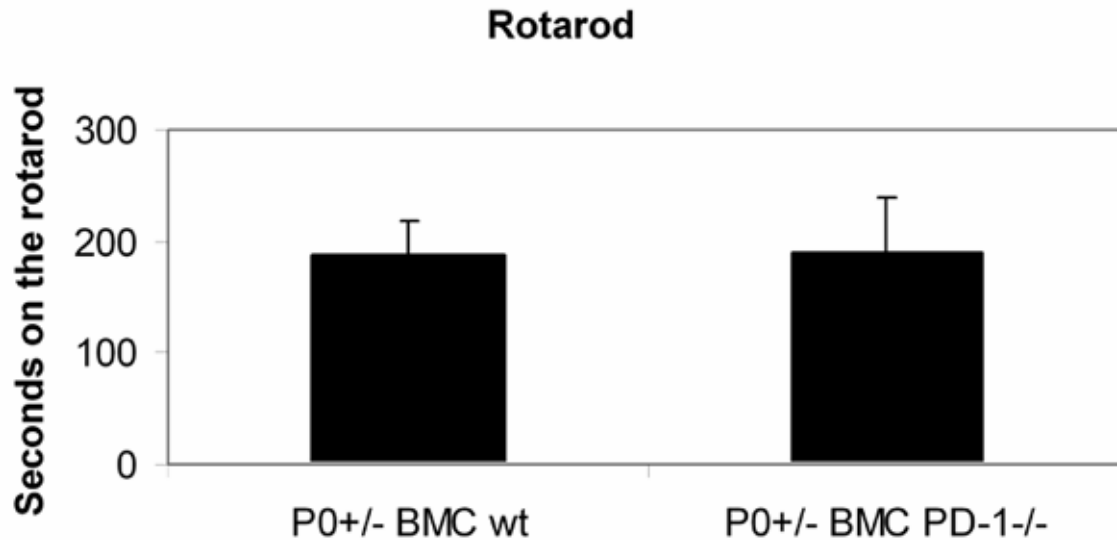


Figure 27: No differences in the rotarod test between myelin mutants in the absence or presence of PD-1

Rotarod test for motor and balancing abilities of P0+/-RAG-1/- BMC wt and PD-1/-/RAG-1/- mice. No significant difference could be detected between the groups. Error bars represent standard deviations.

6.2.4.2 Gait test

To detect more subtle differences of motor behaviour than visible in the rotarod test, gait tests were performed. For this, the hind paws of mice were stained with ink and they had to walk through a tunnel over some sheets of paper. Distance between feet, stride length and rotation of feet was measured. This test revealed no differences in stride length or rotation but a significantly broader distance between feet in the P0+/-RAG-1/- BMC PD-1/- group, suggesting difficulties in weight bearing (**Figure 28**). To exclude that this effect was caused by different size of the investigated mice, we measured the weight which was very similar in both groups (29.4 ± 3.5 g in wt BMCs versus 28.75 ± 4.11 g in PD-1/- BMCs).

6.2.4.3 Thermal sensitivity

To investigate not only the motor behaviour but also sensory parts of the nervous system, the same group of mice was tested for the sensitivity to thermal stimuli. Here, mice are placed on a heated glass plate and the time until they react to the heat and lift their hindlimbs is measured. In this sensory test, a trend towards a delayed reaction of P0+/-RAG-1/- BMC PD-1/- was detected, but statistical significance was not reached. This might be partly due to the fact that the test had to be terminated at a specific time point to prevent heat induced injuries of the mice (not shown).

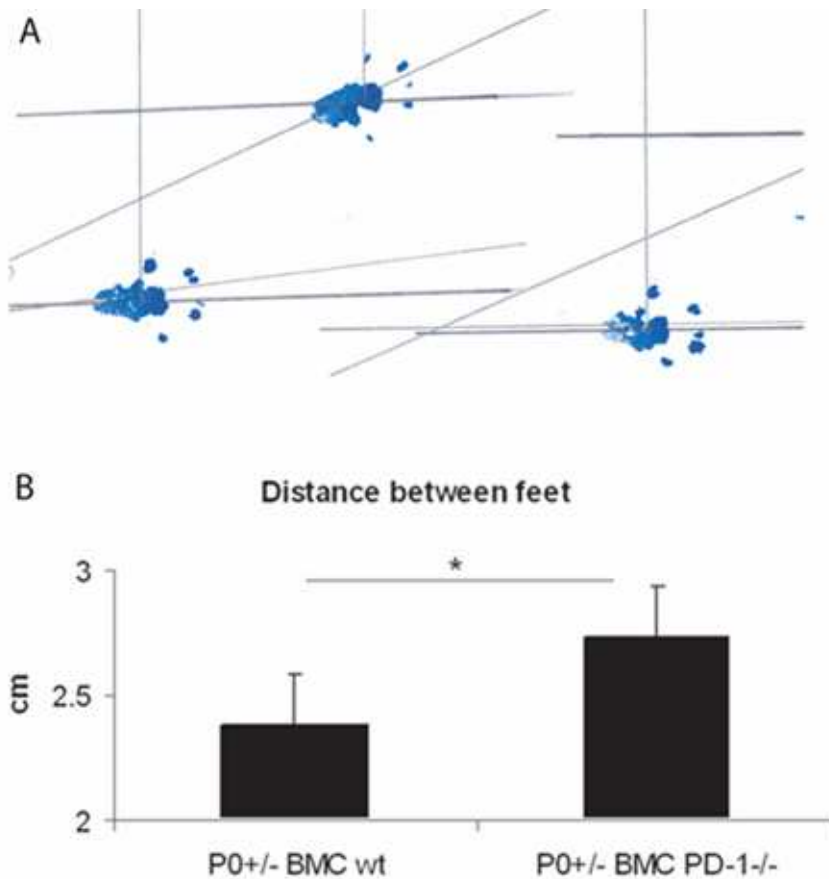


Figure 28: Widened distance between feet in P0+/-RAG-1-/- BMC PD-1-/- mice

PD-1-deficiency in P0+/-RAG-1-/- BMCs leads to increased distance between feet, reflecting impaired straight performance, as demonstrated by a representative step print (A) and the corresponding quantitative analysis (B) in P0+/-RAG-1-/- BMC wt versus P0+/-RAG-1-/- BMC PD-1-/-. Note increased values for P0+/-RAG-1-/- BMC PD-1-/- mice. Error bars represent standard deviations. * = p-value < 0.05.

6.2.4.4 Mechanical sensitivity

Further, we performed an established test for mechanical sensitivity of the hind paw (von Frey test). Mice were positioned on a grid and their hind paws were consecutively stimulated with monofilaments of defined strengths.

In a first test, P0+/-RAG-1-/- BMC wt mice reacted at 0.16 ± 0.13 g compared to P0+/-RAG-1-/- BMC PD-1-/- mice whose withdrawal level was 0.39 ± 0.22 g (p-value < 0.02). A second test also showed higher mechanical withdrawal thresholds in the absence of PD-1: 0.18 ± 0.18 g versus 0.61 ± 0.36 g (p-value = 0.005, **Figure 29**).

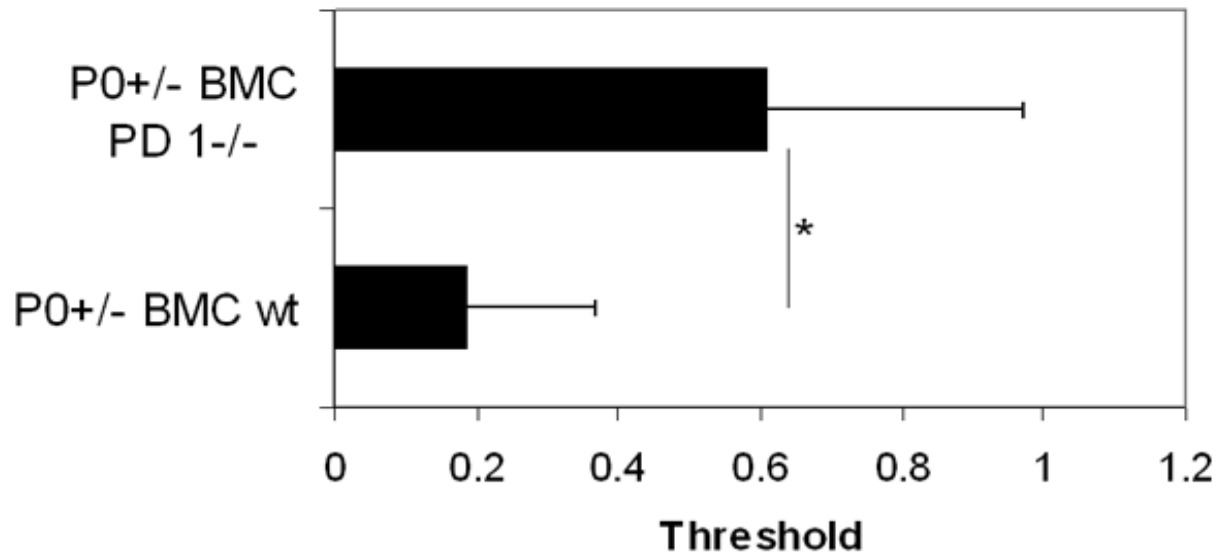


Figure 29: Reduced sensitivity to stimulation in P0+/-/RAG-1-/- BMC PD-1-/-

This figure represents threshold of reaction to stimulation with defined von Frey hairs in P0+/-/RAG-1-/- BMC wt and PD-1-/. This measure represents the point when mice pull off their feet because the touch with the filament is unpleasant. Delayed reaction in the PD-1 deficient group represents reduced sensitivity. Error bars represent standard deviations, * = p-value < 0.05.

6.2.5 Isolated PNS derived T- cells show features indicative of activated effector cells, but do not show evidence of clonal expansions

Isolation and flow-cytometry analysis of CD8+ cells from peripheral nerves of P0+/-/RAG-1-/- BMC wt and P0+/-/RAG-1-/- BMC PD-1-/- mice revealed that lymphocytes expressed the effector cell markers CD44/CD69, but scarcely the marker of immature lymphocytes CD62L. There is a tendency toward an even higher activation status in P0+/-/RAG-1-/- BMC PD-1-/- mice. Splenocytes, in contrast, showed a more balanced composition of naïve (CD62L+) and effector T- lymphocytes (CD44+/CD69+) which did not differ significantly in the absence or presence of PD-1 (**Figure 30**).

Furthermore, spectratyping analysis was performed as described above in collaboration with Nicholas Schwab to detect single clonal expansions of CD8+ T- cells, a feature highly suggestive of antigen specificity. We detected no evidence for mono- or oligoclonal T- cell expansions in the peripheral nerves of P0 mutants, neither in the presence nor in the absence of PD-1 (n = 3 – 7, data not shown). This could, however, be due to technical limitations, related to the relatively small number of T- lymphocytes in the peripheral nerve tissue. Nevertheless, in spleens of P0+/-/RAG-1-/- BMC PD-1-/- mice and in genuine PD-1-/- mice, polyclonal expansions of CD8+ cells could be detected, while spleen-derived CD8+ cells of P0+/- and P0+/-/RAG-1-/- BMC wt mice were not clonally expanded (not shown).

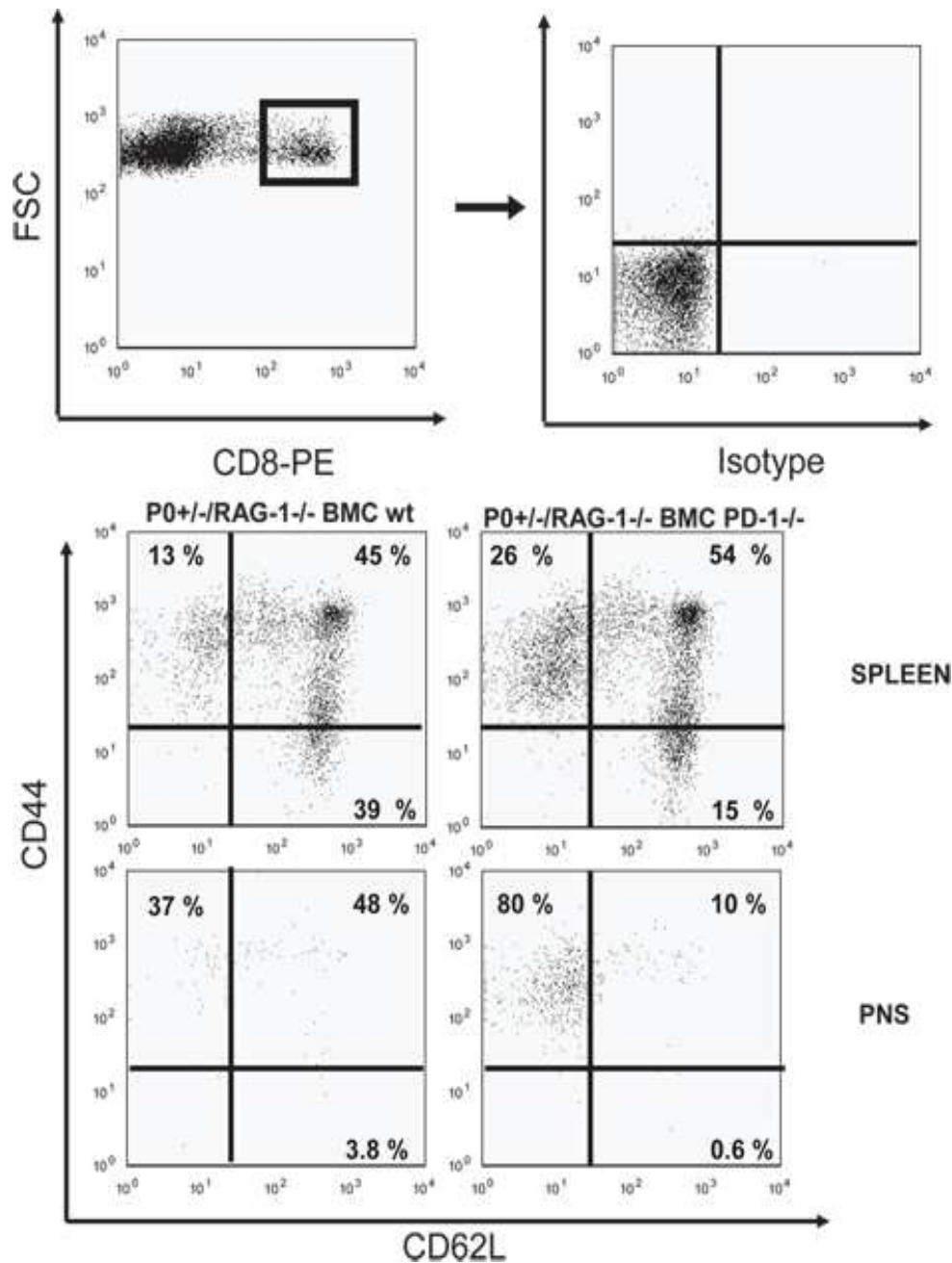


Figure 30: Nerve derived CD8+ lymphocytes display activated phenotype

CD8+ T- lymphocytes from peripheral nerves of P0+/-RAG-1-/- BMC wt and P0+/-RAG-1-/- BMC PD-1-/- mice display features of activated cytotoxic effector cells, as revealed by flow cytometry experiments. Cells are gated to CD8+ (upper diagrams) and investigated for CD44 (activation marker) and CD62L (marker for immature lymphocytes; lower diagrams). Note the similar distribution of naïve (CD62L) and effector cells in splenocytes of both groups, while the nerve derived lymphocytes from P0+/-RAG-1-/- BMC PD-1-/- show a more activated (= CD44+) phenotype.

6.2.6 PNS derived T- cells are prone to IFN- γ secretion in P0+/- mice

To investigate the ability of cells to react towards stimulation and to produce proinflammatory cytokines, IFN- γ ELISPOT assays were performed on lymphocytes derived from the PNS of

P0+/+ and P0+/- mice and from P0+/-/RAG-1/- BMC wt or PD-1/-/. For this, lymphocytes were extracted from the peripheral nervous tissue of the different groups as described above. Equal numbers of cells (1×10^5) were cultured for 24 hours either completely unstimulated or unspecifically stimulated with the PKC-activator PMA and the Ca^{++} ionophor ionomycin. Afterwards colorimetric development of the assay, the number of single dots, representing IFN- γ + cells, was analysed. A higher number of IFN- γ expressing cells was present in peripheral nerves of the myelin mutants (P0+/+: 19 ± 8.5 ; P0+/- 58 ± 4.2), but not in spleens of P0+/- mice compared to P0+/+ mice under unspecific stimulatory conditions with PMA / ionomycin. In peripheral nerves of P0+/-/RAG-1/- BMC PD-1/-/mice, there was a non-significant trend to an increased susceptibility of lymphocyte activation (72 ± 9.9) in comparison to P0+/-/RAG-1/- BMC wt (47 ± 26.16 , **Figure 31**).

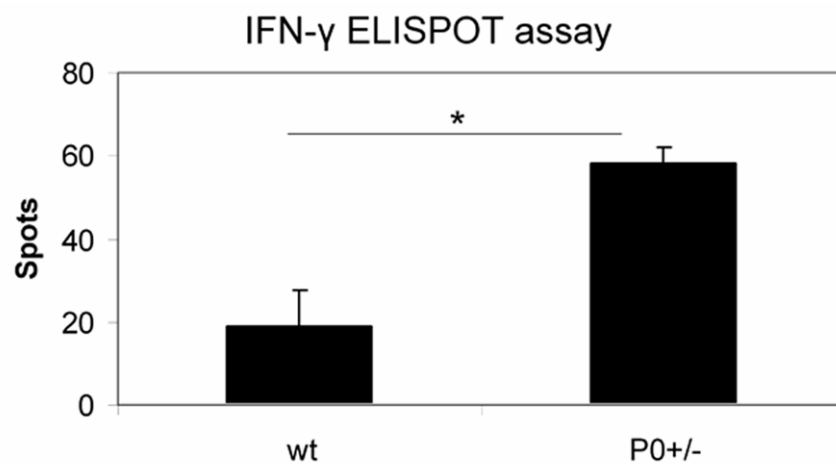


Figure 31: A higher percentage of stimulated nerve derived lymphocytes from myelin mutants produce IFN- γ

IFN- γ ELISPOT assay on PNS derived lymphocytes from wildtype and P0+/- mice. Error bars represent standard deviations, * = p-values < 0.05.

We could show in this study that the absence of PD-1 in our model of CMT1B, the P0+/- mouse, induces increased numbers of CD8+ T- cells, massive increase of myelin damage and also deterioration in some motor and sensory behavioural tests. Importantly, the absence of PD-1 alone is not sufficient to induce neural damage in mice.

7. Discussion

7.1 Presence and influence of inflammation in neurological diseases

Neuroinflammation leads to damage of glial cells and axons and is, thus, a crucial pathogenetic component of several disorders of the nervous system. Apart from infectious diseases of the nervous system with bacteria, viruses, fungi or parasites, there are many neurological diseases which are caused or modulated by the immune system.

In multiple sclerosis (MS), different neuropathological patterns of disease have been described. Pattern I and II are characterized by T- cell mediated autoimmune response while the other patterns (III and IV) are mainly characterized by loss of myelin proteins and therefore suggest primary oligodendrocytic dystrophy (Lucchinetti et al., 2000; Barnett et al., 2004).

Primary oligodendrocyte damage as one pathogenetic pattern of MS might be a reason for cases of MS-like-disease in patients carrying PLP mutations (Warshawsky et al., 2005; Gorman et al., 2007). These examples affirm that there is no clear borderline between inflammatory / autoimmune and mutation derived diseases of the CNS. These findings are further supported by investigations in mice which indicate that a primary glial injury can be causative for neuroinflammation of substantial pathological and clinical relevance (Ip et al., 2006a; Ip et al., 2007; Ip et al., 2006b; Leder et al., 2007; Grundtner et al., 2007; Kassmann et al., 2007).

The presence of immune cells in the CNS and their contribution or even original cause of the damage links MS to another disease type in which immune cells might influence disease course and response to treatment, the leukodystrophies.

Leukodystrophies, like for example X-linked adrenoleukodystrophy or metachromatic leukodystrophy, are heterogenous diseases characterized by extensive white matter loss. In these two forms, immune response inside the CNS is strongly present but distinct: in X-linked adrenoleukodystrophy, T- lymphocytes and macrophages are frequently present and might contribute to the damage, while in metachromatic leukodystrophy, microglia are upregulated but lymphocytes are not detected (Powers et al., 1992; Eichler et al., 2007).

Similarly, in globoid cell leukodystrophy (Krabbe disease) macrophage or microglial activation seems to play an important role. This is underlined by the fact that MHC class II deficiency in the corresponding mouse model, the twitcher mouse, significantly reduces not only inflammation but also ameliorates myelin and functional status (Matsushima et al., 1994).

Even neurodegenerative diseases like Alzheimer's or Parkinson's disease are influenced by immune- related cells. In Alzheimer's disease, microglial cells are protective on the one hand in means of amyloid β protein phagocytosis and, on the other hand, induce tissue injury and

neural death by complement activation, secretion of proinflammatory cytokines and reactive oxygen species (Akiyama et al., 2000; Verdier et al., 2004; Tuppo et al., 2005).

Similarly, in Parkinson's disease, microglial cells accumulate around dystrophic dopaminergic neurons and induce neuronal death when additionally stimulated with LPS (Rogers et al., 2007).

Also in the peripheral nervous system, immune cells play a crucial role. Many polyneuropathies of the peripheral nervous system are caused by inflammation. Some are additional symptoms in severe systemic diseases, among those paraneoplastic polyneuropathies in cancer patients, collagenoses like systemic lupus erythematosus, skleroderma, rheumatoid arthritis or different kinds of vasculitis.

Other diseases of the peripheral nervous system are directly caused by immune influences, like Guillain Barré syndrome (GBS). In this, antibodies against *Campylobacter jejuni* cross react with peripheral myelin and induce quickly ascending paresis and sensory disturbances. Another important example of immune mediated disease of the peripheral nervous system is the chronic idiopathic demyelinating polyneuropathy (CIDP) where patients develop slowly progressive paresis, paresthesia and other sensory symptoms. T- cells and antibodies are involved in the disease, and treatment includes anti- inflammatory regimens like steroids, plasmapheresis and immunoglobulins (Hughes et al., 2006; Meyer zu Horste et al., 2007).

7.2 Myelinopathies and corresponding animal models

In this work, we investigated the impact of immune cell activation status and cytotoxic properties to the neural pathology in different mouse models of central and peripheral hereditary myelinopathies. In these models for central and peripheral myelinopathies, we investigated the role of immune cells and their contribution to the neural damage.

Our model for CNS myelin mutations is a PLPtg mouse which autosomally overexpresses *p/p* (Readhead et al., 1994). PLP is the most abundant myelin protein of the CNS and disturbances of its expression pattern frequently result in severe disease. Pelizeaus-Merzbacher disease for example can be caused by duplications of the *p/p* gene and also by point mutations (Sistermans et al., 1998; Mimault et al., 1999; Regis et al., 2008). Many hereditary myelinopathies of the PNS are members of the demyelinating Charcot-Marie-Tooth disease neuropathies. The most frequent subgroup is CMT1A which is mostly caused by duplications in the *pmp22* gene. CMT1B is less frequent and related to mutations in the *mpz* gene. The mice we use as models for peripheral hereditary myelinopathies are P0+/- mice, which serve as a model for CMT1B (Martini, 1997).

One limitation to this model is the fact that most CMT1B patients do not suffer from a homo- or heterozygous null mutation but from point mutations which induce dominant negative effects and usually result in increased damage. Nevertheless, one family has been described

whose members carry either a heterozygous or homozygous loss of function mutation in *mpz* (Shy, 2006). Clinically, this results in a relatively mild demyelinating phenotype in the heterozygous carriers, comparable to the situation in P0+/- mice, while the homozygous mutation induces a Dejerine- Sottas like dysmyelinating phenotype which can also be seen in P0-/- mutants (Warner et al., 1996; Martini, 1997).

7.3 Role of immune cells in peripheral and central myelinopathies

In the last years, our group demonstrated the influence of immune cells and their contribution to neural damage in a variety of models for hereditary myelinopathies.

Investigation of the PLP_{tg} mouse showed that in several parts of the CNS, CD11b+ macrophage-like cells increase in an age-dependent manner compared to wildtype mice. Furthermore, CD8+ but not CD4+ T- lymphocytes ascend to a significant amount but show much smaller total numbers than CD11b+ macrophage-like cells. Cross breeding of PLP_{tg} mice with RAG-1-/- mice, which lack mature B- and T-lymphocytes, significantly reduced myelin damage in PLP_{tg} mice (Ip et al., 2006a). Interestingly, crossbreeding with mice lacking the macrophage surface marker Siglec-1 (Sialoadhesin) also reduced the neural damage but, in addition, reduced the amount of CD8+ T- lymphocytes to the wildtype level (Ip et al., 2007), indicating a crucial role of Siglec-1 in the activation of T- cells. Remarkably, this molecule was expressed on almost all CD11b+ cells in PLP_{tg} mice but only rarely in wildtype mice (Ip et al., 2007). The critical role of CD8+ lymphocytes as culprit cells in the pathogenesis of PLP_{tg} mice could be proven by bone marrow chimerization experiments (Ip et al., 2006a).

A crucial role of immune cells was also shown in P0+/- (Schmid et al., 2000) mice as well as in Cx32-/- (Kobsar et al., 2002) and PMP22_{tg} mice (Kobsar et al., 2005), where the number of F4/80+ macrophages significantly increased during the lifespan. The pathogenetic impact of macrophages was demonstrated in several experiments where macrophage activation factors were knocked out. The absence of M-CSF (Carenini et al., 2001) or Sialoadhesin (Kobsar et al., 2006) in P0+/- mice resulted in less severe myelin damage compared to P0+/- mice with unaltered immune system. Similarly, heterozygous dose reduction of MCP-1 (MCP-1+/-) significantly ameliorated the myelin phenotype, while complete absence of MCP-1 increased the damage (Fischer et al., 2008a).

Not only macrophages, but also CD8+ T- lymphocytes show elevated numbers in P0+/- and Cx32-/- mice, while CD4+ T- lymphocytes are generally scarce (Ip et al., 2006b; Kobsar et al., 2002; Schmid et al., 2000). The pathogenetic impact of T- lymphocytes has been demonstrated by crossbreeding experiments with RAG-1-/- mice. The absence of RAG-1 also induced a significant amelioration of the myelin phenotype in P0+/- and also Cx32-/- mice compared to immunocompetent myelin mutants. Interestingly, in dysmyelinating P0-/-

mice, the absence of RAG-1 induced a worsening of neural damage, characterized by enlarged axonal loss in the plantar nerves, thus suggesting a certain neuroprotective role of the immune system (Berghoff et al., 2005).

7.3.1 Granzyme B is pathogenetically relevant PLPtg mice

Having shown that CD8⁺ T- lymphocytes are the major culprit cells in myelin damage of PLPtg mice, it was important to define the cytotoxic molecules involved in the pathology. In the present study, we could extend our findings on CD8⁺ effector cells and identified granzyme B as one important mediator of lymphocytic cytotoxicity.

CD8⁺ T- cells can induce apoptosis via two main pathways, either by ligation of death receptor on the surface of cytotoxic T- lymphocytes or by granule exocytosis (Cullen et al., 2008). Cytotoxic T- lymphocytes contain modified lysosomes, so called lytic granules, which contain effector molecules, namely granzymes and perforin. Granzymes are serine proteases which induce apoptosis in the target cell. Upon antigen recognition on a target cell, cytotoxic T- lymphocytes synthesize and secrete perforin and granzymes into the interface between CD8⁺ and target cell, thereby inducing rapid cell death.

Experiments with perforin deficient mice have proven its essential role in granzyme-dependent killing (Kagi et al., 1994; Lowin et al., 1994). Perforin is required for granzyme trafficking but its exact role is controversially discussed. Some authors suggest pore formation in the membrane of the target cell as a necessary mechanism for granzyme B to enter the cell, others propose that perforin is essential for the endosomal disruption and release of granzyme B (Cullen et al., 2008). Granzyme B deficient mice, in contrast, are still able to induce apoptosis but with a remarkable delay, underlining the importance of granzyme B in fast and efficient killing (Cullen et al., 2008). Granzyme B itself induces apoptosis via two different pathways, either by cleavage of caspases or by permeabilization of mitochondria. Caspase-3 is a major substrate among the caspases, which then cleaves downstream caspases like caspase-2, -6, and -9 itself (Adrain et al., 2005).

The fact that oligodendrocyte damage in PLPtg/granzyme B^{-/-} BMCs is not completely abolished suggests the influence of other factors involved in the induction of oligodendrocyte apoptosis, like e.g. perforin, which unfolds its full property when combined with granzymes, or, alternatively, Fas and FasL. Generally, granzymes are thought to induce primarily apoptotic death of their target cells (Chowdhury et al., 2008), but to our knowledge, this issue has not been investigated extensively for target oligodendrocytes. *In vitro* studies could show lysis of oligodendrocytes as a result of granzyme activity (Pouly et al., 1999).

In our model, we detected substantial numbers of cleaved caspase-3⁺ oligodendrocytic profiles in the optic nerve of PLPtg and PLPtg BMC wt mice. These cells were significantly reduced in PLPtg BMC granzyme B^{-/-} mice, reflecting the fact that granzyme B is an

important mediator of CD8+ T- cell-mediated cytotoxicity leading to (pre) apoptosis of oligodendrocytes.

7.3.2 Immune modulation by the coinhibitory molecule PD-1

To investigate the impact of immune-regulatory mechanisms on the adaptive immunity in our myelin mutants, we focussed on the influence of the coinhibitory molecule programmed death (PD)-1 (CD279), which is an important factor in tissue immune homeostasis and tolerance. PD-1 is a CD28 related receptor mainly expressed on activated T- and B-lymphocytes (Zha et al., 2004). Compared to other members of the CD28 family, it is upregulated at later time points: While CD28 is constitutively expressed and CTLA-4 is expressed during the first 24 hours after T- cell activation, PD-1 is only upregulated after 48-72 hours (Iida et al., 2000; Dong et al., 1999; Zha et al., 2004), suggesting distinct functions of the inhibitory molecules. The CTLA-4 pathway seems to play an important role in limiting the immune response already at the site of activation in the secondary lymphoid organs. The PD-1 pathway, in contrast, appears to modulate the immune response within the target tissue (Carter et al., 2003; Nishimura et al., 2001a). Recent data in mice as well as in humans demonstrate that PD-1 is substantially involved in the control of T- cell homeostasis under physiological and pathological conditions (Okazaki et al., 2006) by preventing uncontrolled proliferation of autoreactive T- cells (Sharpe et al., 2007). Suitably, absence of PD-1 leads to autoimmune diseases as lupus-like nephritis in BL/6 mice and autoimmune cardiomyopathy in BALB/c mice (Nishimura et al., 1999; Nishimura et al., 2001b).

Moreover, the clinical and pathological outcome of some autoimmune disorder models, such as autoimmune diabetes or experimental autoimmune encephalomyelitis (EAE), are substantially aggravated in the absence or by pharmacological modulation of PD-1 or its ligand, PD-L1/B7-homologue 1 (B7-H1; Carter et al., 2007; Fife et al., 2006; Keir et al., 2006; Okazaki et al., 2007; Salama et al., 2003). Due to its inhibitory properties PD-1 - PD-L1/B7-H1 interactions have been proposed to contribute to the mechanisms maintaining peripheral tolerance and limiting inflammatory damage in parenchymal organs (Keir et al., 2006; Salama et al., 2003; Sharpe et al., 2007; Magnus et al., 2005).

In accordance with these functional data, certain polymorphisms in the PD-1 gene are associated with human autoimmune disease (Kroner et al., 2005; Prokunina et al., 2002). Our group recently showed that a PD-1.3 polymorphism at position 7146G/A was linked to a more progressive phenotype of multiple sclerosis (MS). T- lymphocytes bearing the polymorphism were hampered in their PD-1 mediated inhibition of T- cell IFN- γ production, thereby providing a potential link between “immune dysregulation” and progression of CNS inflammation (Kroner et al., 2005).

Regarding the effects of lymphocytes in neural damage, variations within the immune system are indeed an interesting parameter to consider when searching for reasons for strong interindividual variations in hereditary neuropathies. For example, CMT patients from the same family, carrying the same mutation, frequently show strongly aberrant disease courses or even CIDP like subforms (Martini, 1997; Martini et al., 2004). These variations in spite of the same genotype are also present in mouse models. Comparison of usually mildly affected P0+/- mice from different animal facilities yielded substantial variations in myelin damage and immune response (Shy et al., 1997; Schmid et al., 2000). Because regulatory mechanisms of immune cells in the nervous system might explain some of these variations, we investigated the influence of PD-1 on immune cells and development of pathology in our myelin mutants of the PNS and CNS.

7.3.2.1 Increased number of immune cells in the CNS in the absence of PD-1

Our present experiments showed that PD-1 plays a major role in modulating immune cell numbers in the demyelinating model of PLP overexpressing mice: in the absence of PD-1 we found significantly elevated numbers of CD8+ cells in the CNS in comparison to PLPtg mice with normal PD-1-expression. Correspondingly, granzyme B+ cytotoxic effector cells were more frequent in ELISPOT assays with CNS immune cells from PLPtg/PD-1-/- mice in comparison to PLPtg mice. Based on our present finding that granzyme B is an important mediator of lymphocytic cytotoxicity in PLPtg mice, the robust elevation of granzyme B+ cytotoxic effector cells in ELISPOT assays from PLPtg/PD-1-/- myelin mutants perfectly fits with the increase of caspase-3+ profiles and the substantially more severe histopathological phenotype of the myelin mutants devoid of PD-1. It is of note in this context that an elevation of granzyme B has been described to be induced by autoreactive T cells in the absence of PD-1 (Martin-Orozco et al., 2006b). It is, therefore, plausible to assume that in our model absence of PD-1 not only leads to an increase in granzyme B+ effector cells, but also to an upregulation of granzyme B per cell, rendering PD-1-deficient effector cells more aggressive than PD-1+ lymphocytes. Remarkably, not only CD8+ but also CD4+ T- lymphocytes were elevated in the PLPtg mice in the absence of PD-1, but the numbers of CD4+ T- cells were only a fractional amount of CD8+ T- cells.

CD11b+ macrophage / microglia like cells in PLPtg/PD-1-/- mice and the corresponding bone marrow chimeras were only elevated in comparison to myelin wildtype mice, as previously described (Ip et al., 2006a). The absence of PD-1 did not induce any further accumulation of CD11b+ cells.

7.3.2.2 Increased number of immune cells in the PNS in the absence of PD-1

In the quadriceps nerves of P0+/- mice at the age of 10 months, we always detected a significant increase of CD8+ lymphocytes compared to wildtype mice, which is a stable affirmation of earlier results (Schmid et al., 2000; Ip et al., 2006b). When we compared P0+/- mice which received wildtype or PD-1-/- bone marrow, we detected a significant increase of CD8+ lymphocytes in the PD-1-/- transplanted group. Importantly, absence of PD-1 alone in P0+/+ mice did not result in higher numbers of endoneurial lymphocytes. These results already indicate a role of PD-1 in the T- lymphocyte reactivity towards damaged nervous tissue and an increased disposition to T- cell proliferation and / or invasion. CD4+ lymphocytes, in contrast, were hardly present in the nerves of wildtypes and myelin mutants and their amount was not significantly influenced by the presence or absence of PD-1. Quantification of F4/80+ macrophages revealed, as expected, a higher number of macrophages in the quadriceps nerves of P0+/- mice compared to wildtype mice (Schmid et al., 2000; Ip et al., 2006b). In contrast to CD8+ lymphocytes, macrophages did not further increase in the absence of PD-1, indicating a strictly lymphocyte restricted influence of PD-1. Importantly, and in line with earlier observations, the saphenous nerve, which is the mainly sensory part of the femoral nerve, never showed any significant differences between cell counts in wildtype mice, myelin mutants and different bone marrow chimeras. This could reflect a different regulation or protection in the distinct parts of the peripheral nervous system.

An unexpected finding was the massive inflammation in terms of very high amounts of CD4+ and CD8+ lymphocytes as well as F4/80+ macrophages in one single P0+/- BMC PD-1-/- mouse. Due to the fact that these cell numbers differed massively also from other PD-1-/- transplanted mice, we excluded this mouse from the statistics because we could not rule out systemic autoimmune effects. Nevertheless, this massive inflammation could be reminiscent to a subgroup of CMT patients. Some of these display a "CIDP-like" phenotype. It is characterized by atypical features like massive inflammation, steroid responsiveness, asymmetrical electrophysiology and allodynia, meaning pain induced by usually non- painful stimuli (Martini et al., 2004). Despite of the similarities, the extraordinary inflammation was only visible in one mouse and the other characteristics like allodynia were not fulfilled. Importantly, one has to keep in mind when comparing mouse mutants with patients, that in our models the sensory nerves are hardly affected and the peripheral nerve biopsies in patients are usually taken from sensory sural nerves.

Interestingly, the absence of PD-1 seems to exhibit a similar influence to immune cells within the target tissue of myelin mutants of the CNS and PNS. In both cases, the numbers of CD8+ T- lymphocytes were significantly higher than in the presence of PD-1 and the amount

of macrophage-like cells was not altered. On the other hand, an increase of CD4+ lymphocytes as detected in the CNS was not seen in the peripheral nerves. These results indicate a comparable pattern of immune modulation in these two different tissue types with a few subtle differences.

7.3.2.3 Worsened myelin damage in PD-1 deficient CNS myelin mutants

With regard of the tight link of increased numbers of CD8+ cells and granzyme B+ T-lymphocytes on the one hand and increased oligodendrocyte apoptosis and myelin destruction on the other, our results are valid in both double mutants and bone marrow chimeric mice, which were used as complementary and parallel approaches to overcome limitations in the interpretation of either strategy. We assessed myelin damage in PLPtg and wildtype mice in the presence and absence of PD-1 by quantifying axonopathic vacuoles in the optic nerve and the distribution of MBP.

Interestingly, not only CNS damage was more pronounced per individual, but most severely affected individuals always belonged to the group of PLPtg mice in combination to functional disruption of PD-1. In one case we even found a marked lesion with substantial myelin loss and cell accumulation in the optic nerve, which was reminiscent of a plaque frequently found and pathognomonic for MS lesions. Such a phenotype has so far never been found in normal PLPtg mice with intact PD-1 function.

7.3.2.4 Worsened myelin damage in PD-1 deficient PNS myelin mutants

We investigated the myelin damage in different nerves of the PNS, namely sciatic and femoral nerves and ventral roots, by ranking (sciatic nerves, roots) and electron microscopy (femoral nerves and roots). All investigations revealed stronger damage in P0+/-/RAG-1-/- mice which received PD-1-/- bone marrow.

By electron microscopy, we quantified thinly myelinated axons, completely demyelinated axons, degenerating axons and axonopathic vacuoles. Abnormally myelinated axons, including thinly myelinated and completely demyelinated axons and also degenerating axons and axonopathic vacuoles were significantly more frequent in P0+/-/RAG-1-/- BMC PD-1-/- mice. Quantification of some individual parameters did not reach statistical significance, which can be explained by high variations within the groups. Nevertheless, the worst pathology was always detected in PD-1-/- transplanted myelin mutants. These results regarding the pathology are nicely correlated with the amount of CD8+ T- lymphocytes accumulating in the peripheral nerve.

Despite sensory disturbances detected in PD-1 deficient P0+/- mutants, myelin damage in the dorsal roots, representing a sensory part of the peripheral nervous system, did not differ significantly between wt and PD-1-/- transplanted mutants. Even more important, and in line

with earlier experiments, pathological features were far less frequent in dorsal roots than in ventral roots and quadriceps nerves, representing the mainly motor parts of the peripheral nervous system.

Again, the influence of PD-1 in our models of hereditary myelinopathies was similar in the CNS and PNS. In both tissues, the absence of PD-1 per se did not induce any damage or increase of immune cells. While it has been reported that PD-1^{-/-} mice on a C57/Bl6 background show lupus-like glomerulonephritis when aging (Nishimura et al., 1999) we did not observe any obvious organ pathology or spontaneous autoimmunity associated with loss of PD-1 in our experiments and routine urine protein and glucose analysis did not reveal any abnormalities in PD-1^{-/-} mice. However, as soon as the susceptibility was increased due to a myelin mutation, the dysregulation of T- cells strongly increased the damage.

Another interesting observation is the fact that in both studies, regarding CNS and PNS, one animal was exceptionally affected, thus underlining the heterogeneity of tissue immune homeostasis even under standardized experimental conditions.

7.3.2.5 Deteriorated electrophysiology, motor and sensory abilities in PD-1 deficient P0^{+/-} mutants

The functional influence of the absence of PD-1 in P0^{+/-} myelin mutants was further confirmed by the fact that the neural damage was also detected in clinical and paraclinical tests. Neurography of peripheral nerves of P0^{+/-}/RAG-1^{-/-} BMC wt and PD-1^{-/-} mice corroborated the more severe damage in PD-1^{-/-} transplanted myelin mutants. We investigated distal and proximal stimulation and the corresponding amplitudes, duration and nerve conduction velocity (NCV) as well as F- wave latency and persistence. The reduction of amplitudes detected in P0^{+/-}/RAG-1^{-/-} BMC PD-1^{-/-} mice represents a marker for axonal disturbances, in our case reflecting, most likely, secondary axonal loss due to demyelination. The most reliable electrophysiological parameter for myelin damage is the F- wave latency, which was significantly deteriorated in P0^{+/-}/RAG-1^{-/-} BMC PD-1^{-/-} mice.

When performing bilateral electrophysiology, we frequently detected diverging test results between the two sides. As this was seen in both groups, asymmetry was not altered by the absence of PD-1.

Having demonstrated significant deterioration of electrophysiological parameters in P0^{+/-}/RAG-1^{-/-} BMC PD-1^{-/-} mice, we investigated their motor and sensory abilities. The rotarod test did not reveal any significant differences between P0^{+/-}/RAG-1^{-/-} BMC PD-1^{-/-} and wt mice. This might be due to the fact that balancing on the rotarod is a very crude test of motor skills, in which more subtle limitations are difficult to detect.

Nevertheless, when choosing a more subtle method to investigate walking abilities, P0^{+/-}/RAG-1^{-/-} BMC PD-1^{-/-} showed an enlarged distance between feet in the gait test compared

to P0+/-/RAG-1-/- BMC wt mice, suggestive of difficulties to balance and carry their weight (Kunkel-Bagden et al., 1993), which might represent a combination of motor and sensory disturbances, a feature which is reminiscent of CMT. Stride length and rotation angle of the feet were not altered.

When we further investigated sensory features, we detected a delayed response towards stimulation with von Frey hairs in P0+/-/RAG-1-/- BMC PD-1-/- mice. The von Frey test is usually applied to detect allodynia (unusually strong response to pain). However, PD-1-/- BMCs showed a delayed response towards unpleasant stimuli which might reflect general sensory disturbances. In line with these observations, when tested for heat sensitivity, P0+/-/RAG-1-/- BMC PD-1-/- mice showed a trend towards a delayed reaction to heat and in many cases, the test had to be aborted to prevent burning injuries. Termination of the test might have prevented statistical significance. On the other hand, it must be taken into account that thermosensory nerve fibers are preferentially non-myelinated, thereby excluding a direct effect of myelin mutation induced damage.

Detection of sensory disturbances in P0+/-/RAG-1-/- BMC PD-1-/- mice was an unexpected result, because in different models of PNS myelinopathies, P0+/- mice and Cx32-/- mice, we observed myelin damage and immune cell increase only in the mainly motor parts of the peripheral nervous system (Ip et al., 2006b). The saphenous nerve, representing a mainly sensory part of the femoral nerve, was spared from the pathology. Possibly, the slightly increased damage we detected in dorsal roots of PD-1 deficient compared to PD-1 competent myelin mutants was already sufficient to surmount a threshold and induce clinically detectable disturbances.

Investigation of functional abilities in CNS myelin mutants on the rotarod also did not reveal any functional differences, possibly due to the same reasons as in PNS mutants. Unfortunately, electrophysiology is more difficult to perform in the CNS and we did not have the possibility to investigate visually evoked potentials (VEP) in our mice. Nevertheless, no crude behavioural and motor differences were detectable in these mice.

7.3.2.6 Absence of PD-1 favours clonal expansion

However, we found clonal expansions of T- cells in the spleen of PD-1-/- mice using CDR3 spectratyping analysis, a finding highly compatible with the known function of PD-1 in T- cell homeostasis. Concurrent CDR3 regions are suggestive for cells derived from the same clone and therefore a sign for reactivity towards the same antigen. While numerically not elevated in the CNS at 12 months, the CD8+ cells of PLPwt/PD-1-/- mice showed multiple clonal T- cell expansions, as opposed to PD-1-expressing CD8+ cells of normal wildtype mice which do not show any repertoire perturbations. The corresponding CD8+ cells of PLPtg mice

display their characteristic mono- or oligoclonal expansion in the CNS as previously described (Leder et al., 2007). In spite of these findings, the presence of clonal expansions per se can not be regarded as a sign of T- cell proliferation as a response to a specific stimulus, it represents merely a higher susceptibility of T- lymphocytes.

Interestingly, in contrast to other observations which were similar in the CNS and PNS, no evidence of clonal expansion could be detected in lymphocytes obtained from peripheral nerves of P0+/- mice and P0+/-/RAG-1-/- BMC wt and P0+/-/RAG-1-/- BMC PD-1-/- mice, while present in spleen derived lymphocytes of P0+/-/RAG-1-/- BMC PD-1-/-.

This could be due to technical limitations, related to the relatively small number of T- lymphocytes in the peripheral nerve tissue.

7.3.2.7 Increased IFN- γ production in the absence of PD-1

The combination of myelin mutations with PD-1 deficiency led to significantly higher numbers of T- cells within the target tissue and, as shown for the CNS, of granzyme B+ effector cells of proven pathological relevance. Moreover, CD8+ T- lymphocytes of PD-1 mutants are aberrant with regard of their prominent clonal expansions in the CNS. This suggests that PD-1 prevents a large number of possible clonal expansions of a variety of T- cell clones in the CNS myelin mutants. PD-1 signalling might quench the T- cell signal transduction below a threshold necessary for activation and proliferation. Indeed, PD-1 signalling is known to attenuate signals of the T- cell receptor such as PKC θ and ZAP-70/CD3 ζ (Sheppard et al., 2004).

This could also be the explanation that only CNS T- cells deficient of PD-1 show markedly enhanced IFN- γ secretion after stimulation with the PKC-activator PMA and the Ca⁺⁺ ionophor ionomycin as revealed by ELISPOT assays, in line with earlier descriptions of increased IFN- γ production in the absence of PD-1 during graft versus host disease (Blazar et al., 2003). Aberrantly, CNS CD8+ cells from genuine PLPtg mice did not show any relevant production of this proinflammatory cytokine. Splenocytes, in contrast, displayed substantial stimulus-related IFN- γ production under any genotype condition. These findings suggest that (1) although prominently expanded and highly susceptible to become activated, PD-1-deficient T- lymphocytes appear to be pathologically “silent” when combined with a normal or healthy environment and that (2) the PD-1 pathway seems critical for homeostasis of cytotoxic T- cells in the tissue.

In the PLP overexpression model, we characterized the pathogenic CD8+ T- lymphocytes as CD44+/CD69+/CD62L- activated effector cells (Ip et al., 2006a). In the P0+/- mutants, we now show that the nerve derived CD8+ T- cells display a similar phenotype and demonstrate – in comparison to P0+/+ mice – an enhanced propensity to secrete proinflammatory cytokines after stimulation with the PKC-activator PMA and the Ca⁺⁺ ionophor ionomycin as

revealed by ELISPOT assays. This propensity also showed a trend towards a further increase in the absence of PD-1. Taken together, PD-1-deficiency leads to a strongly increased pathogenetically relevant increase of immune cells and immune cell activity in both the PLP_{tg} and P0^{+/-} myelin mutants, supporting the view that PD-1 is a regulator of tissue homeostasis of a wide range of disease-relevant conditions (Okazaki et al., 2007; Okazaki et al., 2006; Sharpe et al., 2007).

7.4 Synopsis

Based on earlier studies where we could show the importance and pathogenetic relevance of CD8⁺ T- lymphocytes PLP_{tg} mice (Ip et al., 2006a), it was important to investigate which cytotoxic factors contribute to the neural damage in these mice. In this study, we could identify granzyme B as a relevant molecule inducing myelin damage and oligodendrocyte apoptosis in myelin mutants. Nevertheless, due to the fact that the damage was reduced but not completely abolished, we can speculate that additional cytotoxic molecules, e.g. perforin, might be involved in the pathogenesis. However, not only cytotoxic effector molecules but factors modulating the T- cell activity, like PD-1, are crucially involved in the disease regulation.

It is assumed that interaction of PD-1 with its cognate ligand, the B7-homologue 1 (PD-L1/B7-H1), is required for its co-inhibitory function. Due to its inhibitory properties PD-L1 has been proposed to contribute to the mechanisms maintaining peripheral tolerance and limiting inflammatory damage in parenchymal organs (Keir et al., 2006; Magnus et al., 2005; Sharpe et al., 2007; Ortler et al., 2008). Parenchymal PD-L1 contributes to the limitation of insulinitis and the resolution of inflammation (Martin-Orozco et al., 2006a). Recent publications report that PD-L1 is expressed and upregulated on CNS cells (e.g. microglia cells) under inflammatory conditions (Magnus et al., 2005; Salama et al., 2003), restricts parenchymal neuroantigen-specific T- cell responses and confines inflammatory CNS damage in MOG-induced active experimental autoimmune encephalomyelitis (Ortler et al., 2008). One therefore might assume that PD-L1 - PD-1 interactions counteract T- cell mediated pathology observed in PLP_{tg} mice by limiting clonal expansion and cytokine release of detrimentally self-reactive low avidity clones.

A synoptic view summarizing our recent and previous observations may be as follows (**Figure 32**): one could hypothesize that the presence of myelin mutations may induce intracellular stress that causes several immune-relevant glial reactions, such as expression of cytokines, like MCP-1, in Schwann cells of P0^{+/-} mice (Fischer et al., 2008a) and, as seen in one of our previous studies, upregulation of MHC-I molecules on oligodendrocytes (Ip et al., 2006a) and Sialoadhesin on the surface of CD11b⁺ macrophage-like cells. It is of note that the latter reaction is an important prerequisite for CD8⁺ effector cell activation in PLP_{tg}

mice (Ip et al., 2007). Furthermore, in case of the CNS myelin mutants, supraphysiological concentrations of myelin antigens associated with PLP-overexpression could promote reactivity of low-avidity T- cell clones that survived clonal deletion or ignorance in the thymus (Leder et al., 2007). CNS-derived, but not spleen-derived CD8⁺ cells show mono- or oligoclonal expansions, further suggesting CNS-restricted specificity against yet unidentified CNS-antigens.

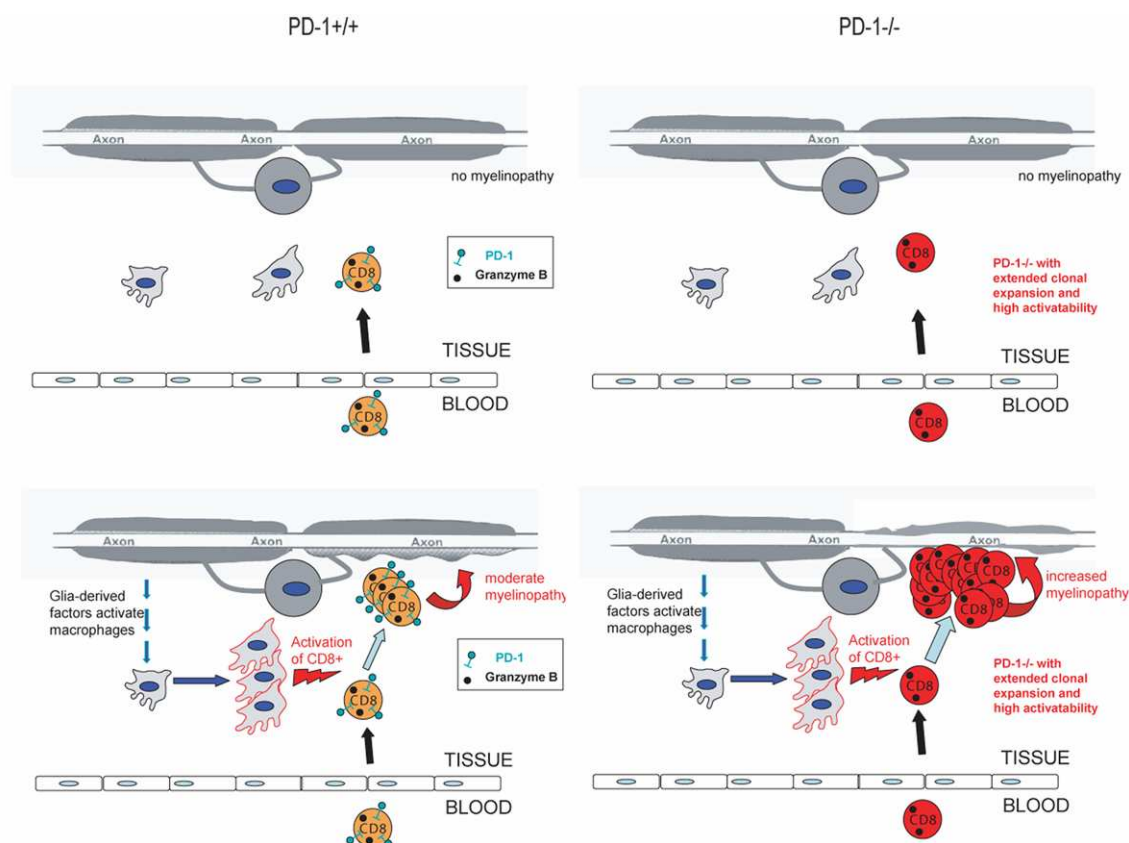


Figure 32: Synoptic view of the pathological mechanisms occurring in the CNS of myelin mutants in the presence and absence of PD-1

Unphysiological myelin protein expression in glial cells may induce intracellular stress that leads to glia-related expression of cytokines, upregulation of MHC-I molecules on oligodendrocytes and Sn expression on the surface of macrophage-like cells. Furthermore, supraphysiological concentrations of myelin antigens could promote reactivity of low-avidity T- cell clones. In the presence of PD-1 on CD8⁺ cells, activation and proliferation is limited (orange cells), as reflected by a moderate elevation of the cells and significant yet limited neural damage. Absence of PD-1, however, leads to substantial increase of CD8⁺ cells and an aggravation of neural damage. The propensity of PD-1 deficient CNS T- cells to secrete proinflammatory cytokines and to perform multiple clonal expansions reflects increased “immunoaggressive” features of the CD8⁺ T- cells (red cells).

PD-1 is critically involved in these processes: in the presence of PD-1 on CD8⁺ effector cells, activation and proliferation is limited, as reflected by a moderate elevation of the cells and

significant yet limited neural damage. Absence of PD-1, however, leads to substantial increase of CD8+ effector cells and an aggravation of neural damage in CNS and PNS, even leading to *bona fide* lesions in rare cases. The additional propensity of PD-1 deficient T- cells in the CNS and PNS to secrete proinflammatory cytokines reflects a higher susceptibility to become activated, resulting in the more “immunoaggressive” features of the CD8+ effector cells. Additionally, multiple clonal expansions of these cells might be an important prerequisite for the high pathogenic capacity of PD-1-deficient T- cells.

Taken together, our study demonstrates that 1) granzyme B is an important mediator of CD8+ cell-mediated cytotoxicity in PLP_{tg} mice and that 2) the co-inhibitory molecule PD-1 modulates glial-injury-related immune responses in the CNS and PNS. As shown for the CNS, PD-1 regulates granzyme B+ effector cells, attenuates the propensity of CD8+ cells to secrete proinflammatory cytokines and limits clonal expansions of CD8+ T- lymphocytes. Importantly, both in the CNS and PNS, PD-1-deficiency is pathogenetically silent as long as tissue-specific molecular or cellular abnormalities are absent. However, the combination of impaired immune-modulation and a low-grade, glial-related inflammation leads to a substantial exacerbation of the primary glial injury and accumulation of immune cells. This impressively reflects the high pathological relevance of immunomodulatory mechanisms under various pathological conditions and should be particularly considered when seeking for mechanisms leading to the high clinical variability of polygenic or even monogenic disorders of the nervous system.

8. Literature

- Adlkofer, K., Frei, R., Neuberg, D. H., Zielasek, J., Toyka, K. V., Suter, U., 1997. Heterozygous peripheral myelin protein 22-deficient mice are affected by a progressive demyelinating tomaculous neuropathy. *J Neurosci.* 17, 4662-71.
- Adlkofer, K., Martini, R., Aguzzi, A., Zielasek, J., Toyka, K. V., Suter, U., 1995. Hypermyelination and demyelinating peripheral neuropathy in Pmp22-deficient mice. *Nat Genet.* 11, 274-80.
- Adrain, C., Murphy, B. M., Martin, S. J., 2005. Molecular ordering of the caspase activation cascade initiated by the cytotoxic T lymphocyte/natural killer (CTL/NK) protease granzyme B. *J Biol Chem.* 280, 4663-73.
- Agata, Y., Kawasaki, A., Nishimura, H., Ishida, Y., Tsubata, T., Yagita, H., Honjo, T., 1996. Expression of the PD-1 antigen on the surface of stimulated mouse T and B lymphocytes. *Int Immunol.* 8, 765-72.
- Akiyama, H., Barger, S., Barnum, S., Bradt, B., Bauer, J., Cole, G. M., Cooper, N. R., Eikelenboom, P., Emmerling, M., Fiebich, B. L., Finch, C. E., Frautschy, S., Griffin, W. S., Hampel, H., Hull, M., Landreth, G., Lue, L., Mrak, R., Mackenzie, I. R., McGeer, P. L., O'Banion, M. K., Pachter, J., Pasinetti, G., Plata-Salaman, C., Rogers, J., Rydel, R., Shen, Y., Streit, W., Strohmeyer, R., Tooyoma, I., Van Muiswinkel, F. L., Veerhuis, R., Walker, D., Webster, S., Wegrzyniak, B., Wenk, G., Wyss-Coray, T., 2000. Inflammation and Alzheimer's disease. *Neurobiol Aging.* 21, 383-421.
- Amici, S. A., Dunn, W. A., Jr., Notterpek, L., 2007. Developmental abnormalities in the nerves of peripheral myelin protein 22-deficient mice. *J Neurosci Res.* 85, 238-49.
- Anderson, T. J., Schneider, A., Barrie, J. A., Klugmann, M., McCulloch, M. C., Kirkham, D., Kyriakides, E., Nave, K. A., Griffiths, I. R., 1998. Late-onset neurodegeneration in mice with increased dosage of the proteolipid protein gene. *J Comp Neurol.* 394, 506-19.
- Anzini, P., Neuberg, D. H., Schachner, M., Nelles, E., Willecke, K., Zielasek, J., Toyka, K. V., Suter, U., Martini, R., 1997. Structural abnormalities and deficient maintenance of peripheral nerve myelin in mice lacking the gap junction protein connexin 32. *J Neurosci.* 17, 4545-51.
- Arroyo, E. J., Scherer, S. S., 2000. On the molecular architecture of myelinated fibers. *Histochem Cell Biol.* 113, 1-18.
- Barbarese, E., Braun, P. E., Carson, J. H., 1977. Identification of prelarge and presmall basic proteins in mouse myelin and their structural relationship to large and small basic proteins. *Proc Natl Acad Sci U S A.* 74, 3360-4.

- Barbarese, E., Nielson, M. L., Carson, J. H., 1983. The effect of the shiverer mutation on myelin basic protein expression in homozygous and heterozygous mouse brain. *J Neurochem.* 40, 1680-6.
- Barnett, M. H., Prineas, J. W., 2004. Relapsing and remitting multiple sclerosis: pathology of the newly forming lesion. *Ann Neurol.* 55, 458-68.
- Baxter, R. V., Ben Othmane, K., Rochelle, J. M., Stajich, J. E., Hulette, C., Dew-Knight, S., Hentati, F., Ben Hamida, M., Bel, S., Stenger, J. E., Gilbert, J. R., Pericak-Vance, M. A., Vance, J. M., 2002. Ganglioside-induced differentiation-associated protein-1 is mutant in Charcot-Marie-Tooth disease type 4A/8q21. *Nat Genet.* 30, 21-2.
- Berghoff, M., Samsam, M., Muller, M., Kobsar, I., Toyka, K. V., Kiefer, R., Maurer, M., Martini, R., 2005. Neuroprotective effect of the immune system in a mouse model of severe dysmyelinating hereditary neuropathy: enhanced axonal degeneration following disruption of the RAG-1 gene. *Mol Cell Neurosci.* 28, 118-27.
- Bergoffen, J., Scherer, S. S., Wang, S., Scott, M. O., Bone, L. J., Paul, D. L., Chen, K., Lensch, M. W., Chance, P. F., Fischbeck, K. H., 1993. Connexin mutations in X-linked Charcot-Marie-Tooth disease. *Science.* 262, 2039-42.
- Bird, T. D., Ott, J., Giblett, E. R., 1982. Evidence for linkage of Charcot-Marie-Tooth neuropathy to the Duffy locus on chromosome 1. *Am J Hum Genet.* 34, 388-94.
- Birouk, N., Gouider, R., Le Guern, E., Gugenheim, M., Tardieu, S., Maisonobe, T., Le Forestier, N., Agid, Y., Brice, A., Bouche, P., 1997. Charcot-Marie-Tooth disease type 1A with 17p11.2 duplication. Clinical and electrophysiological phenotype study and factors influencing disease severity in 119 cases. *Brain.* 120 (Pt 5), 813-23.
- Blazar, B. R., Carreno, B. M., Panoskaltis-Mortari, A., Carter, L., Iwai, Y., Yagita, H., Nishimura, H., Taylor, P. A., 2003. Blockade of programmed death-1 engagement accelerates graft-versus-host disease lethality by an IFN-gamma-dependent mechanism. *J Immunol.* 171, 1272-7.
- Boison, D., Stoffel, W., 1994. Disruption of the compacted myelin sheath of axons of the central nervous system in proteolipid protein-deficient mice. *Proc Natl Acad Sci U S A.* 91, 11709-13.
- Bolino, A., Muglia, M., Conforti, F. L., LeGuern, E., Salih, M. A., Georgiou, D. M., Christodoulou, K., Hausmanowa-Petrusewicz, I., Mandich, P., Schenone, A., Gambardella, A., Bono, F., Quattrone, A., Devoto, M., Monaco, A. P., 2000. Charcot-Marie-Tooth type 4B is caused by mutations in the gene encoding myotubularin-related protein-2. *Nat Genet.* 25, 17-9.
- Bolitho, P., Voskoboinik, I., Trapani, J. A., Smyth, M. J., 2007. Apoptosis induced by the lymphocyte effector molecule perforin. *Curr Opin Immunol.* 19, 339-47.
- Bots, M., Medema, J. P., 2006. Granzymes at a glance. *J Cell Sci.* 119, 5011-4.

- Brunner, C., Lassmann, H., Waehneltd, T. V., Matthieu, J. M., Lington, C., 1989. Differential ultrastructural localization of myelin basic protein, myelin/oligodendroglial glycoprotein, and 2',3'-cyclic nucleotide 3'-phosphodiesterase in the CNS of adult rats. *J Neurochem.* 52, 296-304.
- Cailloux, F., Gauthier-Barichard, F., Mimault, C., Isabelle, V., Courtois, V., Giraud, G., Dastugue, B., Boespflug-Tanguy, O., 2000. Genotype-phenotype correlation in inherited brain myelination defects due to proteolipid protein gene mutations. *Clinical European Network on Brain Dysmyelinating Disease. Eur J Hum Genet.* 8, 837-45.
- Carenini, S., Maurer, M., Werner, A., Blazyca, H., Toyka, K. V., Schmid, C. D., Raivich, G., Martini, R., 2001. The role of macrophages in demyelinating peripheral nervous system of mice heterozygously deficient in p0. *J Cell Biol.* 152, 301-8.
- Carenini, S., Montag, D., Cremer, H., Schachner, M., Martini, R., 1997. Absence of the myelin-associated glycoprotein (MAG) and the neural cell adhesion molecule (N-CAM) interferes with the maintenance, but not with the formation of peripheral myelin. *Cell Tissue Res.* 287, 3-9.
- Carter, L., Fouser, L. A., Jussif, J., Fitz, L., Deng, B., Wood, C. R., Collins, M., Honjo, T., Freeman, G. J., Carreno, B. M., 2002. PD-1:PD-L inhibitory pathway affects both CD4(+) and CD8(+) T cells and is overcome by IL-2. *Eur J Immunol.* 32, 634-43.
- Carter, L. L., Carreno, B. M., 2003. Cytotoxic T-lymphocyte antigen-4 and programmed death-1 function as negative regulators of lymphocyte activation. *Immunol Res.* 28, 49-59.
- Carter, L. L., Leach, M. W., Azoitei, M. L., Cui, J., Pelker, J. W., Jussif, J., Benoit, S., Ireland, G., Luxenberg, D., Askew, G. R., Milarski, K. L., Groves, C., Brown, T., Carito, B. A., Percival, K., Carreno, B. M., Collins, M., Marusic, S., 2007. PD-1/PD-L1, but not PD-1/PD-L2, interactions regulate the severity of experimental autoimmune encephalomyelitis. *J Neuroimmunol.* 182, 124-34.
- Cerghet, M., Bessert, D. A., Nave, K. A., Skoff, R. P., 2001. Differential expression of apoptotic markers in jimpy and in Plp overexpressors: evidence for different apoptotic pathways. *J Neurocytol.* 30, 841-55.
- Chance, P. F., Alderson, M. K., Leppig, K. A., Lensch, M. W., Matsunami, N., Smith, B., Swanson, P. D., Odelberg, S. J., Distech, C. M., Bird, T. D., 1993. DNA deletion associated with hereditary neuropathy with liability to pressure palsies. *Cell.* 72, 143-51.
- Chaplan, S. R., Bach, F. W., Pogrel, J. W., Chung, J. M., Yaksh, T. L., 1994. Quantitative assessment of tactile allodynia in the rat paw. *J Neurosci Methods.* 53, 55-63.
- Chowdhury, D., Lieberman, J., 2008. Death by a thousand cuts: granzyme pathways of programmed cell death. *Annu Rev Immunol.* 26, 389-420.

-
- Cullen, S. P., Martin, S. J., 2008. Mechanisms of granule-dependent killing. *Cell Death Differ.* 15, 251-62.
- D'Urso, D., Brophy, P. J., Staugaitis, S. M., Gillespie, C. S., Frey, A. B., Stempak, J. G., Colman, D. R., 1990. Protein zero of peripheral nerve myelin: biosynthesis, membrane insertion, and evidence for homotypic interaction. *Neuron.* 4, 449-60.
- D'Urso, D., Prior, R., Greiner-Petter, R., Gabreels-Festen, A. A., Muller, H. W., 1998. Overloaded endoplasmic reticulum-Golgi compartments, a possible pathomechanism of peripheral neuropathies caused by mutations of the peripheral myelin protein PMP22. *J Neurosci.* 18, 731-40.
- De Jonghe, P., Timmerman, V., Ceuterick, C., Nelis, E., De Vriendt, E., Lofgren, A., Vercruyssen, A., Verellen, C., Van Maldergem, L., Martin, J. J., Van Broeckhoven, C., 1999. The Thr124Met mutation in the peripheral myelin protein zero (MPZ) gene is associated with a clinically distinct Charcot-Marie-Tooth phenotype. *Brain.* 122 (Pt 2), 281-90.
- De Jonghe, P., Timmerman, V., Nelis, E., Martin, J. J., Van Broeckhoven, C., 1997. Charcot-Marie-Tooth disease and related peripheral neuropathies. *J Peripher Nerv Syst.* 2, 370-87.
- Dickinson, P. J., Fanarraga, M. L., Griffiths, I. R., Barrie, J. M., Kyriakides, E., Montague, P., 1996. Oligodendrocyte progenitors in the embryonic spinal cord express DM-20. *Neuropathol Appl Neurobiol.* 22, 188-98.
- Dong, H., Zhu, G., Tamada, K., Chen, L., 1999. B7-H1, a third member of the B7 family, co-stimulates T-cell proliferation and interleukin-10 secretion. *Nat Med.* 5, 1365-9.
- Duchen, L. W., Eicher, E. M., Jacobs, J. M., Scaravilli, F., Teixeira, F., 1980. Hereditary leucodystrophy in the mouse: the new mutant twitcher. *Brain.* 103, 695-710.
- Eichler, F., Van Haren, K., 2007. Immune response in leukodystrophies. *Pediatr Neurol.* 37, 235-44.
- Evgrafov, O. V., Mersyanova, I., Irobi, J., Van Den Bosch, L., Dierick, I., Leung, C. L., Schagina, O., Verpoorten, N., Van Impe, K., Fedotov, V., Dadali, E., Auer-Grumbach, M., Windpassinger, C., Wagner, K., Mitrovic, Z., Hilton-Jones, D., Talbot, K., Martin, J. J., Vasserman, N., Tverskaya, S., Polyakov, A., Liem, R. K., Gettemans, J., Robberecht, W., De Jonghe, P., Timmerman, V., 2004. Mutant small heat-shock protein 27 causes axonal Charcot-Marie-Tooth disease and distal hereditary motor neuropathy. *Nat Genet.* 36, 602-6.
- Fanarraga, M. L., Dickinson, P. J., Sommer, I., Montague, P., Kyriakides, E., Griffiths, I. R., 1996. Evidence that some oligodendrocyte progenitors in the developing optic pathway express the plp gene. *Glia.* 18, 282-92.

- Fife, B. T., Guleria, I., Gubbels Bupp, M., Eagar, T. N., Tang, Q., Bour-Jordan, H., Yagita, H., Azuma, M., Sayegh, M. H., Bluestone, J. A., 2006. Insulin-induced remission in new-onset NOD mice is maintained by the PD-1-PD-L1 pathway. *J Exp Med.* 203, 2737-47.
- Filbin, M. T., 2006. Recapitulate development to promote axonal regeneration: good or bad approach? *Philos Trans R Soc Lond B Biol Sci.* 361, 1565-74.
- Filbin, M. T., Tennekoon, G. I., 1993. Homophilic adhesion of the myelin P0 protein requires glycosylation of both molecules in the homophilic pair. *J Cell Biol.* 122, 451-9.
- Fischer, S., Kleinschnitz, C., Muller, M., Kobsar, I., Ip, C. W., Rollins, B., Martini, R., 2008a. Monocyte chemoattractant protein-1 is a pathogenic component in a model for a hereditary peripheral neuropathy. *Mol Cell Neurosci.* 37, 359-66.
- Fischer, S., Weishaupt, A., Troppmair, J., Martini, R., 2008b. Increase of MCP-1 (CCL2) in myelin mutant Schwann cells is mediated by MEK-ERK signaling pathway. *Glia.* 56, 836-43.
- Fruttiger, M., Montag, D., Schachner, M., Martini, R., 1995. Crucial role for the myelin-associated glycoprotein in the maintenance of axon-myelin integrity. *Eur J Neurosci.* 7, 511-5.
- Gabreels-Festen, A. A., Gabreels, F. J., Jennekens, F. G., Joosten, E. M., Janssen-van Kempen, T. W., 1992. Autosomal recessive form of hereditary motor and sensory neuropathy type I. *Neurology.* 42, 1755-61.
- Gal, A., Mucke, J., Theile, H., Wieacker, P. F., Ropers, H. H., Wienker, T. F., 1985. X-linked dominant Charcot-Marie-Tooth disease: suggestion of linkage with a cloned DNA sequence from the proximal Xq. *Hum Genet.* 70, 38-42.
- Garcia, C. A., Malamut, R. E., England, J. D., Parry, G. S., Liu, P., Lupski, J. R., 1995. Clinical variability in two pairs of identical twins with the Charcot-Marie-Tooth disease type 1A duplication. *Neurology.* 45, 2090-3.
- Gay, C. T., Hardies, L. J., Rauch, R. A., Lancaster, J. L., Plaetke, R., DuPont, B. R., Cody, J. D., Cornell, J. E., Herndon, R. C., Ghidoni, P. D., Schiff, J. M., Kaye, C. I., Leach, R. J., Fox, P. T., 1997. Magnetic resonance imaging demonstrates incomplete myelination in 18q- syndrome: evidence for myelin basic protein haploinsufficiency. *Am J Med Genet.* 74, 422-31.
- Giese, K. P., Martini, R., Lemke, G., Soriano, P., Schachner, M., 1992. Mouse P0 gene disruption leads to hypomyelination, abnormal expression of recognition molecules, and degeneration of myelin and axons. *Cell.* 71, 565-76.
- Gimmi, C. D., Freeman, G. J., Gribben, J. G., Sugita, K., Freedman, A. S., Morimoto, C., Nadler, L. M., 1991. B-cell surface antigen B7 provides a costimulatory signal that

- induces T cells to proliferate and secrete interleukin 2. *Proc Natl Acad Sci U S A.* 88, 6575-9.
- Gorman, M. P., Golomb, M. R., Walsh, L. E., Hobson, G. M., Garbern, J. Y., Kinkel, R. P., Darras, B. T., Urion, D. K., Eksioglu, Y. Z., 2007. Steroid-responsive neurologic relapses in a child with a proteolipid protein-1 mutation. *Neurology.* 68, 1305-7.
- Gould, R. M., Byrd, A. L., Barbarese, E., 1995. The number of Schmidt-Lanterman incisures is more than doubled in shiverer PNS myelin sheaths. *J Neurocytol.* 24, 85-98.
- Gow, A., Lazzarini, R. A., 1996. A cellular mechanism governing the severity of Pelizaeus-Merzbacher disease. *Nat Genet.* 13, 422-8.
- Greenfield, S., Brostoff, S., Eylar, E. H., Morell, P., 1973. Protein composition of myelin of the peripheral nervous system. *J Neurochem.* 20, 1207-16.
- Greenwald, R. J., Freeman, G. J., Sharpe, A. H., 2005. The B7 family revisited. *Annu Rev Immunol.* 23, 515-48.
- Griffiths, I., Klugmann, M., Anderson, T., Thomson, C., Vouyiouklis, D., Nave, K. A., 1998a. Current concepts of PLP and its role in the nervous system. *Microsc Res Tech.* 41, 344-58.
- Griffiths, I., Klugmann, M., Anderson, T., Yool, D., Thomson, C., Schwab, M. H., Schneider, A., Zimmermann, F., McCulloch, M., Nadon, N., Nave, K. A., 1998b. Axonal swellings and degeneration in mice lacking the major proteolipid of myelin. *Science.* 280, 1610-3.
- Griffiths, I. R., Dickinson, P., Montague, P., 1995a. Expression of the proteolipid protein gene in glial cells of the post-natal peripheral nervous system of rodents. *Neuropathol Appl Neurobiol.* 21, 97-110.
- Griffiths, I. R., Schneider, A., Anderson, J., Nave, K. A., 1995b. Transgenic and natural mouse models of proteolipid protein (PLP)-related dysmyelination and demyelination. *Brain Pathol.* 5, 275-81.
- Griffiths, I. R., Scott, I., McCulloch, M. C., Barrie, J. A., McPhilemy, K., Cattanach, B. M., 1990. Rumpshaker mouse: a new X-linked mutation affecting myelination: evidence for a defect in PLP expression. *J Neurocytol.* 19, 273-83.
- Grohmann, K., Rossoll, W., Kobsar, I., Holtmann, B., Jablonka, S., Wessig, C., Stoltenburg-Didinger, G., Fischer, U., Hubner, C., Martini, R., Sendtner, M., 2004. Characterization of *Ighmbp2* in motor neurons and implications for the pathomechanism in a mouse model of human spinal muscular atrophy with respiratory distress type 1 (SMARD1). *Hum Mol Genet.* 13, 2031-42.
- Grundtner, R., Dornmair, K., Dahm, R., Flugel, A., Kawakami, N., Zeitelhofer, M., Schoderboeck, L., Nosov, M., Selzer, E., Willheim, M., Kagawa, T., 2007. Transition

- from enhanced T cell infiltration to inflammation in the myelin-degenerative central nervous system. *Neurobiol Dis.* 28, 261-75.
- Guenard, V., Montag, D., Schachner, M., Martini, R., 1996. Onion bulb cells in mice deficient for myelin genes share molecular properties with immature, differentiated non-myelinating, and denervated Schwann cells. *Glia.* 18, 27-38.
- Harding, A. E., Thomas, P. K., 1980. The clinical features of hereditary motor and sensory neuropathy types I and II. *Brain.* 103, 259-80.
- Hargreaves, K., Dubner, R., Brown, F., Flores, C., Joris, J., 1988. A new and sensitive method for measuring thermal nociception in cutaneous hyperalgesia. *Pain.* 32, 77-88.
- Hayasaka, K., Himoro, M., Sato, W., Takada, G., Uyemura, K., Shimizu, N., Bird, T. D., Conneally, P. M., Chance, P. F., 1993a. Charcot-Marie-Tooth neuropathy type 1B is associated with mutations of the myelin P0 gene. *Nat Genet.* 5, 31-4.
- Hayasaka, K., Himoro, M., Sawaishi, Y., Nanao, K., Takahashi, T., Takada, G., Nicholson, G. A., Ouvrier, R. A., Tachi, N., 1993b. De novo mutation of the myelin P0 gene in Dejerine-Sottas disease (hereditary motor and sensory neuropathy type III). *Nat Genet.* 5, 266-8.
- Hayasaka, K., Ohnishi, A., Takada, G., Fukushima, Y., Murai, Y., 1993c. Mutation of the myelin P0 gene in Charcot-Marie-tooth neuropathy type 1. *Biochem Biophys Res Commun.* 194, 1317-22.
- Hayasaka, K., Takada, G., Ionasescu, V. V., 1993d. Mutation of the myelin P0 gene in Charcot-Marie-Tooth neuropathy type 1B. *Hum Mol Genet.* 2, 1369-72.
- Hess, B., Saftig, P., Hartmann, D., Coenen, R., Lullmann-Rauch, R., Goebel, H. H., Evers, M., von Figura, K., D'Hooge, R., Nagels, G., De Deyn, P., Peters, C., Gieselmann, V., 1996. Phenotype of arylsulfatase A-deficient mice: relationship to human metachromatic leukodystrophy. *Proc Natl Acad Sci U S A.* 93, 14821-6.
- Hughes, R. A., Allen, D., Makowska, A., Gregson, N. A., 2006. Pathogenesis of chronic inflammatory demyelinating polyradiculoneuropathy. *J Peripher Nerv Syst.* 11, 30-46.
- Huxley, C., Passage, E., Manson, A., Putzu, G., Figarella-Branger, D., Pellissier, J. F., Fontes, M., 1996. Construction of a mouse model of Charcot-Marie-Tooth disease type 1A by pronuclear injection of human YAC DNA. *Hum Mol Genet.* 5, 563-9.
- Iida, T., Ohno, H., Nakaseko, C., Sakuma, M., Takeda-Ezaki, M., Arase, H., Kominami, E., Fujisawa, T., Saito, T., 2000. Regulation of cell surface expression of CTLA-4 by secretion of CTLA-4-containing lysosomes upon activation of CD4+ T cells. *J Immunol.* 165, 5062-8.

- Ionasescu, V. V., Searby, C. C., Ionasescu, R., Chatkupt, S., Patel, N., Koenigsberger, R., 1997. Dejerine-Sottas neuropathy in mother and son with same point mutation of PMP22 gene. *Muscle Nerve*. 20, 97-9.
- Ip, C. W., Kohl, B., Kleinschnitz, C., Reuss, B., Nave, K. A., Kroner, A., Martini, R., 2008. Origin of CD11b+ macrophage-like cells in the CNS of PLP-overexpressing mice: Low influx of haematogenous macrophages and unchanged blood-brain-barrier in the optic nerve. *Mol Cell Neurosci*.
- Ip, C. W., Kroner, A., Bendszus, M., Leder, C., Kobsar, I., Fischer, S., Wiendl, H., Nave, K. A., Martini, R., 2006a. Immune cells contribute to myelin degeneration and axonopathic changes in mice overexpressing proteolipid protein in oligodendrocytes. *J Neurosci*. 26, 8206-16.
- Ip, C. W., Kroner, A., Crocker, P. R., Nave, K. A., Martini, R., 2007. Sialoadhesin deficiency ameliorates myelin degeneration and axonopathic changes in the CNS of PLP overexpressing mice. *Neurobiol Dis*. 25, 105-11.
- Ip, C. W., Kroner, A., Fischer, S., Berghoff, M., Kobsar, I., Maurer, M., Martini, R., 2006b. Role of immune cells in animal models for inherited peripheral neuropathies. *Neuromolecular Med*. 8, 175-90.
- Ishida, Y., Agata, Y., Shibahara, K., Honjo, T., 1992. Induced expression of PD-1, a novel member of the immunoglobulin gene superfamily, upon programmed cell death. *Embo J*. 11, 3887-95.
- Ito, M., Blumberg, B. M., Mock, D. J., Goodman, A. D., Moser, A. B., Moser, H. W., Smith, K. D., Powers, J. M., 2001. Potential environmental and host participants in the early white matter lesion of adreno-leukodystrophy: morphologic evidence for CD8 cytotoxic T cells, cytolysis of oligodendrocytes, and CD1-mediated lipid antigen presentation. *J Neuropathol Exp Neurol*. 60, 1004-19.
- Jacobs, E. C., 2005. Genetic alterations in the mouse myelin basic proteins result in a range of dysmyelinating disorders. *J Neurol Sci*. 228, 195-7.
- Johns, T. G., Bernard, C. C., 1999. The structure and function of myelin oligodendrocyte glycoprotein. *J Neurochem*. 72, 1-9.
- Johnson, R. S., Roder, J. C., Riordan, J. R., 1995. Over-expression of the DM-20 myelin proteolipid causes central nervous system demyelination in transgenic mice. *J Neurochem*. 64, 967-76.
- Kagawa, T., Ikenaka, K., Inoue, Y., Kuriyama, S., Tsujii, T., Nakao, J., Nakajima, K., Aruga, J., Okano, H., Mikoshiba, K., 1994. Glial cell degeneration and hypomyelination caused by overexpression of myelin proteolipid protein gene. *Neuron*. 13, 427-42.

- Kagi, D., Ledermann, B., Burki, K., Seiler, P., Odermatt, B., Olsen, K. J., Podack, E. R., Zinkernagel, R. M., Hengartner, H., 1994. Cytotoxicity mediated by T cells and natural killer cells is greatly impaired in perforin-deficient mice. *Nature*. 369, 31-7.
- Kandel, E., Schwartz, J., Jessell, T.: Principles of Neural Science. New York: 4 th Edition, McGraw- Hill, 2000.
- Kamholz, J., de Ferra, F., Puckett, C., Lazzarini, R., 1986. Identification of three forms of human myelin basic protein by cDNA cloning. *Proc Natl Acad Sci U S A*. 83, 4962-6.
- Kaplan, M. R., Meyer-Franke, A., Lambert, S., Bennett, V., Duncan, I. D., Levinson, S. R., Barres, B. A., 1997. Induction of sodium channel clustering by oligodendrocytes. *Nature*. 386, 724-8.
- Kassmann, C. M., Lappe-Siefke, C., Baes, M., Brugger, B., Mildner, A., Werner, H. B., Natt, O., Michaelis, T., Prinz, M., Frahm, J., Nave, K. A., 2007. Axonal loss and neuroinflammation caused by peroxisome-deficient oligodendrocytes. *Nat Genet*. 39, 969-76.
- Keefe, D., Shi, L., Feske, S., Massol, R., Navarro, F., Kirchhausen, T., Lieberman, J., 2005. Perforin triggers a plasma membrane-repair response that facilitates CTL induction of apoptosis. *Immunity*. 23, 249-62.
- Keir, M. E., Butte, M. J., Freeman, G. J., Sharpe, A. H., 2008. PD-1 and its ligands in tolerance and immunity. *Annu Rev Immunol*. 26, 677-704.
- Keir, M. E., Liang, S. C., Guleria, I., Latchman, Y. E., Qipo, A., Albacker, L. A., Koulmanda, M., Freeman, G. J., Sayegh, M. H., Sharpe, A. H., 2006. Tissue expression of PD-L1 mediates peripheral T cell tolerance. *J Exp Med*. 203, 883-95.
- Kettenmann, H., Ransom, B.: Neuroglia. Oxford University Press, Second Edition, 2005, p50.
- Klugmann, M., Schwab, M. H., Puhlhofer, A., Schneider, A., Zimmermann, F., Griffiths, I. R., Nave, K. A., 1997. Assembly of CNS myelin in the absence of proteolipid protein. *Neuron*. 18, 59-70.
- Kobsar, I., Berghoff, M., Samsam, M., Wessig, C., Maurer, M., Toyka, K. V., Martini, R., 2003. Preserved myelin integrity and reduced axonopathy in connexin32-deficient mice lacking the recombination activating gene-1. *Brain*. 126, 804-13.
- Kobsar, I., Hasenpusch-Theil, K., Wessig, C., Muller, H. W., Martini, R., 2005. Evidence for macrophage-mediated myelin disruption in an animal model for Charcot-Marie-Tooth neuropathy type 1A. *J Neurosci Res*. 81, 857-64.
- Kobsar, I., Maurer, M., Ott, T., Martini, R., 2002. Macrophage-related demyelination in peripheral nerves of mice deficient in the gap junction protein connexin 32. *Neurosci Lett*. 320, 17-20.

- Kobsar, I., Oetke, C., Kroner, A., Wessig, C., Crocker, P., Martini, R., 2006. Attenuated demyelination in the absence of the macrophage-restricted adhesion molecule sialoadhesin (Siglec-1) in mice heterozygously deficient in P0. *Mol Cell Neurosci.* 31, 685-91.
- Kovach, M. J., Lin, J. P., Boyadjiev, S., Campbell, K., Mazzeo, L., Herman, K., Rimer, L. A., Frank, W., Llewellyn, B., Jabs, E. W., Gelber, D., Kimonis, V. E., 1999. A unique point mutation in the PMP22 gene is associated with Charcot-Marie-Tooth disease and deafness. *Am J Hum Genet.* 64, 1580-93.
- Kroner, A., Mehling, M., Hemmer, B., Rieckmann, P., Toyka, K. V., Maurer, M., Wiendl, H., 2005. A PD-1 polymorphism is associated with disease progression in multiple sclerosis. *Ann Neurol.* 58, 50-7.
- Kunkel-Bagden, E., Dai, H. N., Bregman, B. S., 1993. Methods to assess the development and recovery of locomotor function after spinal cord injury in rats. *Exp Neurol.* 119, 153-64.
- Lai, C., Brow, M. A., Nave, K. A., Noronha, A. B., Quarles, R. H., Bloom, F. E., Milner, R. J., Sutcliffe, J. G., 1987. Two forms of 1B236/myelin-associated glycoprotein, a cell adhesion molecule for postnatal neural development, are produced by alternative splicing. *Proc Natl Acad Sci U S A.* 84, 4337-41.
- Lazzarini, R.: *Myelin Biology and Disorders 1*. San Diego: Elsevier Academic Press, 2004.
- Leder, C., Schwab, N., Ip, C. W., Kroner, A., Nave, K. A., Dornmair, K., Martini, R., Wiendl, H., 2007. Clonal expansions of pathogenic CD8+ effector cells in the CNS of myelin mutant mice. *Mol Cell Neurosci.* 36, 416-24.
- Lemke, G., Lamar, E., Patterson, J., 1988. Isolation and analysis of the gene encoding peripheral myelin protein zero. *Neuron.* 1, 73-83.
- Li, C., Tropak, M. B., Gerlai, R., Clapoff, S., Abramow-Newerly, W., Trapp, B., Peterson, A., Roder, J., 1994. Myelination in the absence of myelin-associated glycoprotein. *Nature.* 369, 747-50.
- Lin, S. C., Yen, J. H., Tsai, J. J., Tsai, W. C., Ou, T. T., Liu, H. W., Chen, C. J., 2004. Association of a programmed death 1 gene polymorphism with the development of rheumatoid arthritis, but not systemic lupus erythematosus. *Arthritis Rheum.* 50, 770-5.
- Linsley, P. S., Brady, W., Grosmaire, L., Aruffo, A., Damle, N. K., Ledbetter, J. A., 1991. Binding of the B cell activation antigen B7 to CD28 costimulates T cell proliferation and interleukin 2 mRNA accumulation. *J Exp Med.* 173, 721-30.

- Lowin, B., Beermann, F., Schmidt, A., Tschopp, J., 1994. A null mutation in the perforin gene impairs cytolytic T lymphocyte- and natural killer cell-mediated cytotoxicity. *Proc Natl Acad Sci U S A.* 91, 11571-5.
- Lu, J. F., Lawler, A. M., Watkins, P. A., Powers, J. M., Moser, A. B., Moser, H. W., Smith, K. D., 1997. A mouse model for X-linked adrenoleukodystrophy. *Proc Natl Acad Sci U S A.* 94, 9366-71.
- Lucchinetti, C., Bruck, W., Parisi, J., Scheithauer, B., Rodriguez, M., Lassmann, H., 2000. Heterogeneity of multiple sclerosis lesions: implications for the pathogenesis of demyelination. *Ann Neurol.* 47, 707-17.
- Lupski, J. R., de Oca-Luna, R. M., Slaugenhaupt, S., Pentao, L., Guzzetta, V., Trask, B. J., Saucedo-Cardenas, O., Barker, D. F., Killian, J. M., Garcia, C. A., Chakravarti, A., Patel, P. I., 1991. DNA duplication associated with Charcot-Marie-Tooth disease type 1A. *Cell.* 66, 219-32.
- Magnus, T., Schreiner, B., Korn, T., Jack, C., Guo, H., Antel, J., Ifergan, I., Chen, L., Bischof, F., Bar-Or, A., Wiendl, H., 2005. Microglial expression of the B7 family member B7 homolog 1 confers strong immune inhibition: implications for immune responses and autoimmunity in the CNS. *J Neurosci.* 25, 2537-46.
- Magyar, J. P., Martini, R., Ruelicke, T., Aguzzi, A., Adlkofer, K., Dembic, Z., Zielasek, J., Toyka, K. V., Suter, U., 1996. Impaired differentiation of Schwann cells in transgenic mice with increased PMP22 gene dosage. *J Neurosci.* 16, 5351-60.
- Marrosu, M. G., Vaccargiu, S., Marrosu, G., Vannelli, A., Cianchetti, C., Muntoni, F., 1998. Charcot-Marie-Tooth disease type 2 associated with mutation of the myelin protein zero gene. *Neurology.* 50, 1397-401.
- Martin-Orozco, N., Dong, C., 2006a. New battlefields for costimulation. *J Exp Med.* 203, 817-20.
- Martin-Orozco, N., Wang, Y. H., Yagita, H., Dong, C., 2006b. Cutting Edge: Programmed death (PD) ligand-1/PD-1 interaction is required for CD8+ T cell tolerance to tissue antigens. *J Immunol.* 177, 8291-5.
- Martini, R., 1997. Animal models for inherited peripheral neuropathies. *J Anat.* 191 (Pt 3), 321-36.
- Martini, R., Mohajeri, M. H., Kasper, S., Giese, K. P., Schachner, M., 1995a. Mice doubly deficient in the genes for P0 and myelin basic protein show that both proteins contribute to the formation of the major dense line in peripheral nerve myelin. *J Neurosci.* 15, 4488-95.
- Martini, R., Schachner, M., 1997. Molecular bases of myelin formation as revealed by investigations on mice deficient in glial cell surface molecules. *Glia.* 19, 298-310.

- Martini, R., Toyka, K. V., 2004. Immune-mediated components of hereditary demyelinating neuropathies: lessons from animal models and patients. *Lancet Neurol.* 3, 457-65.
- Martini, R., Zielasek, J., Toyka, K. V., Giese, K. P., Schachner, M., 1995b. Protein zero (P0)-deficient mice show myelin degeneration in peripheral nerves characteristic of inherited human neuropathies. *Nat Genet.* 11, 281-6.
- Mastronardi, F. G., Ackerley, C. A., Arsenault, L., Roots, B. I., Moscarello, M. A., 1993. Demyelination in a transgenic mouse: a model for multiple sclerosis. *J Neurosci Res.* 36, 315-24.
- Matsushima, G. K., Taniike, M., Glimcher, L. H., Grusby, M. J., Frelinger, J. A., Suzuki, K., Ting, J. P., 1994. Absence of MHC class II molecules reduces CNS demyelination, microglial/macrophage infiltration, and twitching in murine globoid cell leukodystrophy. *Cell.* 78, 645-56.
- Maurer, M., Schmid, C. D., Bootz, F., Zielasek, J., Toyka, K. V., Oehen, S., Martini, R., 2001. Bone marrow transfer from wild-type mice reverts the beneficial effect of genetically mediated immune deficiency in myelin mutants. *Mol Cell Neurosci.* 17, 1094-101.
- Mersiyanova, I. V., Perepelov, A. V., Polyakov, A. V., Sitnikov, V. F., Dadali, E. L., Oparin, R. B., Petrin, A. N., Evgrafov, O. V., 2000. A new variant of Charcot-Marie-Tooth disease type 2 is probably the result of a mutation in the neurofilament-light gene. *Am J Hum Genet.* 67, 37-46.
- Meyer zu Horste, G., Hartung, H. P., Kieseier, B. C., 2007. From bench to bedside--experimental rationale for immune-specific therapies in the inflamed peripheral nerve. *Nat Clin Pract Neurol.* 3, 198-211.
- Meyer zu Horste, G., Prukop, T., Nave, K. A., Sereda, M. W., 2006. Myelin disorders: Causes and perspectives of Charcot-Marie-Tooth neuropathy. *J Mol Neurosci.* 28, 77-88.
- Mimault, C., Giraud, G., Courtois, V., Cailloux, F., Boire, J. Y., Dastugue, B., Boespflug-Tanguy, O., 1999. Proteolipoprotein gene analysis in 82 patients with sporadic Pelizaeus-Merzbacher Disease: duplications, the major cause of the disease, originate more frequently in male germ cells, but point mutations do not. The Clinical European Network on Brain Demyelinating Disease. *Am J Hum Genet.* 65, 360-9.
- Montag, D., Giese, K. P., Bartsch, U., Martini, R., Lang, Y., Bluthmann, H., Karthigasan, J., Kirschner, D. A., Wintergerst, E. S., Nave, K. A., et al., 1994. Mice deficient for the myelin-associated glycoprotein show subtle abnormalities in myelin. *Neuron.* 13, 229-46.
- Moser, H., Dubey, P., Fatemi, A., 2004. Progress in X-linked adrenoleukodystrophy. *Curr Opin Neurol.* 17, 263-9.

- Moser, H. W., 1997. Adrenoleukodystrophy: phenotype, genetics, pathogenesis and therapy. *Brain*. 120 (Pt 8), 1485-508.
- Moser, H. W., 2006. Peripheral nerve involvement in Krabbe disease: a guide to therapy selection and evaluation. *Neurology*. 67, 201-2.
- Moser, H. W., Moser, A. B., Naidu, S., Bergin, A., 1991. Clinical aspects of adrenoleukodystrophy and adrenomyeloneuropathy. *Dev Neurosci*. 13, 254-61.
- Muller, H. W., 2000. Tetraspan myelin protein PMP22 and demyelinating peripheral neuropathies: new facts and hypotheses. *Glia*. 29, 182-5.
- Nave, K. A., Lai, C., Bloom, F. E., Milner, R. J., 1987. Splice site selection in the proteolipid protein (PLP) gene transcript and primary structure of the DM-20 protein of central nervous system myelin. *Proc Natl Acad Sci U S A*. 84, 5665-9.
- Nelles, E., Butzler, C., Jung, D., Temme, A., Gabriel, H. D., Dahl, U., Traub, O., Stumpel, F., Jungermann, K., Zielasek, J., Toyka, K. V., Dermietzel, R., Willecke, K., 1996. Defective propagation of signals generated by sympathetic nerve stimulation in the liver of connexin32-deficient mice. *Proc Natl Acad Sci U S A*. 93, 9565-70.
- Nicholson, G. A., Valentijn, L. J., Cherryson, A. K., Kennerson, M. L., Bragg, T. L., DeKroon, R. M., Ross, D. A., Pollard, J. D., McLeod, J. G., Bolhuis, P. A., et al., 1994. A frame shift mutation in the PMP22 gene in hereditary neuropathy with liability to pressure palsies. *Nat Genet*. 6, 263-6.
- Nielsen, C., Hansen, D., Husby, S., Jacobsen, B. B., Lillevang, S. T., 2003. Association of a putative regulatory polymorphism in the PD-1 gene with susceptibility to type 1 diabetes. *Tissue Antigens*. 62, 492-7.
- Nishimura, H., Agata, Y., Kawasaki, A., Sato, M., Imamura, S., Minato, N., Yagita, H., Nakano, T., Honjo, T., 1996. Developmentally regulated expression of the PD-1 protein on the surface of double-negative (CD4-CD8-) thymocytes. *Int Immunol*. 8, 773-80.
- Nishimura, H., Honjo, T., 2001a. PD-1: an inhibitory immunoreceptor involved in peripheral tolerance. *Trends Immunol*. 22, 265-8.
- Nishimura, H., Minato, N., Nakano, T., Honjo, T., 1998. Immunological studies on PD-1 deficient mice: implication of PD-1 as a negative regulator for B cell responses. *Int Immunol*. 10, 1563-72.
- Nishimura, H., Nose, M., Hiai, H., Minato, N., Honjo, T., 1999. Development of lupus-like autoimmune diseases by disruption of the PD-1 gene encoding an ITIM motif-carrying immunoreceptor. *Immunity*. 11, 141-51.
- Nishimura, H., Okazaki, T., Tanaka, Y., Nakatani, K., Hara, M., Matsumori, A., Sasayama, S., Mizoguchi, A., Hiai, H., Minato, N., Honjo, T., 2001b. Autoimmune dilated cardiomyopathy in PD-1 receptor-deficient mice. *Science*. 291, 319-22.

- Ohno, M., Komiyama, A., Martin, P. M., Suzuki, K., 1993. Proliferation of microglia/macrophages in the demyelinating CNS and PNS of twitcher mouse. *Brain Res.* 602, 268-74.
- Okazaki, T., Honjo, T., 2006. The PD-1-PD-L pathway in immunological tolerance. *Trends Immunol.* 27, 195-201.
- Okazaki, T., Honjo, T., 2007. PD-1 and PD-1 ligands: from discovery to clinical application. *Int Immunol.* 19, 813-24.
- Okazaki, T., Maeda, A., Nishimura, H., Kurosaki, T., Honjo, T., 2001. PD-1 immunoreceptor inhibits B cell receptor-mediated signaling by recruiting src homology 2-domain-containing tyrosine phosphatase 2 to phosphotyrosine. *Proc Natl Acad Sci U S A.* 98, 13866-71.
- Ortler, S., Leder, C., Mittelbronn, M., Zozulya, A. L., Knolle, P. A., Chen, L., Kroner, A., Wiendl, H., 2008. B7-H1 restricts neuroantigen-specific T cell responses and confines inflammatory CNS damage: Implications for the lesion pathogenesis of multiple sclerosis. *Eur J Immunol.*
- Pannetier, C., Even, J., Kourilsky, P., 1995. T-cell repertoire diversity and clonal expansions in normal and clinical samples. *Immunol Today.* 16, 176-81.
- Parry, R. V., Chemnitz, J. M., Frauwirth, K. A., Lanfranco, A. R., Braunstein, I., Kobayashi, S. V., Linsley, P. S., Thompson, C. B., Riley, J. L., 2005. CTLA-4 and PD-1 receptors inhibit T-cell activation by distinct mechanisms. *Mol Cell Biol.* 25, 9543-53.
- Pellegatta, S., Tunici, P., Poliani, P. L., Dolcetta, D., Cajola, L., Colombelli, C., Ciusani, E., Di Donato, S., Finocchiaro, G., 2006. The therapeutic potential of neural stem/progenitor cells in murine globoid cell leukodystrophy is conditioned by macrophage/microglia activation. *Neurobiol Dis.* 21, 314-23.
- Pham-Dinh, D., Jones, E. P., Pitiot, G., Della Gaspera, B., Daubas, P., Mallet, J., Le Paslier, D., Fischer Lindahl, K., Dautigny, A., 1995. Physical mapping of the human and mouse MOG gene at the distal end of the MHC class Ib region. *Immunogenetics.* 42, 386-91.
- Poliak, S., Peles, E., 2003. The local differentiation of myelinated axons at nodes of Ranvier. *Nat Rev Neurosci.* 4, 968-80.
- Pouly, S., Antel, J. P., 1999. Multiple sclerosis and central nervous system demyelination. *J Autoimmun.* 13, 297-306.
- Powers, J. M., Liu, Y., Moser, A. B., Moser, H. W., 1992. The inflammatory myelinopathy of adreno-leukodystrophy: cells, effector molecules, and pathogenetic implications. *J Neuropathol Exp Neurol.* 51, 630-43.
- Privat, A., Jacques, C., Bourre, J. M., Dupouey, P., Baumann, N., 1979. Absence of the major dense line in myelin of the mutant mouse "shiverer". *Neurosci Lett.* 12, 107-12.

- Prokunina, L., Castillejo-Lopez, C., Oberg, F., Gunnarsson, I., Berg, L., Magnusson, V., Brookes, A. J., Tentler, D., Kristjansdottir, H., Grondal, G., Shapiro, L., 2002. A regulatory polymorphism in PDCD1 is associated with susceptibility to systemic lupus erythematosus in humans. *Nat Genet.* 32, 666-9.
- Pujol, A., Hindelang, C., Callizot, N., Bartsch, U., Schachner, M., Mandel, J. L., 2002. Late onset neurological phenotype of the X-ALD gene inactivation in mice: a mouse model for adrenomyeloneuropathy. *Hum Mol Genet.* 11, 499-505.
- Quarles, R. H., 2007. Myelin-associated glycoprotein (MAG): past, present and beyond. *J Neurochem.* 100, 1431-48.
- Raeymaekers, P., Timmerman, V., Nelis, E., De Jonghe, P., Hoogendijk, J. E., Baas, F., Barker, D. F., Martin, J. J., De Visser, M., Bolhuis, P. A., et al., 1991. Duplication in chromosome 17p11.2 in Charcot-Marie-Tooth neuropathy type 1a (CMT 1a). The HMSN Collaborative Research Group. *Neuromuscul Disord.* 1, 93-7.
- Readhead, C., Popko, B., Takahashi, N., Shine, H. D., Saavedra, R. A., Sidman, R. L., Hood, L., 1987. Expression of a myelin basic protein gene in transgenic shiverer mice: correction of the dysmyelinating phenotype. *Cell.* 48, 703-12.
- Readhead, C., Schneider, A., Griffiths, I., Nave, K. A., 1994. Premature arrest of myelin formation in transgenic mice with increased proteolipid protein gene dosage. *Neuron.* 12, 583-95.
- Regis, S., Biancheri, R., Bertini, E., Burlina, A., Lualdi, S., Bianco, M. G., Devescovi, R., Rossi, A., Uziel, G., Filocamo, M., 2008. Genotype-phenotype correlation in five Pelizaeus-Merzbacher disease patients with PLP1 gene duplications. *Clin Genet.* 73, 279-87.
- Roach, A., Takahashi, N., Pravtcheva, D., Ruddle, F., Hood, L., 1985. Chromosomal mapping of mouse myelin basic protein gene and structure and transcription of the partially deleted gene in shiverer mutant mice. *Cell.* 42, 149-55.
- Rogers, J., Mastroeni, D., Leonard, B., Joyce, J., Grover, A., 2007. Neuroinflammation in Alzheimer's disease and Parkinson's disease: are microglia pathogenic in either disorder? *Int Rev Neurobiol.* 82, 235-46.
- Rosenbluth, J., 1980. Peripheral myelin in the mouse mutant Shiverer. *J Comp Neurol.* 193, 729-39.
- Rosenthal, J. J., Bezanilla, F., 2000. Seasonal variation in conduction velocity of action potentials in squid giant axons. *Biol Bull.* 199, 135-43.
- Roth, H. J., Kronquist, K. E., Kerlero de Rosbo, N., Crandall, B. F., Campagnoni, A. T., 1987. Evidence for the expression of four myelin basic protein variants in the developing human spinal cord through cDNA cloning. *J Neurosci Res.* 17, 321-8.

-
- Runker, A. E., Kobsar, I., Fink, T., Loers, G., Tilling, T., Putthoff, P., Wessig, C., Martini, R., Schachner, M., 2004. Pathology of a mouse mutation in peripheral myelin protein P0 is characteristic of a severe and early onset form of human Charcot-Marie-Tooth type 1B disorder. *J Cell Biol.* 165, 565-73.
- Salama, A. D., Chitnis, T., Imitola, J., Ansari, M. J., Akiba, H., Tushima, F., Azuma, M., Yagita, H., Sayegh, M. H., Khoury, S. J., 2003. Critical role of the programmed death-1 (PD-1) pathway in regulation of experimental autoimmune encephalomyelitis. *J Exp Med.* 198, 71-8.
- Samsam, M., Mi, W., Wessig, C., Zielasek, J., Toyka, K. V., Coleman, M. P., Martini, R., 2003. The Wlds mutation delays robust loss of motor and sensory axons in a genetic model for myelin-related axonopathy. *J Neurosci.* 23, 2833-9.
- Scherer, S. S., 1997. Molecular genetics of demyelination: new wrinkles on an old membrane. *Neuron.* 18, 13-6.
- Scherer, S. S., Deschenes, S. M., Xu, Y. T., Grinspan, J. B., Fischbeck, K. H., Paul, D. L., 1995. Connexin32 is a myelin-related protein in the PNS and CNS. *J Neurosci.* 15, 8281-94.
- Schmid, C. D., Stienekemeier, M., Oehen, S., Bootz, F., Zielasek, J., Gold, R., Toyka, K. V., Schachner, M., Martini, R., 2000. Immune deficiency in mouse models for inherited peripheral neuropathies leads to improved myelin maintenance. *J Neurosci.* 20, 729-35.
- Schneider, A. M., Griffiths, I. R., Readhead, C., Nave, K. A., 1995. Dominant-negative action of the jimpy mutation in mice complemented with an autosomal transgene for myelin proteolipid protein. *Proc Natl Acad Sci U S A.* 92, 4447-51.
- Senderek, J., Bergmann, C., Weber, S., Ketelsen, U. P., Schorle, H., Rudnik-Schoneborn, S., Buttner, R., Buchheim, E., Zerres, K., 2003. Mutation of the SBF2 gene, encoding a novel member of the myotubularin family, in Charcot-Marie-Tooth neuropathy type 4B2/11p15. *Hum Mol Genet.* 12, 349-56.
- Sereda, M., Griffiths, I., Puhlhofer, A., Stewart, H., Rossner, M. J., Zimmerman, F., Magyar, J. P., Schneider, A., Hund, E., Meinck, H. M., Suter, U., Nave, K. A., 1996. A transgenic rat model of Charcot-Marie-Tooth disease. *Neuron.* 16, 1049-60.
- Shapiro, L., Doyle, J. P., Hensley, P., Colman, D. R., Hendrickson, W. A., 1996. Crystal structure of the extracellular domain from P0, the major structural protein of peripheral nerve myelin. *Neuron.* 17, 435-49.
- Sharpe, A. H., Wherry, E. J., Ahmed, R., Freeman, G. J., 2007. The function of programmed cell death 1 and its ligands in regulating autoimmunity and infection. *Nat Immunol.* 8, 239-45.

- Sheppard, K. A., Fitz, L. J., Lee, J. M., Benander, C., George, J. A., Wooters, J., Qiu, Y., Jussif, J. M., Carter, L. L., Wood, C. R., Chaudhary, D., 2004. PD-1 inhibits T-cell receptor induced phosphorylation of the ZAP70/CD3zeta signalosome and downstream signaling to PKC θ . *FEBS Lett.* 574, 37-41.
- Shinohara, T., Taniwaki, M., Ishida, Y., Kawaichi, M., Honjo, T., 1994. Structure and chromosomal localization of the human PD-1 gene (PDCD1). *Genomics.* 23, 704-6.
- Shy, M. E., 2006. Peripheral neuropathies caused by mutations in the myelin protein zero. *J Neurol Sci.* 242, 55-66.
- Shy, M. E., Arroyo, E., Sladky, J., Menichella, D., Jiang, H., Xu, W., Kamholz, J., Scherer, S. S., 1997. Heterozygous P0 knockout mice develop a peripheral neuropathy that resembles chronic inflammatory demyelinating polyneuropathy (CIDP). *J Neuropathol Exp Neurol.* 56, 811-21.
- Simard, A. R., Rivest, S., 2004. Bone marrow stem cells have the ability to populate the entire central nervous system into fully differentiated parenchymal microglia. *Faseb J.* 18, 998-1000.
- Sisttermans, E. A., de Coo, R. F., De Wijs, I. J., Van Oost, B. A., 1998. Duplication of the proteolipid protein gene is the major cause of Pelizaeus-Merzbacher disease. *Neurology.* 50, 1749-54.
- Skoff, R. P., 1995. Programmed cell death in the dysmyelinating mutants. *Brain Pathol.* 5, 283-8.
- Stroobants, S., Leroy, T., Eckhardt, M., Aerts, J. M., Berckmans, D., D'Hooge, R., 2008. Early signs of neuropilidosis-related behavioural alterations in a murine model of metachromatic leukodystrophy. *Behav Brain Res.* 189, 306-16.
- Suter, U., Moskow, J. J., Welcher, A. A., Snipes, G. J., Kosaras, B., Sidman, R. L., Buchberg, A. M., Shooter, E. M., 1992a. A leucine-to-proline mutation in the putative first transmembrane domain of the 22-kDa peripheral myelin protein in the trembler-J mouse. *Proc Natl Acad Sci U S A.* 89, 4382-6.
- Suter, U., Scherer, S. S., 2003. Disease mechanisms in inherited neuropathies. *Nat Rev Neurosci.* 4, 714-26.
- Suter, U., Snipes, G. J., 1995. Biology and genetics of hereditary motor and sensory neuropathies. *Annu Rev Neurosci.* 18, 45-75.
- Suter, U., Welcher, A. A., Ozcelik, T., Snipes, G. J., Kosaras, B., Francke, U., Billings-Gagliardi, S., Sidman, R. L., Shooter, E. M., 1992b. Trembler mouse carries a point mutation in a myelin gene. *Nature.* 356, 241-4.
- Tang, B. S., Zhao, G. H., Luo, W., Xia, K., Cai, F., Pan, Q., Zhang, R. X., Zhang, F. F., Liu, X. M., Chen, B., Zhang, C., Shen, L., Jiang, H., Long, Z. G., Dai, H. P., 2005. Small

- heat-shock protein 22 mutated in autosomal dominant Charcot-Marie-Tooth disease type 2L. *Hum Genet.* 116, 222-4.
- Thomas, P. K., King, R. H., Small, J. R., Robertson, A. M., 1996. The pathology of charcot-marie-tooth disease and related disorders. *Neuropathol Appl Neurobiol.* 22, 269-84.
- Timmerman, V., Nelis, E., Van Hul, W., Nieuwenhuijsen, B. W., Chen, K. L., Wang, S., Ben Othman, K., Cullen, B., Leach, R. J., Hanemann, C. O., et al., 1992. The peripheral myelin protein gene PMP-22 is contained within the Charcot-Marie-Tooth disease type 1A duplication. *Nat Genet.* 1, 171-5.
- Topilko, P., Schneider-Maunoury, S., Levi, G., Baron-Van Evercooren, A., Chennoufi, A. B., Seitanidou, T., Babinet, C., Charnay, P., 1994. Krox-20 controls myelination in the peripheral nervous system. *Nature.* 371, 796-9.
- Trapp, B. D., Quarles, R. H., 1982. Presence of the myelin-associated glycoprotein correlates with alterations in the periodicity of peripheral myelin. *J Cell Biol.* 92, 877-82.
- Tuppo, E. E., Arias, H. R., 2005. The role of inflammation in Alzheimer's disease. *Int J Biochem Cell Biol.* 37, 289-305.
- Uceyler, N., Kobsar, I., Biko, L., Ulzheimer, J., Levinson, S. R., Martini, R., Sommer, C., 2006. Heterozygous P0 deficiency protects mice from vincristine-induced polyneuropathy. *J Neurosci Res.* 84, 37-46.
- van Geel, B. M., Bezman, L., Loes, D. J., Moser, H. W., Raymond, G. V., 2001. Evolution of phenotypes in adult male patients with X-linked adrenoleukodystrophy. *Ann Neurol.* 49, 186-94.
- Vance, J. M., Nicholson, G. A., Yamaoka, L. H., Stajich, J., Stewart, C. S., Speer, M. C., Hung, W. Y., Roses, A. D., Barker, D., Pericak-Vance, M. A., 1989. Linkage of Charcot-Marie-Tooth neuropathy type 1a to chromosome 17. *Exp Neurol.* 104, 186-9.
- Verdier, Y., Zarandi, M., Penke, B., 2004. Amyloid beta-peptide interactions with neuronal and glial cell plasma membrane: binding sites and implications for Alzheimer's disease. *J Pept Sci.* 10, 229-48.
- Verhoeven, K., De Jonghe, P., Coen, K., Verpoorten, N., Auer-Grumbach, M., Kwon, J. M., FitzPatrick, D., Schmedding, E., De Vriendt, E., Jacobs, A., Van Gerwen, V., Wagner, K., Hartung, H. P., Timmerman, V., 2003. Mutations in the small GTP-ase late endosomal protein RAB7 cause Charcot-Marie-Tooth type 2B neuropathy. *Am J Hum Genet.* 72, 722-7.
- Warner, L. E., Hiltz, M. J., Appel, S. H., Killian, J. M., Kolodry, E. H., Karpati, G., Carpenter, S., Watters, G. V., Wheeler, C., Witt, D., Bodell, A., Nelis, E., Van Broeckhoven, C., Lupski, J. R., 1996. Clinical phenotypes of different MPZ (P0) mutations may include

- Charcot-Marie-Tooth type 1B, Dejerine-Sottas, and congenital hypomyelination. *Neuron*. 17, 451-60.
- Warner, L. E., Mancias, P., Butler, I. J., McDonald, C. M., Keppen, L., Koob, K. G., Lupski, J. R., 1998. Mutations in the early growth response 2 (EGR2) gene are associated with hereditary myelinopathies. *Nat Genet*. 18, 382-4.
- Warshawsky, I., Rudick, R. A., Staugaitis, S. M., Natowicz, M. R., 2005. Primary progressive multiple sclerosis as a phenotype of a PLP1 gene mutation. *Ann Neurol*. 58, 470-3.
- Wenger, D. A., Rafi, M. A., Luzi, P., 1997. Molecular genetics of Krabbe disease (globoid cell leukodystrophy): diagnostic and clinical implications. *Hum Mutat*. 10, 268-79.
- Wenger, D. A., Rafi, M. A., Luzi, P., Datto, J., Costantino-Ceccarini, E., 2000. Krabbe disease: genetic aspects and progress toward therapy. *Mol Genet Metab*. 70, 1-9.
- Werner, H., Jung, M., Klugmann, M., Sereda, M., Griffiths, I. R., Nave, K. A., 1998. Mouse models of myelin diseases. *Brain Pathol*. 8, 771-93.
- Wrabetz, L., D'Antonio, M., Pennuto, M., Dati, G., Tinelli, E., Fratta, P., Previtali, S., Imperiale, D., Zielasek, J., Toyka, K., Avila, R. L., Kirschner, D. A., Messing, A., Feltri, M. L., Quattrini, A., 2006. Different intracellular pathomechanisms produce diverse Myelin Protein Zero neuropathies in transgenic mice. *J Neurosci*. 26, 2358-68.
- Xu, W., Shy, M., Kamholz, J., Elferink, L., Xu, G., Lilien, J., Balsamo, J., 2001. Mutations in the cytoplasmic domain of P0 reveal a role for PKC-mediated phosphorylation in adhesion and myelination. *J Cell Biol*. 155, 439-46.
- Yeager, A. M., Brennan, S., Tiffany, C., Moser, H. W., Santos, G. W., 1984. Prolonged survival and remyelination after hematopoietic cell transplantation in the twitcher mouse. *Science*. 225, 1052-4.
- Young, P., Wiebusch, H., Stogbauer, F., Ringelstein, B., Assmann, G., Funke, H., 1997. A novel frameshift mutation in PMP22 accounts for hereditary neuropathy with liability to pressure palsies. *Neurology*. 48, 450-2.
- Zang, X., Allison, J. P., 2007. The B7 family and cancer therapy: costimulation and coinhibition. *Clin Cancer Res*. 13, 5271-9.
- Zha, Y., Blank, C., Gajewski, T. F., 2004. Negative regulation of T-cell function by PD-1. *Crit Rev Immunol*. 24, 229-37.
- Zielasek, J., Martini, R., Toyka, K. V., 1996. Functional abnormalities in P0-deficient mice resemble human hereditary neuropathies linked to P0 gene mutations. *Muscle Nerve*. 19, 946-52.
- Zuchner, S., Mersyanova, I. V., Muglia, M., Bissar-Tadmouri, N., Rochelle, J., Dadali, E. L., Zappia, M., Nelis, E., Patitucci, A., Senderek, J., Parman, Y., Evgrafov, O., Jonghe, P. D., Takahashi, Y., Tsuji, S., Pericak-Vance, M. A., Quattrone, A., Battaloglu, E., Polyakov, A. V., Timmerman, V., Schroder, J. M., Vance, J. M., 2004. Mutations in

the mitochondrial GTPase mitofusin 2 cause Charcot-Marie-Tooth neuropathy type 2A. Nat Genet. 36, 449-51.

9. Acknowledgements

I would like to thank Prof. Dr. Rudolf Martini for giving me the opportunity to do my PhD thesis in his lab, for countless discussions, excellent supervision, permanent support and a lot of fun!

Many thanks go to PD Dr. Mathias Mäurer and Prof. Dr. Heinz Wiendl and their groups, with whom we had a fruitful collaboration on the topics investigated during this thesis.

Furthermore, I would like to thank Prof. Dr. Toyka, in who's department this work was performed and Prof. Dr. Roessler for the second survey.

I am also indebted to the MD/PhD program of the IZKF for funding me during my PhD thesis and the coordinators Prof. Dr. Walter, Prof. Dr. A. Rethwilm and Prof. Dr. J. Schulz for help and encouragement. I also thank Prof. Dr. T. Hünig and the Graduate College for Immunomodulation who supported me as an associate member and contributed profoundly to my education in immunology.

A very cordial thanks goes to all current and former members of the AG Martini (in strict alphabetical order), namely Henryk Blazyca, Stefan Fischer, Janos Groh, Christiane Hammerschmidt, Dr. Chi Wang Ip, Carolin Kiesel, Bianca Kohl, Silke Loserth, Bettina Meyer and Nadine Weckesser for the great time, lots of help and many useful discussions.

Bianca and Erik were also invaluablely helpful with correction of the manuscript and artwork. A big thanks also goes to Helga Brünner and Karl- Heinz Aulenbach for expert animal care and lots of patience for unusual wishes. Furthermore, I thank Carsten Wessig for doing the electrophysiology, Nicholas Schwab for the spectratyping and Lydia Biko for the sensory testing.

And, last but not least, I thank my dear husband Erik Milsch and my family for the constant support during the last years.

10. Appendices

10.1. Appendix 1: Reagents and consumables

10.1.1 Reagents

Acetone	Invitrogen (Karlsruhe, Germany)
Ammonium chloride (NH ₄ Cl)	Merck (Darmstadt, Germany)
Agarose	Sigma (Munich, Germany)
Ampicillin	Roth (Karlsruhe, Germany)
AmpliTaq DNA Polymerase	Applied Biosystems (Foster City, CA, USA)
Aquatex	Merck (Darmstadt, Germany)
Boric acid	Merck (Darmstadt, Germany)
Bovine Serum albumine (BSA) 96% DER 736	Sigma (Munich, Germany) ServaElectrophoresis (Heidelberg, Germany)
Diaminobenzidine (DAB)	KemEnTecDiagnostics (Copenhagen, Denmark)
Dimethylaminoethanol	ServaElectrophoresis (Heidelberg, Germany)
Di-sodium hydrogen phosphate (Na ₂ HPO ₄)	Merck (Darmstadt, Germany)
Dulbecco`s Modified Eagle`s medium (D-MEM)	Gibco Invitrogen (Karlsruhe, Germany)
Ethanol	J.T.Baker (Deventer, Netherlands)
Ethidium bromide	Sigma (Munich, Germany)
EDTA	Merck (Darmstadt, Germany)
Fetal Calf Serum (FCS)	Gibco Invitrogen (Karlsruhe, Germany)
Fixation / Permeabilization Diluent	BD Biosciences Pharmingen (San Jose, CA USA)
Glutamat	Gibco Invitrogen (Karlsruhe, Germany)
Glycine	Sigma (Munich, Germany)
Glycerol	Merck (Darmstadt, Germany)
Goat serum	DAKO (Hamburg, Germany)
Heparin	Ratiopharm (Ulm, Germany)
Hydrochloric acid (HCl)	Merck (Darmstadt, Germany)
Hydrogen peroxide (H ₂ O ₂)	Merck (Darmstadt, Germany)
Ketanest	Parke-Davis (Karlsruhe, Germany)
Methanol	J.T.Baker (Deventer, Netherlands)
2-Methylbutane	Roth (Karlsruhe, Germany)
O.C.T. matrix	DiaTec, Nuernberg, Germany
O Range Ruler 600bp DNA ladder	Fermentas (St. Leon-Rot, Germany)

6x Orange Loading Dye	Fermentas (St. Leon-Rot, Germany)
Phosphate-buffered saline (PBS)	Biochrom AG (Berlin, Germany)
Penicillin / Streptomycin	Biochrom AG (Berlin, Germany)
Percoll	GE Healthcare (Munich, Germany)
Perm / Wash Solution	eBioscience (San Diego, CA, USA)
Primers	Sigma (Munich, Germany)
Potassium di-hydrogen phosphate (KH ₂ PO ₄)	Merck (Darmstadt, Germany)
Potassium chloride (KCl)	Merck (Darmstadt, Germany)
Potassium hydrogen carbonate (KHCO ₃)	Merck (Darmstadt, Germany)
RPMI	PAA (Coelbe, Germany)
Rompun	BayerVital (Leverkusen, Germany)
RPMI-Medium (Roswell Park Memorial Institute Medium)	Gibco Invitrogen (Karlsruhe, Germany)
D (+)-Saccharose	Roth (Karlsruhe, Germany)
StreptABComplex kit	DakoCytomation (Hamburg, Germany)
Sodium azide (NaN ₃)	Merck (Darmstadt, Germany)
Sodium chloride solution (NaCl)	Merck (Darmstadt, Germany)
Tris	Merck (Darmstadt, Germany)
TritonX-100	Roth (Karlsruhe, Germany)
Tween20	Roth (Karlsruhe, Germany)
Vinyl/ERL4221D (Epoxy-cyclohexyl-carboxylat)	ServaElectrophoresis (Heidelberg, Germany)
Vitro-Clud	Langenbrinck (Teningen, Germany)

10.1.2 Consumables

Cell strainer 40 and 70 µm	BD Biosciences Pharmingen (San Jose, CA USA)
Cell culture flasks	Sarstedt (Nuembrecht, Germany)
Cell culture dishes	Nunc (Roskilde, Danmark)
CombiScreen® urine tests	Biocon Diagnostik (Voehl-Marienhagen, Germany)
FACS Tubes	BD Biosciences Pharmingen (San Jose, CA USA)
Object slides superfrost	Langenbrinck (Teningen, Germany)
PapPen	SCI (Munich, Germany)

PCR tubes	Sarstedt (Nuembrecht, Germany)
Reaction tubes (0.5 ml/ 1.5 ml, 2ml)	Sarstedt (Nuembrecht, Germany)
Reaction tubes (15 ml, 50 ml)	Greiner Bio-one (Frickenhausen, Germany)

10.2. Appendix 2: Equipment

Algesiometer		Ugo Basile (Comerico, Italy)
BioPhotometer 6131		Eppendorf (Hamburg, Germany)
Centrifuges	Biofuge 15R	Heraeus (Hanau, Germany)
	Centrifuge 5810R	Eppendorf (Hamburg, Germany)
	Rotofix 32	Hettich Zentrifugen (Tuttlingen, Germany)
	Biofuge Pico	Heraeus (Hanau, Germany)
	Centrifuge 5415C	Eppendorf (Hamburg, Germany)
ELISA reader	Original Multiskan	EX Labsystems (Helsinki, Finland)
FACSCalibur		BD Biosciences Pharmingen (San Jose, CA USA)
Freezer		Liebherr (Biberach, Germany)
Gel chamber (horizontal)		PeqLab (Erlangen, Germany)
Heater		Eppendorf (Hamburg, Germany)
Incubators	HeraCell150	Heraeus (Hanau, Germany)
	TH25	E. Bühler GmbH (Tuebingen, Germany)
Kryostat	CM 1900	Leica (Wetzlar, Germany)
	CM 3050S	Leica (Wetzlar, Germany)
Microscopes	CX31	Olympus (Hamburg, Germany)
	BH2	Olympus (Hamburg, Germany)
	CKX41	Olympus (Hamburg, Germany)
	Axiophot 2	Zeiss (Oberkochen, Germany)
	906 E	Zeiss (Oberkochen, Germany)
Pipettes		Abimed (Berlin, Germany)
		Eppendorf (Hamburg, Germany)
		Gilson (Bad Camberg, Germany)
ProScan Slow Scan CCD camera		Pro Scan (Lagerlechfeld, Germany)
Rotarod (for mice)		Ugo Basile (Comerico, Italy)
Thermocycler Mastercycler gradient		Eppendorf (Hamburg, Germany)
<u>Software</u>		
Adobe Photoshop CS		Adobe Systems, Saggart, Republic of Ireland
Adobe Illustrator CS		Adobe Systems, Saggart, Republic of Ireland
CellQuest Pro		BD Biosciences Pharmingen (San Jose, CA USA)
FlowJo7 software		Tree Star Inc. (Ashland, OR, USA)
iTEM		Olympus Soft Imaging Solutions GmbH, (Muenster, Germany)

10.3. Appendix 3: Media, buffers and solutions

10.3.1 Cell culture media

RPMI-Medium:	RPMI basic medium	
	FCS	20%
	Glutamat	1%
	PenStrep	1%
	Sterile filtration	

10.3.2 Buffers and solutions

Anesthetic	Ketanest	0.6 %
	Rompun	0.08 %
	NaCl	8.3 %
10x PBS:	NaCl	80g
	Na ₂ HPO ₄ ⁻ * 2H ₂ O	14.2g
	KCl	2g
	KH ₂ PO ₄	2g
	Aqua dest	ad 1l
	Adjustion of pH to 6.8	
1x PBS:	1:10 dilution of 10x PBS in A. dest	
1x PBST:	1:10 dilution of 10x PBS in A. dest Addition 0.1% Tween 20	
10x TBE:	Tris	108g
	Boric acid	55g
	0.5 M EDTA	40ml
	A. dest	ad 1l
1x TBE:	1:10 dilution of 10x TBE in A. dest	
3M NaAc:	NaAc	24.6g
	A. dest	ad 100ml
	Adjustion of pH to 5.3 with 25% HCl	

DABCO:	1x PBS	25ml
	Glycerol	75ml
	DABCO	2.5g
	(Final concentration of 25mg/ml)	
	Storage at +4°C protected from light	
Erythrocyte lysis buffer:	NH ₄ Cl	0.15M
	KHCO ₃	1mM
	Na ₂ EDTA	0.1mM
	In A. dest	
	Adjustion of pH to 7.2-7.4	
Sterile filtration through 0.2µm filter		
FACS buffer:	1 x PBS	
	0.1 – 1 % BSA	
	0.1 % NaAzide	
Spurr's Medium:	Vinyl/ERL	10g
	DER 736	6g
	NSA	26g
	Dimethylaminoethanol	0.4g

If not specified otherwise, all buffers and solutions were stored at room temperature.

10.4. Appendix 4: List of antibodies

10.4.1 Primary antibodies

Reactivity	Company	Clone	Host	Target species	Application
B220, PE conjugated	BD Biosciences San Jose, CA, USA # 553085	RA3-6B2	Rat IgG2a	Mouse	FC
Cleaved Caspase-3, Purified	Cell Signaling Danvers, MA, USA # 9664	polyclonal	Rabbit	Mouse	IHC
CD4, Purified	Serotec Oxford, UK #MCA1767	YTS191.1	Rat IgG2b	Mouse	IHC
CD4, PerCP conjugated	BD Biosciences #553052	RM4-5	Rat IgG2a	Mouse	FC
CD8, purified	Chemicon Temecula, CA, USA #CBL 1325	IBL-3/25	Rat	Mouse	IHC
CD8, FITC conjugated	BD Biosciences #553031	53-6.7	Rat IgG2a	Mouse	FC
CD8, PE conjugated	BD Biosciences #553033	53-6.7	Rat IgG2a	Mouse	FC
CD11b, purified	Serotec #MCA74G	M1/70.15	Rat IgG2b	Mouse	IHC
CD11b, PerCP conjugated	BD Biosciences #550993	M1/70	Rat IgG2b	Mouse	FC
CD44, FITC conjugated	BD Biosciences #553133	IM7	Rat IgG2b	Mouse	FC

CD62L, APC conjugated	BD Biosciences #553152	MEL-14	Rat IgG2a	Mouse	FC
CD169 , (Siglec-1) purified	Serotec #MCA884GA	3D6.112	Rat IgG2a	Mouse	IHC
F4/80, purified	Serotec #MCA497B	A3-1	Rat	Mouse	IHC
MBP, purified	MBL Woburn, MA, USA #PD004	polyclonal	Rabbit	Mouse	IHC
PD-1, PE conjugated	ebioscience San Diego, CA, USA #12-9981-82	RMP1-30	Rat IgG2b	Mouse	FC
Isotype FITC conjugated	BD Biosciences #553929	R35-95	Rat IgG2a	(none)	FC
Isotype PE Conjugated	BD Biosciences #556925	A95-1	Rat IgG2b	(none)	FC
Isotype PerCP conjugated	BD Biosciences #550764	A95-1	Rat IgG2b	(none)	FC
Isotype APC conjugated	BD Biosciences #554690	R35-95	Rat IgG2a	(none)	FC

10.4.2 Secondary antibodies

IgG biotinylated	Vector Burlingame, CA, USA #BA-1000		goat	Rabbit	IHC
IgG biotinylated	Vector #BA-9400		goat	Rat	IHC

11. Abbreviations

APC	antigen presenting cell
APC	allophycocyanin
BMC	bone marrow chimera
CD	cluster of differentiation
CDR	complementarity determining region
CIDP	chronic idiopathic demyelinating polyneuropathy
CMAP	compound muscle action potential
CMT	Charcot-Marie-Tooth
CNS	central nervous system
Cx	connexin
DSS	Dejerine- Sottas Syndrome
ELISA	enzyme linked immunosorbent assay
FC	flow cytometry
FSC	forward sideward scatter
FITC	fluoreszeinisothiocyanat
Gy	Gray
IFN	interferon
IHC	immunohistochemistry
IL	interleukin
MAG	myelin associated glycoprotein
MHC	major histocompatibility complex
MBP	myelin basic protein
MCSF	macrophage colony stimulating factor
MCP-1	monocyte chemoattractant protein -1
N	Newton
NCV	Nerve conduction velocity
op	osteopetrotic
PD-1	programmed death 1
PE	phycoerythrin
PerCP	peridinin chlorophyll protein
PMP22	peripheral myelin protein 22
PLP	proteolipid protein
PMA	phorbol myristate acetate
PMD	Pelizaeus Merzbacher disease
PNS	peripheral nervous system

P0	myelin protein zero
RAG	recombinase activating gene
Sn	Sialoadhesin, Siglec-1
tg	transgene / transgenic
wt	wildtype
X-ALD	X-linked adrenoleukodystrophy

12. Curriculum vitae

Employment and Education

1995 - 2002	Studies of medicine, Bayerische Julius-Maximilians University, Würzburg
2001 - 2002	Practical year: Kantonales Spital Herisau, Switzerland Neurologische Universitätsklinik, Würzburg, Germany Universidad de Granada, Spain
2002	Final exam at the University of Wuerzburg (Grade 1.0 / Overall Score 1.0)
2003	Dissertation as an MD at the institute for hygiene and microbiology (Head: Prof. Dr. M. Frosch, Supervisor Prof. K. Brehm). Title of doctoral thesis: "Cloning and Characterization of Receptorkinases from the EGF- and TGF β - Family in the fox tapeworm, Echinococcus multilocularis" (magna cum laude).
2002 - 2004	"Aerztin im Praktikum"(equivalent to residency) and scientific work in MS genetics, University of Wuerzburg, Neurology, Multiple Sclerosis Research Group, Wuerzburg, Germany (Prof. Dr. Peter Rieckmann)
2004	Approbation as MD
2004	Postdoctoral fellow, University of Würzburg, Neurology, Developmental Neurobiology (Head: Prof. Dr. Rudolf Martini)
2004 - 2007	Member of the MD/PhD program, IZKF University of Würzburg Doctoral thesis at the Department of Neurology, Developmental Neurobiology (Prof. Dr. Rudolf Martini). Title of dissertation: "Role of immune cells in hereditary myelinopathies"

Awards and Scholarships

- MD/ PhD program: Three years scholarship 2004 - 2007, Wuerzburg, Germany
- Graduate School Immunomodulation (Speaker Prof. T. Huenig):
Associated member 2005 - 2007, Wuerzburg, Germany
- Wyeth Young Investigator Award "Multiple Sclerosis", Germany, 2005
- Travel grant, ECTRIMS 2007

- Chairs fund travel grant, Travel grant Gordon Research Conference Myelin, Italy, 2008

13. List of publications

13.1 Publications in peer-reviewed international journals

2008

Ip C.W., Kohl B., Kleinschnitz C., Reuss B., Nave K.A., Kroner A., Martini R. (2008)

Origin of CD11b+ macrophage-like cells in the CNS of PLP overexpressing mice: Low influx of haematogenous macrophages and unchanged blood brain barrier in the optic nerve. *Mol Cell Neurosci* (in press)

Ortler S., Leder C., Mittelbronn M., Zozulya AL., Knolle PA., Chen L., Kroner A., Wiendl H. (2008) **B7-H1 restricts neuroantigen-specific T cell responses and confines inflammatory CNS damage: Implications for the lesion pathogenesis of Multiple Sclerosis.** *Eur J Immunol.* 38: 1734 – 1744

Yu X., Koczan D., Sulonen AM., Akkad DA., Kroner A., Comabella M., Costa G., Corongiu D., Goertsches R., Camina-Tato M., Thiesen HJ., Nyland HI., Mørk SJ., Montalban X., Rieckmann P., Marrosu MG., Myhr KM., Epplen JT, Janna Saarela, Ibrahim SM. (2008) **mtDNA nt13708A Variant Increases the Risk of Multiple Sclerosis.** *PlosOne.* 13; 3 (2): e1530

Weber F., Fontaine B., Cournu-Rebeix I., Kroner A., Knop M., Lutz S., Müller-Sarnowski F., Uhr M., Bettecken T., Kohli M., Ripke S., Ising M., Rieckmann P., Brassat D., Semana G., Babron MC., Mrejen S., Gout C., Lyon-Caen O., Yaouanq J., Edan G., Clanet M., Holsboer F., Clerget-Darpoux F., Müller-Myhsok B. (2008) **IL2RA and IL7RA genes confer susceptibility for Multiple Sclerosis in two independent European populations.** *Genes and Immunity* 9 (3):259-263

Buttmann M, Nowak E, Kroner A, Hemmer B, Lesch KP, Rieckmann P (2008) **Analysis of the stathmin rs182455 single nucleotide promoter polymorphism in patients with multiple sclerosis.** *J Neurogenetics* 22 (3) in press

2007

Leder C*, Schwab N*, Ip CW*, Kroner A*, Nave KA, Dornmair K, Martini R, Wiendl H (2007) **Clonal expansions of pathogenic CD8+ effector cells in the CNS of myelin mutant mice.** *Mol Cell Neurosci.* 36 (3): 416-424

*equal contribution

Kroner A, Grimm A, Johannssen K, Maurer M, Wiendl H. (2007)

The Genetic Influence of the Nonclassical MHC Molecule HLA-G on Multiple Sclerosis. *Hum Immunol.* 68(5):422-425

Ey B, Kobsar I, Blazyca H, Kroner A, Martini R. (2007)

Visualization of degenerating axons in a dysmyelinating mouse mutant with axonal loss. *Mol Cell Neurosci.* 35(1):153-60.

Ip CW, Kroner A, Crocker PR, Nave KA, Martini R. (2007)

Sialoadhesin deficiency ameliorates myelin degeneration and axonopathic changes in the CNS of PLP overexpressing mice.

Neurobiol Dis. 25 (1):105-111

2006

Buck D*, Kroner A*, Rieckmann P, Mäurer M, Wiendl H (2006)

Analysis of the C/T(-1)) single nucleotide polymorphism in the CD40 gene in multiple sclerosis.

Tissue Antigens. 68(4):335- 338

*equal contribution

Gronen F, Ruprecht K, Weissbrich B, Klinker E, Kroner A, Hofstetter HH, Rieckmann P. (2006)

Frequency analysis of HLA-B7-restricted Epstein-Barr virus-specific cytotoxic T lymphocytes in patients with multiple sclerosis and healthy controls.

J Neuroimmunol. 180(1-2):185-192

Ip CW, Kroner A, Bendszus M, Leder C, Kobsar I, Fischer S, Wiendl H, Nave KA, Martini R. (2006)

Immune cells contribute to myelin degeneration and axonopathic changes in mice overexpressing proteolipid protein in oligodendrocytes.

J Neurosci. 26:8206-8216.

Salih HR, Wintterle S, Krusch M, Kroner A, Huang YH, Chen L, Wiendl H (2006)

The role of leukemia-derived B7-H1 (PD-L1) in tumor-T- cell interactions in humans

Experimental Hematology 34(7): 888-894

Linker RA, Kroner A, Horn T, Gold R, Maurer M, Bendszus M. (2006)

Iron particle-enhanced visualization of inflammatory central nervous system lesions by high resolution: preliminary data in an animal model.

AJNR Am J Neuroradiol. 27(6):1225-9

Kobsar I, Oetke C, Kroner A, Wessig C, Crocker P, Martini R. (2006)

Attenuated demyelination in the absence of the macrophage-restricted adhesion molecule sialoadhesin (Siglec-1) in mice heterozygously deficient in P0.

Mol Cell Neurosci, 31(4): 685-691

Zavala-Gongora R, Kroner A, Bernthaler P, Knaus P, Brehm K (2006)

A member of the transforming growth factor- β receptor family from *Echinococcus multilocularis* is activated by human bone morphogenetic protein 2.

Mol Biochem Parasit, 146(2):265-271

2005

Vogler S, Goedde R, Milterski B, Gold R, Kroner A, Koczan D, Zettl UK, Rieckmann P, Epplen JT, Ibrahim SM. (2005)

Association of a common polymorphism in the promoter of UCP2 with susceptibility to multiple sclerosis. *J Mol Med*, 83(10): 806- 811

Kroner A*, Mehling M*, Hemmer B, Rieckmann P, Toyka KV, Mäurer M, and Wiendl, H (2005)

A PD-1 polymorphism is associated with impaired T- cell inhibition and progression in multiple sclerosis. *Ann Neurol*, 58(1): 50-57

*equal contribution

Kroner A, Vogel F, Kolb- Mäurer A, Kruse N, Toyka KV, Hemmer B, Rieckmann P, Mäurer M (2005)

Impact of the Asp299Gly polymorphism in the toll-like receptor 4 (*tlr-4*) gene on disease course of multiple sclerosis. *J Neuroimmunol*, 165 (1-2): 161- 165

2004

Rosche B, Cepok S, Stei S, Vogel F, Grummel V, Hoffmann S, Kroner A, Mäurer M, Rieckmann P, Sommer N, Hemmer B (2004)

The role of the Polio Virus Receptor and the Herpes Virus entry mediator B genes for the development of MS. *J Neuroimmunol*, 156: 171- 177

Kroner A, Mäurer M, Loserth S, Kleinschnitz C, Hemmer B, Rosche B, Toyka KV, Rieckmann P (2004)

Analysis of the monocyte chemoattractant protein 1 -2518 promoter polymorphism in patients with multiple sclerosis. *Tissue Antigens* 64: 70-73

2003

Konrad C, Kroner A, Spiliotis M, Zavala- Gongora R & Brehm K(2003)

Identification and molecular characterisation of a gene encoding a member of the insulin receptor family in *Echinococcus multilocularis*.

Int J Parasitol, 33: 301- 312

Brehm K, Wolf M, Beland H, Kroner A, Frosch M (2003)

Analysis of differential gene expression in *Echinococcus multilocularis* larval stages by means of spliced leader differential display.

Int J Parasitol, 33: 1145- 1159

Zavala- Gongora R, Kroner A, Wittek B, Knaus P, & Brehm K (2003)

Identification and characterization of two distinct Smad proteins from the fox tapeworm *Echinococcus multilocularis*.

Int J Parasitol, 33: 1665- 1677

Spiliotis M, Kroner A, Brehm K (2003)

Identification, molecular characterization and expression of the gene encoding the epidermal growth factor orthologue from the fox tapeworm *Echniococcus multilocularis*.

Gene, 323:57-65

13.2 Reviews

Wang Ip C, Kroner A, Fischer S, Berghoff M, Kobsar I, Maurer M, Martini R. (2006)

Role of immune cells in animal models for inherited peripheral neuropathies.

Neuromolecular Med. 8 (1-2):175- 190 Review

13.3 Oral presentations

Kroner A., Schwab N., Ip C.W., Nave K.A., Honjo T., Wiendl H., Martini R. (2007)

Programmed cell death 1 is a key regulator of tissue immune- homeostasis in the CNS: lessons from a model of oligodendropathy induced inflammation.

ECTRIMS, Prague, Czech republic, 11.10.-14.10.2007

Multiple Sclerosis, 13, Supplement 2, October 2007

Kroner A., Kohl B., Kobsar I., Mäurer M., Martini R. (2005)

Enoneurial fibroblast like cells express the hematopoetic stem cell marker CD34 and form cell contacts with resident and phagocytosing macrophages in normal mice and demyelinating mutants.

Biennial Meeting of the Peripheral Nerve Society, Il Ciocco, Italy, 09.07.-13.07.2005,

JPNS, 10, Supplement 1, 46

Kroner A., Rosche B., Hemmer B., Wiendl H., Toyka K.V., Rieckmann P., Mäurer M. (2004)

Analysis of a functional polymorphism within the *programmed cell death protein- 1* gene in patients with multiple sclerosis.

14th Meeting of the European Neurological Society, Barcelona, Spain, 26.-30.06.2004,

J Neurol 251, Supplement 3, 83

Kroner A., Toyka K., Rieckmann P., Mäurer M (2003)

Analysis of the Asp299Gly Polymorphism in the toll-like –receptor 4 (*tlr4*) gene in patients with multiple sclerosis.

13th Meeting of the European Neurological Society, Istanbul, Turkey, 14.- 18.06.2003.

J Neurol 250, Supplement 2, 121

13.4 Posters

Kroner A., Ip C.W., Schwab N., Nave K.A., Maeurer M., Wiendl H., Martini R. (2008)

PD-1 is a key regulator of tissue-homoeostasis in a model of oligodendrocyte induced inflammation. Gordon Research Conference Myelin, Il Ciocco, Lucca, Italy, 4.05.-9.05.08

Kroner A., Rieckmann P. (2005)

Impact of the Val66Met BDNF polymorphism on multiple sclerosis. 21st Congress of the European Committee / 10th Annual Meeting of the Americas Committee for Treatment and Research in Multiple Sclerosis, Thessaloniki, Greece, 28.09. – 1.10.2005.

Multiple Sclerosis, Supplement 1 2005, P451

Kroner A., B.D. Kohl, I. Kobsar, R. Martini, M. Maeurer (2005)

Endoneural CD34+ Macrophages Activation in the Peripheral Nerve?

FOCIS, 5th Annual Meeting, Boston, USA, 12.05.- 16.05.2005

Clin Immunol, Supplement 1 2005, Sa1.09.

Kroner A., Rosche B., Kolb- Mäurer A., Kruse N., Toyka K., Hemmer B., Rieckmann P., Mäurer M. (2004)

Analysis of the Asp 299 Gly Polymorphism in the Toll- like receptor 4 (TLR-4) gene in patients with Multiple Sclerosis.

7th International Congress of Neuroimmunology, Venice, Italy, 28.09.- 02.10.2004,

J Neuroimmunol, 154 (1-2), P83

Kroner A., Mäurer M., Loserth S., Kleinschnitz Ch., Toyka K.V., Rieckmann P. (2003)

Analyse des MCP-1 (Monocyte- Chemoattractant- Protein 1) -2518 Promotorpolymorphismus bei Patienten mit Multipler Sklerose.

76. Kongress der DGN, Hamburg, 03.- 06.09.2003,

Aktuel Neurol, Supplement S1, 30: P 478